การปรับปรุงไฮโดรโฟบิซิตีและเสถียรภาพของไทเทเนียม-เอ็มซีเอ็ม-41

นาย เดโชชัย วิไลรัตน์

IMPROVEMENT OF HYDROPHOBICITY AND STABILITY OF Ti-MCM-41

Mr. Dachochai Wilairat

Thesis Title	IMPROVEMENT OF HYDROPHOBICITY AND STABILITY OF Ti-MCM-41
By	Mr. Dachochai Wilairat
Field of Study	Chemistry
Thesis Advisor	Aticha Chaisuwan, Ph.D.

Accepted by the Faculty of Science, Chulalongkorn University in Partial Fulfillment of the Requirements for the Master 's Degree

……………………………………….Dean of Faculty of Science

(Associate Professor Wanchai Phothiphichitr, Ph.D.)

Thesis Committee

………………………………………Chairman

(Associate Professor Siri Varothai, Ph.D.)

…………………………………….…. Thesis Advisor

(Aticha Chaisuwan, Ph.D.)

……………………………………….Member

(Associate Professor Wimonrat Trakarnpruk, Ph.D.)

……………………………………….Member

(Assistant Professor Santi Tip-pyang, Ph.D.)

เดโชชัย   วิไลรัตน์ : การปรับปรุงไฮโดรโฟบิซิตีและเสถียรภาพของไทเทเนียม-เอ็มซีเอ็ม-41. (IMPROVEMENT OF HYDROPHOBICITY AND STABILITY OF Ti-MCM-41) อ. ที่ปรึกษา : ดร.อธิชา ฉายสุวรรณ, 112 หน้า. ISBN 974-17-3189-2.

ในการศึกษานี้ได้สังเคราะห์วัสดุไทเทเนียม-เอ็มซีเอ็ม-41 ที่มีขนาดโพรงและอัตราส่วนซิลิกอนต่อไทเทเนียมแตกต่างกันเพื่อเปรียบเทียบสมบัติของมัน ได้สำรวจภาวะของการปรับโครงสร้างใหม่   และซิลิเลชันแยกจากกันและพร้อมกันเพื่อปรับปรุงไฮโดรโฟบิซิตีและความเสถียรของไทเทเนียม-เอ็มซีเอ็ม-41 ใช้เทคนิคการเลี้ยวเบนรังสีเอ็กซ์ ดิฟฟิวซ์รีเฟลกแทนซ์-ยูวี-วิสิเบิลและฟูเรียร์ทรานส์ฟอร์มอินฟราเรด ไทเทเนียม-เอ็มซีเอ็ม-41 ที่มีโพรงใหญ่มีความเสถียรน้อยเนื่องจากมีการสร้างผนังโพรงที่บางรอบโพรง   ไม่ใช่ซิลิกอนทั้งหมดที่ควบแน่นได้อย่างสมบูรณ์ที่ผนังโพรงจึงมีหมู่ซิลานอลเหลืออยู่ที่ผิวผนังและสามารถถูกปรับโครงสร้างระหว่างกรรมวิธีที่เหมาะสม   การปรับโครงสร้างเพียงอย่างเดียวในน้ำร้อนทำให้มีการเพิ่มความเสถียรของผลิตภัณฑ์ โดยเฉพาะอย่างยิ่งไทเทเนียม-เอ็มซีเอ็ม-41 ที่มีโพรงใหญ่ ซิลิเลชันของวัสดุเหล่านี้ภายใต้การเปลี่ยนค่าของอุณหภูมิ ปริมาณที่มากเกินพอและชนิดของของซิลิลรีเอเจนต์ ได้ทดสอบตัวอย่างที่ผ่านกรรมวิธีเพื่อหาความเสถียรต่อกรรมวิธีไฮโดรเทอร์มัลและต่อความชื้นเปรียบเทียบกับตัวอย่างที่ไม่ผ่านกรรมวิธี   การใช้การปรับโครงสร้างในน้ำร้อนร่วมกับซิลิเลชันได้รับการพิสูจน์ว่า   เป็นกระบวนการที่ดีที่สุดสำหรับเตรียมผลิตภัณฑ์ไทเทเนียม-เอ็มซีเอ็ม-41 ที่มีความเสถียรสูงสุดและมีไฮโดรโฟบิกซิตีที่สูงขึ้น

ภาควิชา.เคมี........เคมี............................ลายมือชื่อนิสิต...

สาขาวิชา............เคมี.........................ลายมือชื่ออาจารย์ที่ปรึกษา...................................

ปีการศึกษา..........2545....................

4272281123 : MAJOR CHEMISTRY
KEY WORD: MCM-41 / MESOPOROUS MOLECULAR SIEVE / SILYLATION / STABILITY / TITANOSILICATE

DACHOCHAI WILAIRAT : IMPROVEMENT OF HYDROPHOBICITY AND STABILITY OF Ti-MCM-41.
THESIS ADVISOR : ATICHA CHAISUWAN, Ph.D. 112 pp., ISBN 974-17-3189-2.

In this study, Ti-MCM-41 materials with various pore sizes and Si/Ti ratios were synthesized to compare their properties. Several conditions of restructuring and silylation were investigated separately and in duality to improve the hydrophobicity and stability of Ti-MCM-41. The crystallinity change was followed up using X-ray diffraction, diffuse reflectance-UV-visible and Fourier transform infrared techniques. Low stability of large pore Ti-MCM-41 is on account of the thin wall formed around the pores. Not all silicon was completely condensed at the pore wall therefore silanol groups were left at the wall surface and can be restructured during appropriate treatment. A single treatment of restructuring in hot water results in the increase of the stability of the products, especially for small pore Ti-MCM-41. Silylation of the materials was studied under a variation of temperature, excess amount, and types of a silyl reagent. All treated samples were tested for their stabilities to hydrothermal treatment and to moisture in comparison with the untreated samples. The post-synthesis combination of restructuring in hot water and silylation is proven as the best treatment for making the highest stable Ti-MCM-41 product with great hydrophobicity.

Department..........Chemistry....................................Student's signature…………………

Field of study.......Chemistry....................................Advisor's signature………………….

Academic year.....2002...

ACKNOWLEDGEMENTS

CONTENTS

CONTENTS (continued)

CONTENTS (continued)

CONTENTS (continued)

LIST OF FIGURES

LIST OF FIGURES (continued)

LIST OF FIGURES (continued)

LIST OF FIGURES (continued)

LIST OF SCHEMES

LIST OF TABLES

LIST OF TABLES (continued)

LIST OF TABLES (continued)

LIST OF ABBRIVATIONS

CTMACl	=	*n*-Hexadecyltrimethylammonium chloride
DR UV VIS	=	Diffuse reflectance ultraviolet spectroscopy
DTMACl	=	*n*-Dodecyltrimethylammonium chloride
FTIR	=	Fourier transform infrared spectroscopy
HMDS	=	Hexamethyldisilazane
HMDSO	=	Hexamethyldisiloxane
ICP-AES	=	Inductively Coupled Plasma-Atomic Emission Spectroscopy
KM	=	Kubelka-Munk function
TBOT	=	Tetra-*n*-butyl orthotitanate
TEOS	=	Tetraethyl orthosilicate
TMAOH	=	Tetramethylammonium hydroxide
TMCS	=	Trimethylchlorosilane
TMES	=	Trimethylethoxysilane
TMSTFA	=	Trimethylsilyl trifluoroacetate
XRD	=	X-ray diffraction or diffractometer

CHAPTER I

INTRODUCTION

1.1 Statement of Problem

Two classes of materials that are used extensively as heterogeneous catalysts and adsorption media are microporous (pore diameter ≤ 20 Å) and mesoporous (20-500 Å) inorganic solids.[1] The utility of these materials is manifested in their microporous structures which allow molecules access to large internal surfaces and cavity. A major subclass of the microporous is molecular sieves. These materials are exemplified by the large family of aluminosilicates known as zeolites in which the micropores are regular arrays of uniformly-sized channels. Zeolites have been used as catalysts, supports, and adsorbents because of their peculiar characteristics: large internal surface area and easily controlled uniform pores with molecular dimensions. When used as catalysts, zeolites exhibit remarkable shape selectivity; the diffusion of bulky reactants and products into the pore are often obstructed.[2]

In 1992, Beck *et al.*,[3-4] the researchers at Mobil, discovered a new family of mesoporous molecular sieves named M41S. The M41S family is classified into several members: MCM-41 (hexagonal), MCM-48 (cubic) and MCM-50 (lamellar). These materials have uniform pores, and their pore size can be varied from approximately 16 Å to greater than 100 Å through the choice of surfactant as the template, auxiliary chemicals and reaction conditions. These materials typically have surface areas above 1000 m^2/g by nitrogen adsorption and more than 700 m^2/g by hydrocarbon adsorption. There is no doubt that the synthesis of these materials opens definitive new

possibilities for preparing catalysts with uniform pores in the mesoporous region, which should importantly allow the relatively large molecules present in crude oils and in the production of fine chemicals to react.

After the discovery of M41S family of mesoporous materials, a considerable effort was made in order to adapt their structures and properties. Most of the research in that field was devoted to MCM-41 silicate and aluminosilicates molecular sieves, which exhibit hexagonal arrays of cylindrical mesopores. Chemical properties of these materials were modified by framework incorporation of various heteroatoms, such as transition metal and non-transition metal etc. with the purpose of creating specific catalytic sites.

Titanium compounds have been widely used as catalysts in oxidation of various organic substrates.[5] Following the discovery of the titanosilicate-1 (TS-1), which incorporates Ti in the MFI framework, in the early 1980s, TS-1 has been proved to be an excellent catalyst for selective oxidation of various organic substrates in the presence of hydrogen peroxide.[6] Microporous titanium-containing silicalite has been attractive for a decade owing to their unique oxidation properties. They are known to be effective in the oxidation of a variety of small substrate, when hydrogen peroxide is employed as the oxidant. Although amorphous TiO_2-SiO_2 also exhibits oxidation activity, it can hardly utilize hydrogen peroxide as an oxidant.[5] Thus, strenuous efforts have been made to synthesize titanium-containing molecular sieves with larger pore which are able to oxidize bulky substrates with hydrogen peroxide; such as Ti-β[7-8] was synthesized and found to be active for oxidation of cycloalkanes and cycloalkenes.[8-9] Ti-zeolite application is still limited to molecules smaller than 7 Å. There is no doubt that this is a limitation for the use of Ti zeolites as selective oxidation catalysts in the filed of fine chemicals. There was, therefore, a need for producing molecular sieve oxidation catalysts with a pore diameter larger than 7 Å.

In 1994, Corma *et al.*[10-11] reported the possibility of synthesizing a mesoporous Ti-MCM-41 with a regular pore diameters of 35 Å. It was obtained by direct synthesis. The OH/SiO$_2$ ratio and alkali metal cation content were found to be important variables to prepare good materials. Ti-MCM-41 samples were prepared with Ti in framework position and no extraframework TiO$_2$ was detected. The materials prepared are selective catalysts for oxidation of different types of olefins. Although the intrinsic activity of Ti-MCM-41 was lower than TS-1 and Ti-β when using H$_2$O$_2$ as oxidant with using tertbutyl hydroperoxide (TBHP) as oxidation, the activity of Ti-MCM-41 was closer to that of Ti-β and much higher than that of TS-1. Ti-MCM-41 has a clear advantage over other Ti-zeolites in the oxidation of large organic molecules of interest for production of fine chemicals. For the oxidation of larger organic molecules, such as α-terpineol, which are diffusion-limited even in a large pore zeolite such as Ti-β, the mesoporous Ti-MCM-41 catalyst is much more active than the above zeolites, and opens new possibilities for the production of oxygenated fine chemicals.

The application limitation of Ti-MCM-41 is the instability of its structure. Poor thermal and hydrothermal stabilities are limiting factors in the potential application of these materials to several types of hydrocarbon processing procedures and adsorption processes requiring heavy-duty regeneration. Although, the thermal stability of pure silica MCM-41 is relatively good, and the materials is stable at temperatures of 850°C but less was found in many zeolites.[12] Ti-MCM-41 is nevertheless usually destroyed, and its surface area is reduced to virtually nil on calcination at 1000°C.[13] Its hydrothermal stability especially in boiling water is also very poor. For example, Ti-MCM-41 lost their hexagonal structure and became amorphous upon boiling in water for 2 days due to silicate hydrolysis.[14] The d_{100} peak height of Ti-MCM-41 decreased by 80% upon exposure to water vapor over a saturated aqueous solution of NH$_4$Cl at room temperature for 3 days.[15] Full structure collapse of MCM-41 was found to occur

when the MCM-41 sample was left in air for three months.[16] Particularly, the stability of Ti-MCM-41 was found low compared to pure-silica MCM-41 so that the substitution of Ti for Si in the silica framework of MCM-41 greatly reduced the stability of the structure.[17] Ti-MCM-41 structure collapsed and titanium was leached out of the framework by hydrolysis under mild reaction conditions for phenol hydroxylation with H_2O_2.[18]

The M41S material has poor mechanical stability compared to other to other materials such as alumina and silica gels.[19-20] The mesoporous molecular sieves structure of MCM-41 and MCM-48 was collapsed by mechanically pressing in the presence of adsorbed water.[21-22]

Because of the instability of M41S mesoporous materials, the Ti-MCM-41 development obtained with the high activity and high stability is widely interested. There have been enormous efforts being devoted to the improvement of stability of these materials. These techniques can be categorized into 3 methods.

1. The increase in the wall thickness and wall polymerization technique,[13,19,23] the simplest one among these techniques, is utilized for improvement of thermal stability and mechanical stability of these materials but not hydrothermal stability. The examples of this technique are the well-known technique of pH-adjustment[12,24-29] and the post-synthesis hydrothermal restructuring method.[30-33]

2. The post-synthesis silylation,[4,15,21-22,34-50] this method is employed to decrease the concentration of silanol groups on the pore wall by the reaction with silanes. The degree of the silylation may be controlled so that the increase in hydrophobicity of the pore walls leads to a systematic enhancement of the hydrothermal stability. This kind of treatment is useful for hydrophobic applications but can be undesirable for hydrophilic application. Undesirable

trimethylsilyl groups of M41S may be lost due to the thermal decomposition leading to surface silanols at 450°C and the condensation of silanols on the silica surface at above 550°C.[50]

3. The Salt Effects,[14,51-55] this treatment is performed by addition of some sodium salts such as sodium chloride, potassium chloride, sodium chloride, sodium acetate, ethylenediamineteraacetic acid terasodium salt (Na_4EDTA), K_4EDTA, and so on during synthesis, or by ion exchange with Na^+, K^+, Ca^{2+} Y^{3+}, La^{3+} and Fe^{3+}. This method causes no changes in the silanol group concentration of the calcined sample but nevertheless was claimed to be effective for the improvement of the hydrothermal stability. However, more recent experiments to exploit the salt effect pointed out its poor reproducibility.[52]

These three techniques have advantages and disadvantages. A combination of them that has not been attempted before, may promote the stability and catalytic activity of Ti-MCM-41 better than using a single technique. A combination of the post-synthesis hydrothermal restructuring treatment and the silylation is very attractive in this study to obtain the higher quality Ti-MCM-41.

1.2 Objectives

1. To prepare high stable and high hydrophobic Ti-MCM-41.

2. To evaluate the stability of these samples by several tests, the samples were characterized for their structure change using XRD.

1.3   Scope of This Work

Ti-MCM-41 samples with two pore sizes were synthesized with *n*-dodecyltrimethylammonium chloride ($C_{12}H_{25}$TMACl) and *n*-hexadecyltrimethylammonium chloride ($C_{16}H_{33}$TMACl) as templates. The Ti-MCM-41 was prepared to improve its stability using the post-synthesis hydrothermal restructuring method and to reduce hydrophilicity by replacing the silanol group with trimethylsilyl group by the trimethylsilylation. The samples were tested for the stability to moisture by exposing to moisture over a saturated aqueous solution of NH_4Cl at room temperature and for the hydrothermal stability on the boil water for 12 h. Some samples were selected to be tested for the mechanical stability, which was performed by pressing the samples in a steel die at various pressures.

1.4   Related Works

Poor thermal and hydrothermal stabilities are limiting factors in the potential application of these MCM-41 typed materials to several types of hydrocarbon processing procedures and adsorption processes requiring heavy-duty regeneration. The relevance of thermal stability has been evident since earliest disclosure of the materials.

When Si-MCM-41, Al-MCM-41, and Ti-MCM-41 were calcined in air at elevated temperature above 800°C. The pore structures of Si-MCM-41 and Al-MCM-41 collapse at a calcination temperature above 800°C, while Ti-MCM-41 structural collapse occurs at about 900°C.[56] It was reported that the control polymerization of silicates during synthesis of MCM-41 led to thicker walls, and hence to higher thermal and hydrothermal stability.[23] Whereas, the increase of the wall thickness from 7 to 11 Å of MCM-41 structure did not improve the hydrothermal stability. After steam treatment at 750°C for 5 h, the pores collapsed and the surface area was dramatically

reduced like amorphous. The structure was not stable enough to resist the conditions in an fluidized catalytic cracking (FCC) regenerator.[57]

The stability of MCM-41 after wetting with neutral, basic, and acidic aqueous solutions and further recalcination was studied by Landau *et al.*[58] Calcined Si-MCM-41 synthesized at room temperature was fully degraded under wetting with neutral water. Crystallization under hydrothermal conditions improved their wetting stability. Adjustment of pH and NaCl addition during hydrothermal crystallization let to a further improvement. The water-stable Si-MCM-41 synthesized with pH adjustment and salt addition was also insensitive to wetting with acidic aqueous solution. However, treatment of this non-strained material with a basic solution at pH 7.8-8.9 resulted in silica leaching and a reduction in crystallinity, the mean pore diameter and the pore volume. The rod shape and surface area remained relatively unchanged after wetting at pH 7.8. It was proposed, based on spectroscopic data, that the structural degradation during wetting was caused by hydration of the siloxane structure at the wetting stage followed by siloxane hydrolysis, or hydroxylation of strained $Si(-OSi-)_4$ units and their rearrangement, or redehydroxylation during recalcination.

Landau *et al.*[58] proposed a model of structural changes occurring in Si-MCM-41 during base treatment and recalcination as shown in Figure 1.1. Some of the $[SiO_4]^{4-}$ units at the pore wall surface leached out resulting in the transformation of Q^4 to Q^3 and Q^3 to Q^2 units as observed in ^{28}Si-NMR spectra. Calcination was performed to remove ammonia and leave silanol groups that disappeared partially as a result of condensation of adjacent silanol groups. The intergrowth of hexagonal crystal rods, reduction of the surface area and pore volume of the material, and formation of a disordered pore structure with increased pore wall thickness supported the proposed schematic model in Figure 1.2.
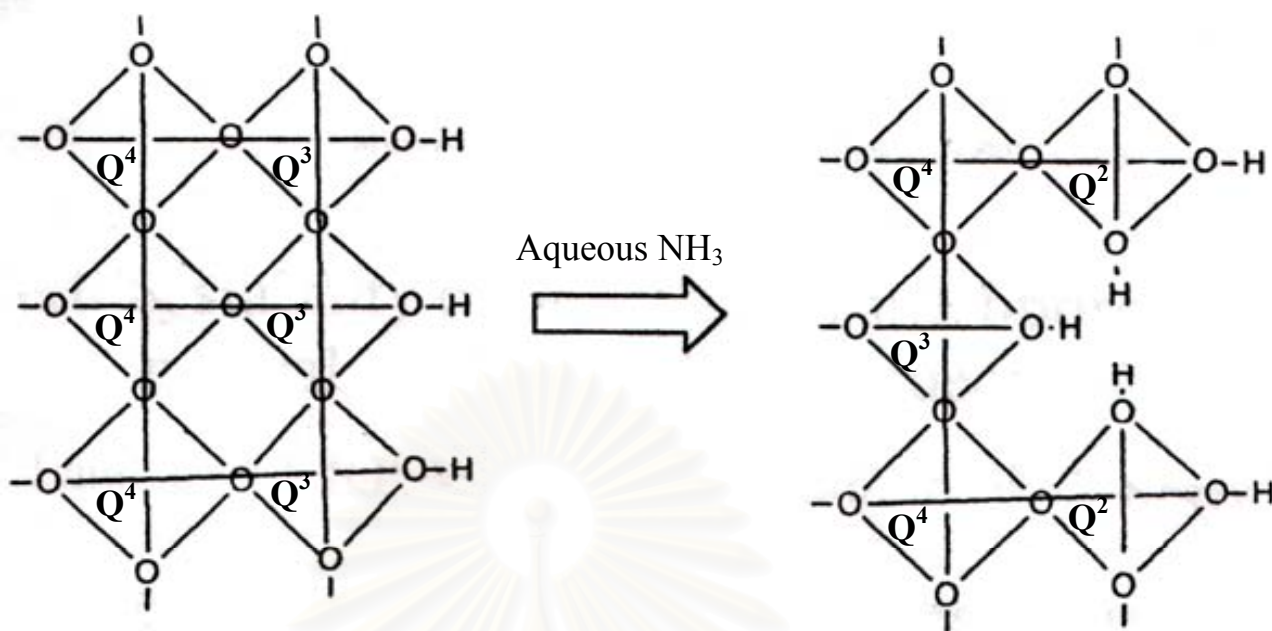
Figure 1.1 Leaching of Si from the pore walls in the Si-MCM-41 creates Q^3 and Q^2 silica units causing roughness of the pores surface.
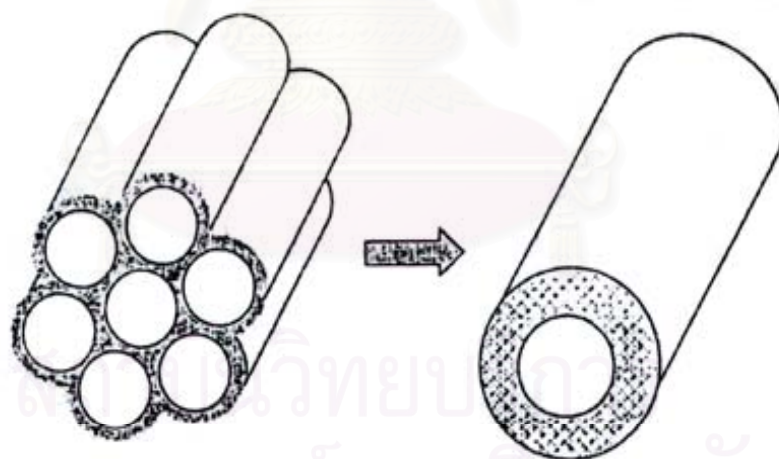
Figure 1.2 Model for the collapse of hexagonal tubular arrays in the Si-MCM-41 structure during wetting and recalcination.

The mechanical stability of MCM-48 is higher than that of MCM-41,[59] but still low compared to zeolites, silica gels and alumina.[19] The structural collapse by

mechanical pressing was believed to occur through the hydrolysis of Si-O-Si bond in the presence of adsorbed water.[21-22] It was recently shown that similar hexagonal mesoporous material FSM-16 also became less ordered by pressing.[20] The magnitudes of applied external pressures which appreciably changed the ordered structure were in the range of routine high-pressure techniques used in handling these materials. The structural collapse of mesoporous molecular sieves MCM-41 and MCM-48 materials is expressed in Scheme 1.1.

Scheme 1.1 Mechanism of mechanical collapse of the M41S structure.

$$\text{—Si—O—Si} \quad + \quad H_2O \quad \xrightarrow{\text{mechanical compression}} \quad 2\text{—Si—OH}$$
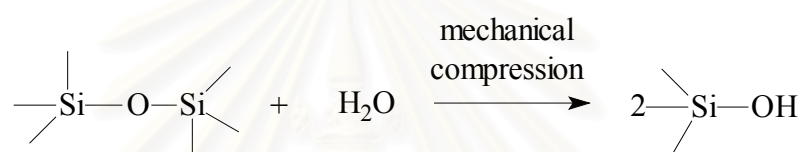
The structure was, perhaps, be strained by pressing then made susceptible to hydrolysis, resulting in the reaction of the ordered structure. MCM-48 adsorbed relatively large amount of water. When water was absent, however, the cleavage of siloxane bonds hardly occurred. The noticeable loss of the regularity of the structures by applying pressure under dry N_2 might have been due to the incomplete removal of adsorbed water and/or intrusion of moisture during the stability test. The samples were inevitably contacted with ambient air ever through momentarily because they were calcined in a muffle furnace. Other factors related to stability of MCM-41 and MCM-48 are pore size, silica source, and adsorption amount of water, which depends also on the humidity of ambient air. Pore wall thickness and particle size may also affect the mechanical stability.

It was known that the increases in pore wall thickness and extent of silica condensation of prepared MCM-41 were significantly improved in thermal and hydrothermal stability. The pore wall thickness of MCM-41 may be controlled by careful choice of synthesis condition[13,19,23] or by post-synthesis restructuring.[30-33] The

stability of MCM-41 may also be improved *via* post-synthesis hydrothermal restructuring of the as-synthesized (surfactant-containing) material in water.[31]

Ryoo *et al.*[12,24-25,28] found that the textural uniformity and thermal stability of MCM-41 and Al-MCM-41 were remarkably improved by repeating pH adjustment to about 11 during hydrothermal reaction of acetic acid. The XRD peak width and intensity of as-synthesized samples was not significantly affected by pH adjustment during the synthesis. Conversely, the XRD peak width and intensity for calcined sample were affected very markedly by the pH adjustment procedure. Each peak was well resolved in the case of MCM-41 samples synthesized using the pH adjustment procedure, while the XRD peaks were severely broadened for samples synthesized without the pH adjustment as shown in Figure 1.3.

The effect of acetic acid addition to the reactant mixture MCM-41 synthesis was found to be reversible by addition of NaOH and heating to 100°C for 24 h. The reversibility of the synthesis reaction, or decomposition of MCM-41 and the long-term product stability under the reaction conditions indicated that the MCM-41 phase is in equilibrium with the reactants. Thus, addition of acetic acid to the reactant mixture shifts the equilibrium toward formation of MCM-41. The MCM-41 yield, based on the SiO_2 increased from 62 to 83, 88 and 90% as for the pH adjustment and subsequent heating was repeated twice. If the acid was quickly added at once to the initial reaction mixture, the XRD pattern was found to be poor. If the acid was properly added, the product exhibited higher uniformity and higher crystallinity.
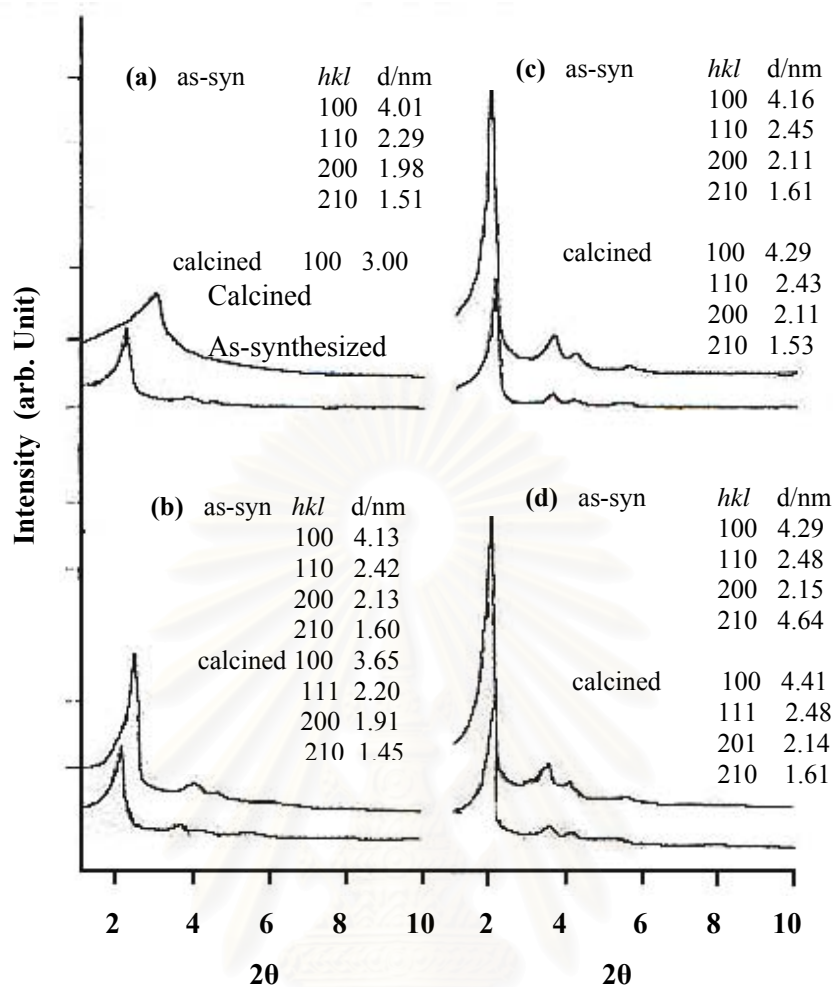
Figure 1.3 XRD patterns of MCM-41 a) synthesized without pH adjustment, b) synthesized with pH readjustment to 11 using acetic acid, c) synthesized by repeating the pH adjustment procedure twice, and d) three times. The as-synthesized MCM-41 samples were transformed to the so-called samples by calcinations in a muffle furnace in air at 500°C.

White *et al.*[26] developed a method by optimizing the mineral acids (i.e., hydrochloric acid, sulfuric acid, and acetic acid) or salts (i.e., ammonium bromide, and sodium acetate). The synthesis was performed at a number of different pH values (pH = 7-11). The highest crystallinity of MCM-41 occurs when the pH is held between 9 and 10 during synthesis in the presence of the sulfate anion. Besides, the addition of different tetraalkylammonium (TAA$^+$) such as tetramethylammonium (TMA$^+$) tetraethyl-ammonium (TEA$^+$) or tetrapropylammonium (TPA$^+$) to the synthesis gel[27] obtained high crystallinity products without the necessity of multiple pH-adjustment steps.

In addition, pH adjustment with NaF addition[28-29] produced MCM-41 with well-defined long-range structure and high hydrothermally stablility. The improvement of the hydrothermal stability of MCM-41 material is most likely attributed to the formation of Si-F bonds on the surface of the mesopores of MCM-41, leading to the natural resistance of the fluorinated surface to the hydrolysis by water molecules.

A few reports showed a fascinating restructuring process upon post-synthesis hydrothermal treatment of the as-synthesized MCM-41 (inorganics + template). In 1995, Khushalani *et al.*[60] reported an increase in d_{100} spacing of 3-4 Å a day, when a MCM-41 was aged in its mother liquor at 150°C for up to 10 days. This increase in *d* spacing was accompanied by an increase in mesoporus volume and an increase in average pore diameter. A silica mesostucture with a mesoporous volume as high as 1.6 ml/g and an average pore diameter as high as 60 Å was obtained after aging a silica mesostructure in deioninzed water at 100°C for four weeks.[61] Even more puzzling was the observation that phase transformation of MCM-41 occurred upon post-synthesis hydrothermal treatment, for example, lamellar to hexagonal, hexagonal to lamellar and lamellar to cubic phase tranformation upon post-synthesis hydrothermal treatment of silica-only M41S.[61]

Horiuchi *et al.*[31] described that the as-synthesized MCM-41 was hydrothermally treated with water, the XRD peak intensity as well as the unit cell parameter was found to increase and with prolonging the synthesis time, the pore size was also increased even in the normal synthesis. However, the most apparent advantage of the post-synthesis water treatment was the significant improvement in product quality, compared to the normal synthesis method. A comparison of XRD patterns showed that the water-treated MCM-41 exhibits much higher XRD intensities than that of normally prepared sample. A phase transformation from lamellar to hexagonal during the restructuring in water was also observed similarly to that noticed upon pH adjustment. This indicated that the post-synthesis water treatment was widely applicable to the further improvement of the quality of MCM-41. Another significant difference between the uncalcined MCM-41 obtained by a normal synthesis and water treatment was the extent of the unit cell shrinkage during calcination. The water-treated sample showed much less shrinkage upon calcination as a result of better wall polymerization of further agglomeration of isolated small MCM-41 particles by the condensation of silanol groups toward a better local atomic arrangement. The observation of the crystallite size increment after the water treatment was also supportive of this conclusion. This possibly can account for the enhancement of the long-distance order in MCM-41 by the post-synthesis water treatment.

The role of the pH solution would play a crucial parameter in the improvement in the quality of MCM-41. In a typical synthesis under basic conditions, the pH of the initial synthesis gel mixture was 11.2; it rose to 11.6 after 1 day synthesis at 150°C. When the mother liquor was replaced with water, the pH of the resulting mixture was in the range of 8–10 depending on the amount water added. It was believed that a pH lower than 10 favored the condensation of silanols and the redeposition of silicate anions. The product quality was greatly improved by maintaining pH during synthesis. Possibly the as-synthesized material with defective

anionic sites and terminal silanol groups restructured toward a higher polymerization to form more $Si(OSi)_4$ bonds at a lower pH. The promoted condensation of silanols led to a higher order of local atomic arrangement. Hence, the lowering of the pH by the replacement of the mother liquor with water was responsible for the better polymerization of the silica wall. The repeated post-synthesis hydrothermal treatments of the as-synthesized sample (containing template) had a beneficial effect on the adsorptive volume of MCM-41. For example, the mesopore volume of MCM-41 increased by 53% after three post-synthesis hydrothermal treatments, and increased by 27% after two post-synthesis hydrothermal treatments. The dramatic increase in mesopores volume was neither the result of phase transformation, as probed by XRD pattern, nor the consequence of an increase in average pore diameter.

White *et al.*[33] described why the post-synthesis hydrothermal treatment improved the condensation of the mesostructure walls with related wall transport and recondensation process the different reasons. At first silicate species was dissolved easily in aqueous solution at the pH between 8 and 11, at which the post-synthesis hydrothermal treatment was performed. The second, at the temperature about 110°C, the species in solution were very mobile with respect to others in the organic core and at the organic/inorganic interface. The silica species located in the surface region of Q^1 and Q^2 were likely to dissolve in the synthesis medium upon post-synthesis hydrothermal treatment and recondense elsewhere. This restructuring process was believed to improves the cross-linking of the inorganic species lining the walls, giving solids with a higher thermal stability. Therefore, the treated mesostructures were more resistant to the calcination treatment and developed, after template removal, a mesopore volume larger than the parent material.

It could be argued that a portion of the amorphous phase crystallized into hexagonal phase during the post-synthesis hydrothermal treatment, explaining the increase in mesopore volume. However, the solid was extensively washed before

hydrothermal treatment so as to remove surfactant ions from the solution and therefore prevent further crystallization. When the MCM-41 was treated in surfactant solution, the volume increased for 3% compared to when the solid was treated in deionized water, the volume increased for 13%. So that the process occurring during hydrothermal treatment was not merely the continuation of the synthesis, but a restructuring process that affected the hexagonal framework.

Since the unstable structure of the mesoporous molecular sieves M41S seems to be due to the adsorbed water, Many researchers[34-49] investigated the methodology for preparation of hydrophobic of surface of silicas with the post-synthesis silylation with various silane compounds. The results were all in agreement that MCM-41 and its analogues exhibited poor activities in olefin epoxidation with H_2O_2 and oxidation of other organic substrates. After silylation with various types of silylating reagents, their activities were remarkably enhanced.[39,40-41] Those silylation reagent studied were trimethylchlorosilane (TMCS),[15,21,22,43,41] MPTMS,[46] APTMS,[46] hexamethylsdisilazane (HMDS),[38,47] silazane analog,[43] hexamethyldisiloxane (HMDSO),[15,21,22,40-41] ipropyltrimetyltrimethoxysilane,[36] phenyltrimethoxysilane,[36] decyltrichlorosilane. methyltriethoxysilane,[36] and N,O-*bis*(trimethylsilyl)trifluoroacetamide) (BSTFA).[39] Besides enhancement of the activity in catalytic oxidation, the wall thickness of the materials was also increased after silylation. This was responsible for their increasing thermal, hydrothermal, and water stability.[21,22,37] Durations for silylation were varied from 3 to 16 h depending on conditions.[34-49]

The procedures may be one-step or two-step silylation with different silylating reagents.[36,44-45] The stabilizing effect was maintained even after removal of methyl groups at elevated temperature.[40-41] Organosilane addition in the reactant mixture for synthesis of Ti-MCM-41 was also attempted.[48-49] Similar effects of sillyation were studies with other materials such as TS-1,[39] Ti-MCM-48,[40-41,50] SBA-15,[46,47] Ti-SBA-15,[47] and amorphous silica.

Besides, the addition trivalent elements of Al^{3+}, La^{3+} and Fe^{3+} to Si-MCM-41[55] showed the effect on the thermal and hydrothermal stability of MCM-41. Al^{3+} decreased the thermal and hydrothermal stability of MCM-41, whereas La^{3+} and Fe^{3+} especially Fe^{3+} improved the thermal and hydrothermal stability. In addition, the La^{3+} and Fe^{3+} addition improved the thermal and hydrothermal of Al-MCM-41 and Ti-MCM-41 as a result of thicker channel wall and salt effect during the crystallization process.

The salts effect on hydrothermal stability[51] that the formation of surfactant-silicate mesostructures from HTA^{+} and sodium silicate solution following the electrostatic templating route can be affected by the electrostatic interaction with ions constituting salts under high salts concentration. In fact, the addition of salt can either decrease or increase the thermal stability of the calcined MCM-41 product very significantly, depending on the nature and the amount of salt the addition time during the MCM-41 crystallization process. The salt effect on hydrothermal stability due to moderation of the electrostatic interaction between cationic surfactant micelles and the silicates was attenuated by the salt while the surfactant-silicate mesostructure is formed. It may be speculated that the silicates was released from strong electrostatic binding with the surfactant under circumstances, and consequently the degree of silicate polymerization (i.e. silanol group condensation) was expected to increase compared to a situation without such electrostatic attenuation.

CHAPTER II

THEORY

2.1   General Background

In 1932, McBain proposed the term "molecular sieve" to describe a class of materials that exhibited selective sorption properties when he found that chabazite, a zeolite mineral, had a property of selective adsorption of molecules smaller than 5 Å in diameter. He proposed that for a material to be a molecular sieve, it must separate components of a mixture on the basis of molecular size and shape. Two classes of molecular sieves were known when McBain put forward his definition: natural zeolites and certain microporous charcoals. This list has now been expanded to include, in addition to zeolites and carbon, microporous materials with pure silica, as well as vastly different elemental compositions. These are silica, metal silicates, metal aluminates, aluminophosphates ($AlPO_4$s) and silicoaluminophosphates. The continually expanding field of molecular sieves is shown in Scheme 2.1. All materials represented in the list are molecular sieves based on McBain's definition, as they can separate components of a mixture on the basis of size and shape. Only the aluminosilicates generally can be considered as classical zeolites.[62]
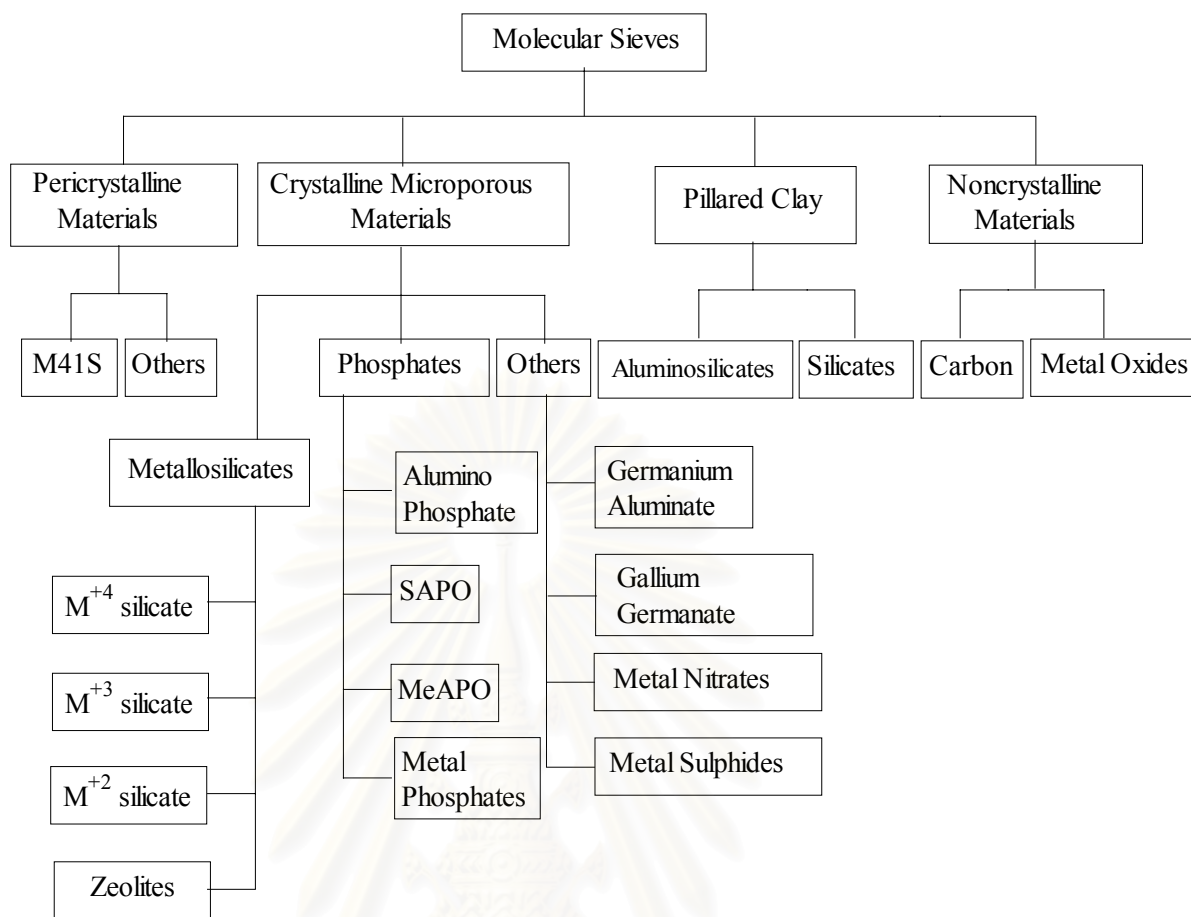
Scheme 2.1 Classification of molecular sieves and related materials indicating the extensive variation in composition (zeolites occupy a subcategory of the metallosilicates).

2.2 Classification of Pore Size of Molecular Sieves

According to the International Union of Pure and Applied Chemistry (IUPAC) classification,[63] molecular sieves can be classified into three main categories. Table 2.1 typically lists some zeolites and molecular sieves with variable pore sizes, mostly in the microporous range prior to the discovery of MCM-41. So far, no macroporous molecular sieves have been discovered.

Table 2.1 Pore size definition of zeolites and molecular sieves

Pore size (Å)	Definition	Typical material	Ring size	Pore diameter (Å)
>500	Macroporous	-	-	-
20-500	Mesoporous	MCM-41	-	15 – 100
		MCM-48		
		SBA-15		
<20	Microporous with			
	Ultra-large pores	Cloverite	20	6.0 x 13.2
		JDF-20	20	6.2 x 14.5
		VPI-5	18	12.1
		AlPO$_4$-8	14	7.9 x 8.7
	Large-pores	Faujasite	12	7.4
		AlPO$_4$-5	12	7.3
		ZSM-12	12	5.5 x 5.9
	Medium-pores	ZSM-48	10	5.3 x 5.6
		ZSM-5		5.3 x 5.6
				5.1 x 5.5
	Small-pores	CaA	8	4.2
		SAPO-34	8	4.3

2.3 Zeolites

Zeolites are crystalline, microporous aluminosilicates with a framework based on an infinitely extending three-dimensional network of AlO$_4$ and SiO$_4$ tetrahedral linked to each other by sharing all of the oxygens. Zeolites may be represented by the formula $M_{2/n}[(AlO_2)_x(SiO_2)_y].wH_2O$ where cations M of valency n neutralize the

negative charges on the aluminosilicates framework. Zeolites are the most widely used for catalysts in industry and have become extremely successful catalysts for oil refining, petrochemistry, and organic synthesis in the production of fine and specialty chemicals, particularly when dealing with molecule having kinetic diameter below 10 Å. The reason for their success in catalysis is related to the following specific features of these materials.[64]

1. Zeolites have very high surface area and adsorption capacity.

2. The adsorption properties of zeolites can be controlled, and their surface can be modified from hydrophobic to hydrophilic properties.

3. Active sites, such as acid sites for can be generated in the framework and their strength and concentration can be tailored for a particular application.

4. The sizes of their channels and cavities are in the typical range for many molecules of interest (5–12 Å), and the strong electric fields existing in those micropores together with an electronic confinement of the guest molecules are responsible for a preactivation of the reactants.

5. Their highly ordered channel structure allows the zeolites to present different types of shape selectivity, i.e., product, reactant, and transition state, which can be used to direct a given catalytic reaction toward the desired product avoiding undesired side reaction.

6. All of these properties of zeolites, which are of importance in catalysis and make them attractive choices for types of desired processes, depending on the thermal and hydrothermal stability of these materials. In the case of zeolites, they can be activated to produce very stable materials not just resistant to heat and steam but also to chemicals.

Despite their catalytically desirable properties, zeolites are limited to small substrates. Therefore, mesoporous materials with ordered structure would be the alternative.

2.4 MCM-41

Beck *et al.*[3-4] extended the templating strategy commonly used for molecular sieve synthesis to the preparation of a new family of periodic mesoporous silicates designated M41S by using long-chain surfactants as templates. Depending on the synthesis conditions, the obtained materials consisted of three different members: a hexagonal phase MCM-41, a cubic phase MCM-48, or a non-stable lamellar phase MCM-50. Then typical XRD patterns are shown in Figure 2.1. By selecting the carbon chain length of a surfactant molecule, the pore size was systematically varied from about 15 to 100 Å. Besides, they present long-range ordered structure, and surface area above 1000 m^2/g.
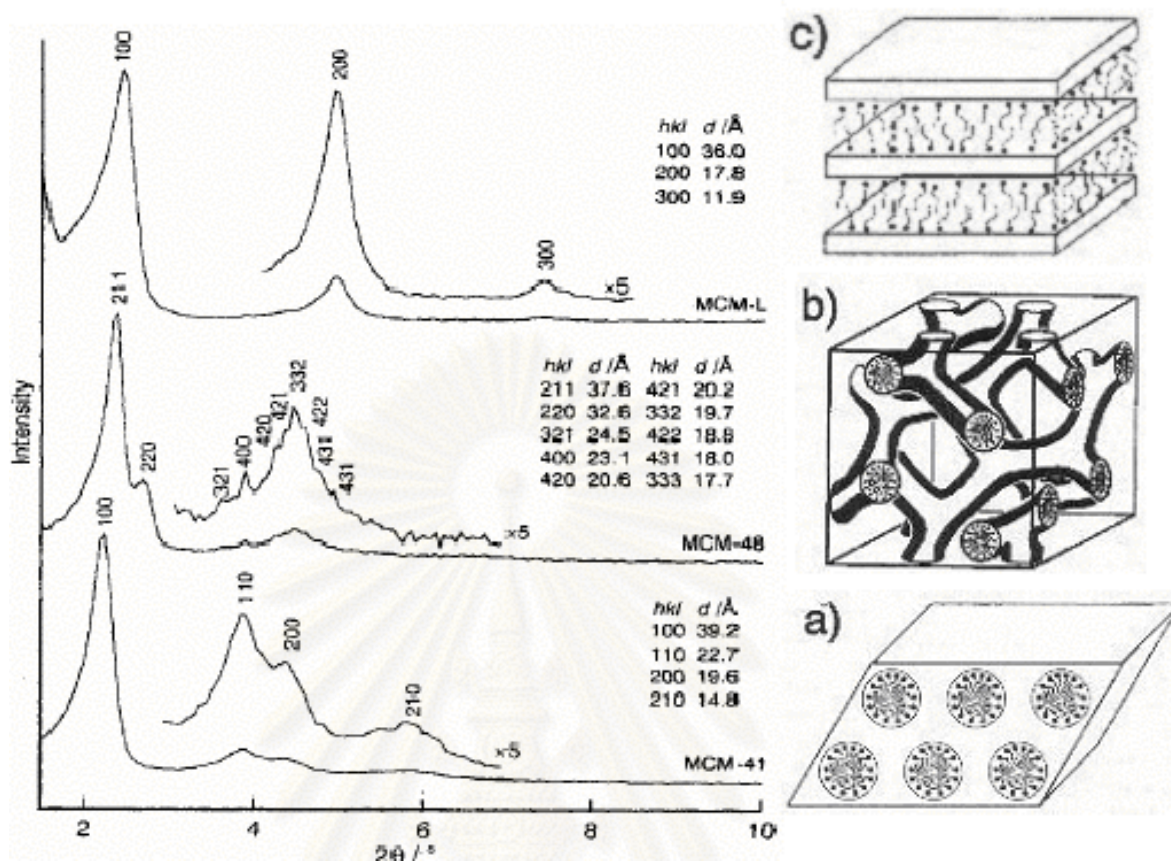
Figure 2.1 XRD patterns of M41S materials: a) hexagonal MCM-41, b) cubic

MCM-48, c) lamellar MCM-50.[65]

MCM-41, one member of this family, possesses highly regular arrays of uniform channels whose pore dimensions can be changed in the range from 15 to 100 Å by using different templates, the addition of auxiliary organic compounds, or the preparation conditions. The pores of this material are considered remarkably larger than those present in zeolites. This discovery, thus offers new opportunities for applications in catalysis, chemical separation, adsorption media, advanced composite materials, and other relevant areas. MCM-41 has been investigated extensively because the other members in this family are either thermally unstable as MCM-50 or obtained as MCM-48.[3-4]

2.5   Mechanism for the Formation of MCM-41

2.5.1   Liquid Crystal Templating (LCT) Mechanism

A liquid crystal templating (LCT) mechanism[4] as shown in Figure 2.2. was proposed by Beck *et al.*[4] to explain formation of MCM-41 since his first discovery.

In a LCT mechanism process, it was the liquid crystalline surfactant micelles that acted as the templates rather than the individual single molecules or ions. Two possible mechanistic pathways were included in this type of mechanism. The first pathway was that the liquid-crystal micelles were formed prior to the addition of silicate species. The second pathway was that the silicate species added to the reactant mixture had influence on the formation of the isotropic rod-like micelles to the desired liquid crystal phase, i.e., hexagonal mesostructure. Therefore, the mesostructure formed was structurally and morphologically directed by the pre-existed liquid crystal micelles and/or the isolated rod micelles, or even a single micelle. These randomly ordered composite species spontaneously packed into a high ordered mesoporous phase with an energetically favorable hexagonal arrangement, accompanied by silicate condensation. With the increase in heating time, the inorganic species continued to condense.
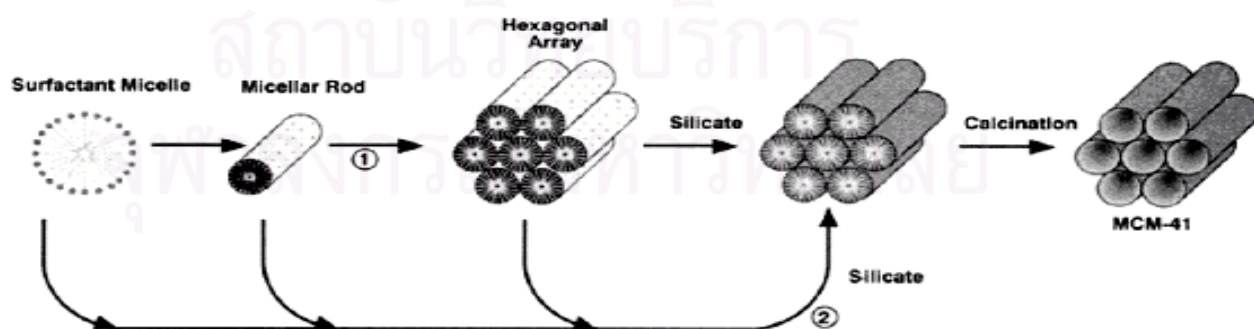
Figure 2.2 Possible mechanistic pathways for the formation of MCM-41: 1) liquid crystal initiated and 2) silicate anion initiated.

2.5.2 Silicate-Encapsulated Rods

Davis *et al.*[66], by carrying out in situ ^{14}N NMR spectroscopy, concluded that the liquid crystalline phase was not present in the synthesis medium during the formation of MCM-41, and consequently, this phase could not be the structure-directing agent for the synthesis of the mesoporous material in agreement with the already proposed mechanism through 2 routes. Thus, the randomly ordered rod-like organic micelles interacted with silicate species to yield two or three monolayers of silica around the external surface of the micelles. Subsequently, the long-range order MCM-41 was spontaneously formed. The mechanism was illustrated in Figure 2.3.

If one tries to remove the surfactant by calcination, just at the point when the long-range order is achieved, i.e., short synthesis times, the material is not stable as a consequence of the still large number of non-condensed silicate species. Longer synthesis time and/or higher temperature increase the amount of condensated silanols giving a resulted stable materials.
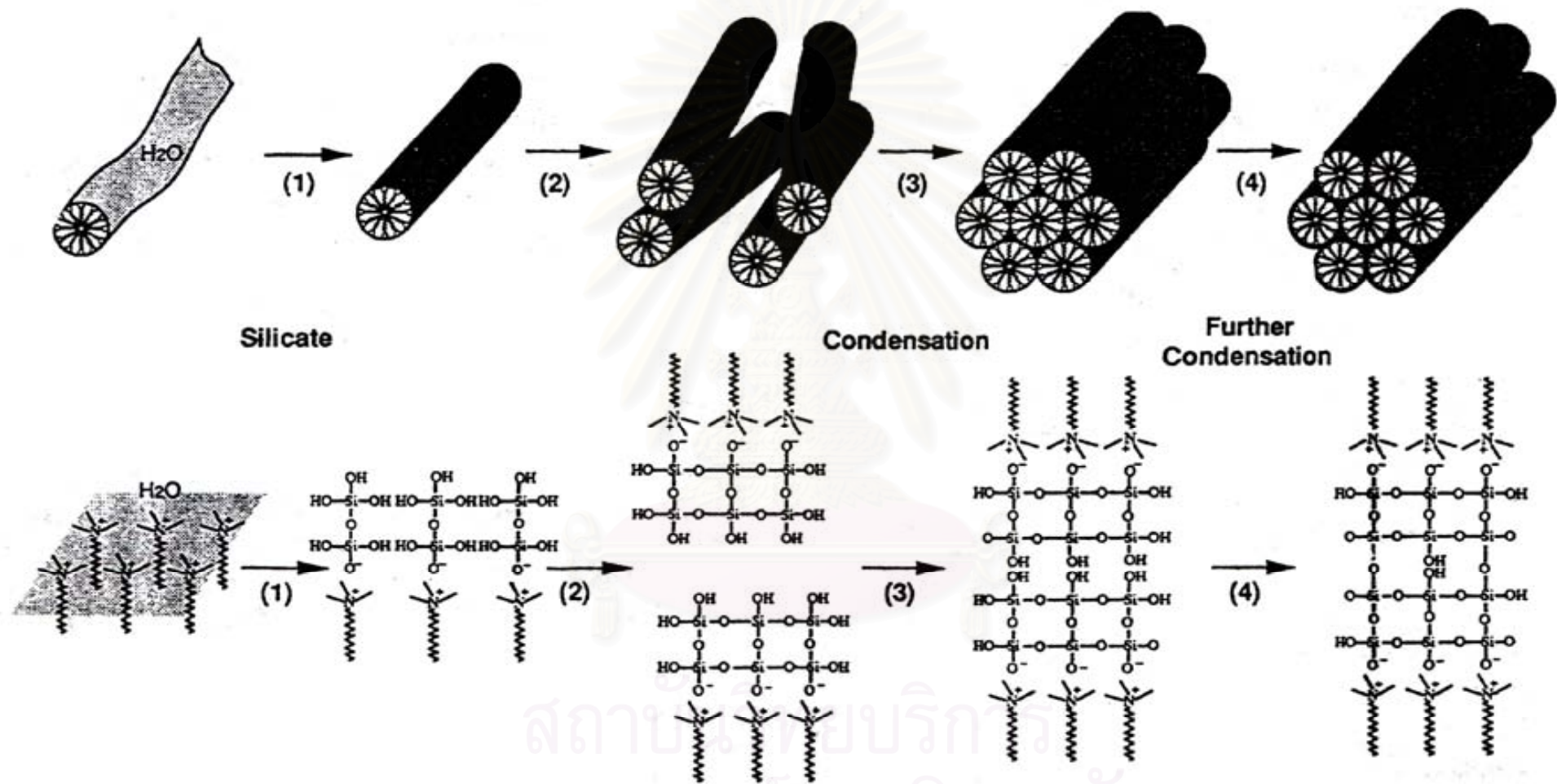
Figure 2.3 Assembly of silicate-encapsulated rods produced by Davis *et al.*[66]

2.5.3   Silicatropic Liquid Crystals

Stucky *et al.*[67] developed a model that made use of the cooperative organization of inorganic and organic molecular species into three dimensionally structured arrays. The global process was divided into three reaction steps as shown in Figure 2.4.

The first step, driven by electrostatic interactions, was the formation of ion pairs between polydentate and polycharged inorganics species on the one hand and the surfactant on the other. The ion pairs then self-organize into a mesostructure, having most often a liquid-crystal structure, i.e., hexagonal, lamellar, or cubic. The structure of the mesostructure depended on the composition of the mixture, the pH, and the temperature. The last step was the condensation of the inorganic species leading to a rigid structure.
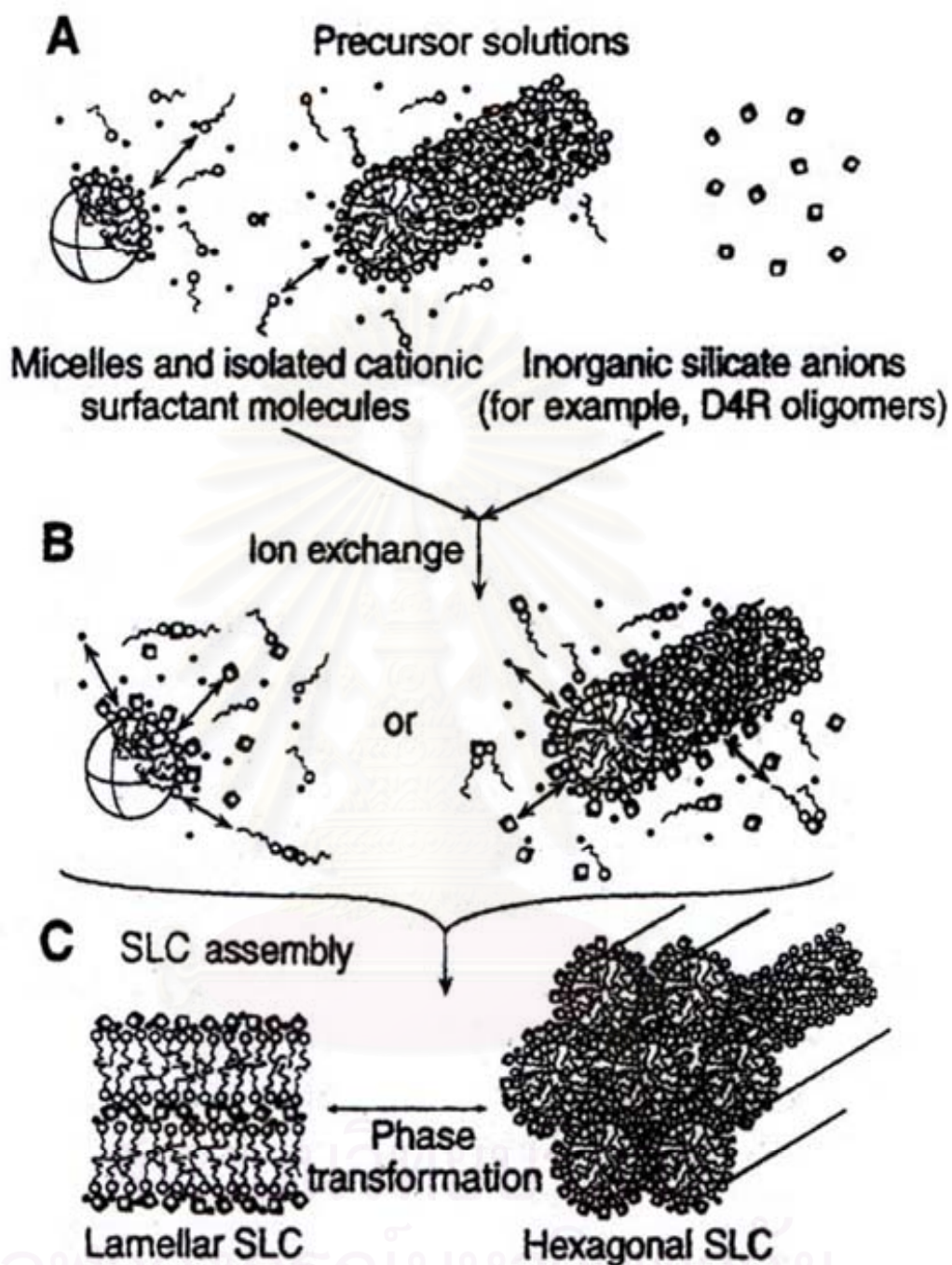
Figure 2.4 Formation of a silicatropic liquid crystal phase.

2.5.4   Generalized Liquid Crystal Templating Mechanism

Four pathways[68-70] were presented in the synthesis of mesostructured surfactant-inorganic biphasic arrays as shown in Figure 2.5. In the two direct pathways, cationic surfactants S^+ were used for matching with negatively charged inorganic species I^- to form S^+I^- mesostructure and anionic surfactants (S^-) were employed for cationic inorganic species (I^+) to form S^-I^+ mesostructure. Organic-inorganic combinations with identically charged partners are possible. In the two mediated pathways, the formation of the mesostructure was mediated by the countercharged ions which must be present in stoichiometric amounts i.e. $S^+X^-I^+$ (X^- was a counter anion), and $S^-M^+I^-$ (M^+ was a metal cation). In cases where the degree of condensation of the oligomeric ions which form the walls is low, the removal of the template leads to the collapse of the ordered mesostructure. It would then be of both fundamental and practical interest to develop new synthetic routes which allow the template to be more easily removed.

Following this mechanism, the criteria of charge density matching at the surfactant inorganic interfaces governs the assembly process, and consequently, the final type of structure generated. From this, it can be seen how the principle methodology can be extrapolated to prepare mesostructures with different metal oxides as far as there is an electrostatic complementarily among the inorganic ions in solution, the charged surfactant head groups, and, when these charges both have the same sign, inorganic counter ions.[68-69]

	Surfactant		Inorganic solution species		
Direct pathways	1) Cationic	+	Anionic	S^+I^-	Antimony oxide Tungsten oxide (pH<7) M41S, MCM-48
	2) Anionic	+	Cationic	S^-I^+	Iron oxide Lead oxide Aluminum oxide
Mediated pathways	3) Cationic	+	Cationic	$S^+X^-I^+$	Silica (pH<2) Zinc phosphate (pH<3)
	4) Anionic	+	Anionic	$S^-M^+I^-$	Zinc oxide (pH>12.5)
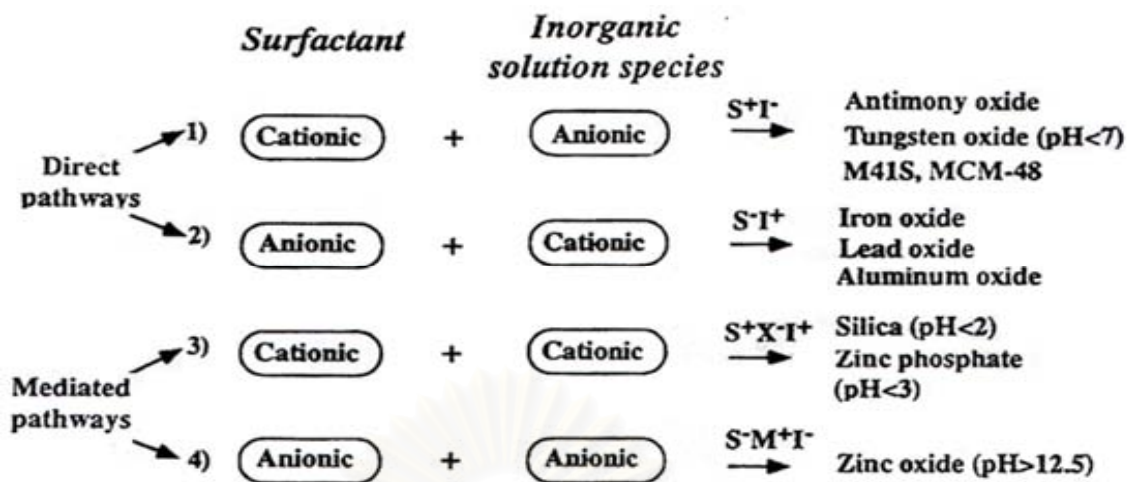
Figure 2.5 A general scheme for the self-assembly reaction of different surfactant and inorganic species.

It is worth discussing here a new procedure for synthesizing silica and silica-alumina MCM-41 materials, which involves highly acidic synthesis conditions instead of the basic or mildly acid conditions commonly used. Maintaining consistencies with the charge density matching principle, it has been proposed[68] that the templating mechanism during the acid synthesis of MCM-41 follows a path in which $S^+X^-I^+$ mesostructures are involved, where I^+ is a positively charged silica precursor, S^+ is the alkyltrimethylammonium cation, and X^- is the compensating anion of the surfactant. The fact that in the samples prepared under a highly acidic synthesis medium, the template can be removed from the core of the MCM-41 by a simple washing with water at room temperature. The removal of the liquid crystal template is accompanied by a decrease in the structural order of the MCM-41 and by a polymerization of the silica layer. The easy removal of the template indicate that the interaction between the silica layer and the surfactant should be very weak and more probably associated with the Van der Waals interaction between oligomers of silicic acid-like species and the anions that compensate the surfactant cation.

2.6   **Synthesis of Ti-Containing MCM-41**

In 1994, Corma *et al.*,[10] have reported the firstly successful direct synthesis of a mesoporous Ti-MCM-41 material with the same regular hexagonal shape of the pore openings (35 Å) as in the silica-based MCM-41 material. In the synthesis of Ti-MCM-41, *n*-hexadecyltrimethylammonium bromide (CTMABr) was used as template, titanium isoproxide as a titanium source, trimethylammonium hydroxide as base. The typical silica sources were varied such as fumed silica, teramethylammonium silicate and sodium silicate. It was found that the optimal OH/SiO$_2$ ratio for the preparation of good crystalline materials was 0.26, providing that the other compositional parameters remain unchanged.

After the successful synthesis of Ti-MCM-41, several techniques have been developed to incorporate Ti into silica wall of MCM-41 by different routes. The direct synthesis[71-74] with different recipes in hydrothermal synthesis is the most general method. Post-synthesis method[75-77] is the alternative way for incorporating Ti into the silica framework of MCM-41.

2.6.1   **Direct Synthesis**

Ti-MCM-41 was prepared Klinowski *et al.*[72-73] using Cab-O-sil fused silica and sodium silicate as the source of silicate and titanium (IV) ethoxide as a source of titanium. The 25%wt CTMACl/OH template solution was prepared by batch exchange of 25%wt CTMACl using the IRA-420 (OH) ion-exchange resin. The solid product was characterized by various techniques to interpret the isomorphous substitution of Ti on Si surface. In 1997, Tatsumi *et al.*[18] investigated the optimal conditions for synthesis of Si-MCM-41 and Ti-MCM-41 in detail by the alkali-free method. For the preparation of Ti-MCM-41, tetraethyl orthosilicate (TEOS), which was free from Na and Al, was used as a silicon source and *n*-dodecyltrimethylammonium ion (DTMA$^+$) was used as a template. They have intensively investigated the optimal

conditions for the synthesis of Ti-MCM-41 such as silicon source, surfactant/Si ratio, counter anion effect, pH, surfactant concentration, surfactant chain length, the gel preparation method, etc.

Pinnavaia et $al.$[74] compared both synthesized products prepared by colloidal silica or TEOS as a source of silica, tetraisopropryl orthotitanate (TIPOT) as a titanium source, $CTMA^+$ as surfactant. For S^+I^- assembly, the molar gel composition of the reactant mixture was $SiO_2 : TiO_2 : CTMA^+ : TMAOH : H_2O = 1 : 0.020 : 0.50 : 1.0 : 160$. Before the static crystallization at 100ºC, the pH of the gel was adjusted to 12 with TMAOH. For $S^+X^-I^+$, strongly acidic condition (pH = 1.5) was utilized in order to generate and assemble positively charged silicon from TEOS. The use of excess Ti for this preparation was necessitated by the high solubility. The composition of the reactant mixture was $SiO_2 : TiO_2 : CTMA^+ : HCl : H_2O = 1 : 0.1 : 0.20 : 1.0 : 160$. The resulted gel showed the S^+I^- pathways, allow for the essentially complete incorporation of the Ti in the product, whereas the $S^+X^-I^+$ pathway required a 4-fold excess of Ti in the reactant mixture in order to achieve a similar Ti loading to S^+I^- pathway. In addition, the yields of crystalline product for the S^+I^- pathways were more than 85%, whereas that for the $S^+X^-I^+$ pathway was only about 50%. But, the XRD patterns of calcined Ti-MCM-41 for $S^+X^-I^+$ pathway showed hexagonal structure with greater long-range than for S^+I^- pathway.

2.6.2   Post-Synthesis

The post-synthesis of Ti-containing MCM-41 by atom-planting was reported by Iwamoto *et al.*[75] Si-MCM-41 was treated with $TiCl_4$ vapor in a continuous flow system at atmospheric pressure. The MCM-41 powder was placed in a quartz reactor and dehydrated under a helium stream at 500ºC for 2 hours, The reactor was cooled down and reheated for desired temperature, with the helium stream containing $TiCl_4$ vapor flowed through the MCM-41 bed for 5-6 mins, the $TiCl_4$ reacted with the silanol group of the silica surface. Then, the unreacted $TiCl_4$ was removed by purging with the pure helium at the same temperature for 1 hour. By the different method, Ahn[76] and Gao *et al.*[77] reported another post-synthesis method for Ti-MCM-41. A calcined MCM-41 was washed at 40ºC for 2 h with TBOT in dry ethanol solution. To eliminate the excess TBOT, the solid was washed with dry ethanol and filtered 3 times, and then recalcined at 550ºC for 4 hours. This post-synthetically prepared Ti-MCM-41 was catallytically active for the selective oxidation of 2,6-di-*tert*-butylphenol with H_2O_2[61] and good photocatalytic activity for oxidizing phenol to carbon dioxide and water.[62]

2.7   Effect of Parameters on MCM-41 Synthesis

2.7.1   Surfactant Template

Beck *et al.*[78] studied the boundaries of reaction conditions and surfactant chain length for formation of microporous zeolites or mesoporous M41S material. It was found that zeolites preferred high temperature for crystallization, whereas the mesoporous material preferred lower temperature for crystallization. As shown in Figure 2.6. At the lowest synthesis temperature 100ºC, the C_6 and the C_8 surfactant preparation produce amorphous material with no evidence of the formation of either zeolites or microporous material. As the surfactant chain length increased,

CM-41 materials were formed and no zeolites were observed. Well-defined MCM-41 exhibiting three or four XRD peaks, which could be indexed on a hexagonal lattices, was synthesized from C_{12}, C_{14}, and C_{16} surfactant containing mixtures. At 150ºC, both the C_6 and the C_8 surfactant preparations produced well-crystallized zeolitic ZSM-5 type products. Ill-defined MCM-41 having one or two low-angle XRD peaks were produced from both the C_{10} and C_{12} preparations while the C_{14} and C_{16} surfactant derived products were well crystallized MCM-41. At 200ºC, the formation of zeolites, ZSM-5 for the C_6 surfactant and mixtures of ZSM-5, ZSM-48, dense phase for the C_8-C_{14} surfactants, and amorphous for the C_{16} surfactant. MCM-41 products are not observed suggesting that even for these longer alkyl chain length surfactant systems, micellar formation is not favorable or has been disrupted.
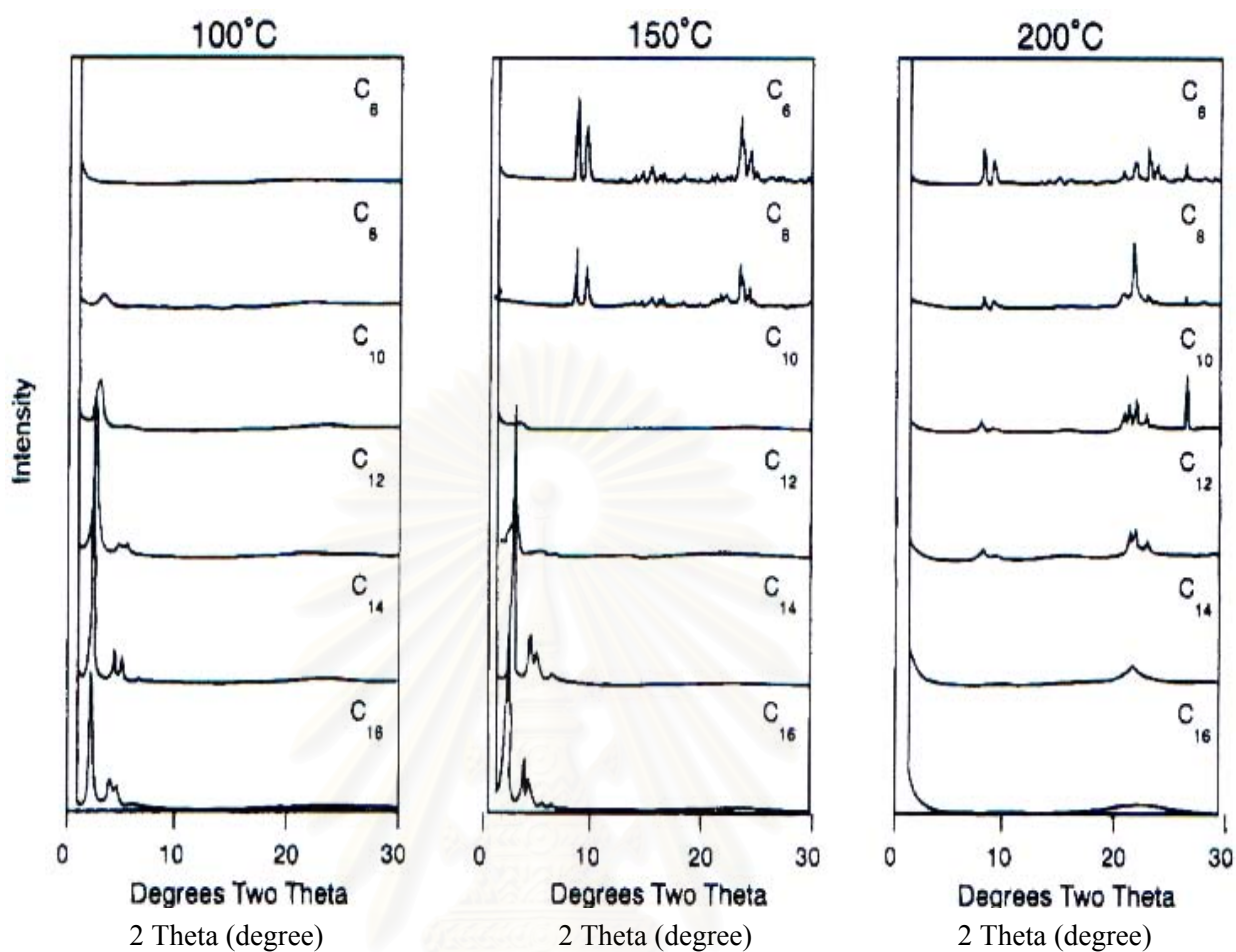
Figure 2.6 XRD patterns of calcined products formed using surfactant having alkyl chain lengths of n = 6, 8, 10, 12, 14, and 16 at 100, 150, and 200ºC.

Grün *et al.*[79] reported the preparation of MCM-41 using different *n*-alkyltrimethylammonium bromides (n = C_{12}-C_{20}) and the results are shown in Table 2.2. The pore diameter became larger with increasing carbon chain length of the alkyl group in the template. The specific surface area gradually decreased from 1450 m^2/g (C_{12}) to 980 m^2/g (C_{20}) while the values of the specific pore volume increased from 0.63 ml/g (C_{12}) up to 1.2 ml/g (C_{20}) with increasing carbon chain length of the alkyl group in the template. Thus the pore size and the pore volume can be controlled by varying the chain length in template.

Table 2.2 Properties of MCM-41 samples prepared by different *n*-alkyltrimethyl-ammonium bromides as temple

Template	BET surface area (m^2/g)	Pore volume (ml/g)	Pore diameter (Å)
$C_{12}TMABr$	1450	0.63	25
$C_{14}TMABr$	1120	0.74	29
$C_{16}TMABr$	1070	0.85	33
$C_{18}TMABr$	1050	1.09	38
$C_{20}TMABr$	980	1.20	Very broad

2.7.2 Crystallization Time

Tatsumi *et al.*[18] found that in the preparation of Si-MCM-41, performed by the hydrothermal crystallization at 100ºC during 10 days, the mesostructure was formed even before the hydrothermal crystallization. The XRD peak width became narrower and the regularity of the products increased with the synthesis times. After 10 days the pattern of typical hexagonal structure with a strong peak and three characteristic peak in the *2θ* range of 2-7º became prominent.

Corma *et al.*[80] reported the method for Si-MCM-41 preparation with different pore diameters from the gel with molar composition of SiO_2 : CTMABr : M_2O : H_2O = 1 : 0.06-0.15 : 0.14 : 0.26, where M represented cations such as tetramethylammonium (TMA^+), tetraethylammonium (TEA^+), or Na^+ as hydroxides. The gel reactant mixture was sealed in Teflon-lined stainless steel autoclaves and heated at 150ºC under static condition, allowing the crystallization time to be varied between 1 and 10 days.

It was shown in Figure 2.7 that a typical MCM-41 material with d_{100} = 42.5 Å was formed in the presence of TMA^+ when the crystallization time was 24 h. With longer crystallization time under these conditions, the pore diameter of the

sample was increased, until reaching a maximum of 70 Å after 10 days. If crystallization is prolonged beyond that a loss of crystallinity accompanied by a decrease in the pore volume of the mesoporous material was observed.
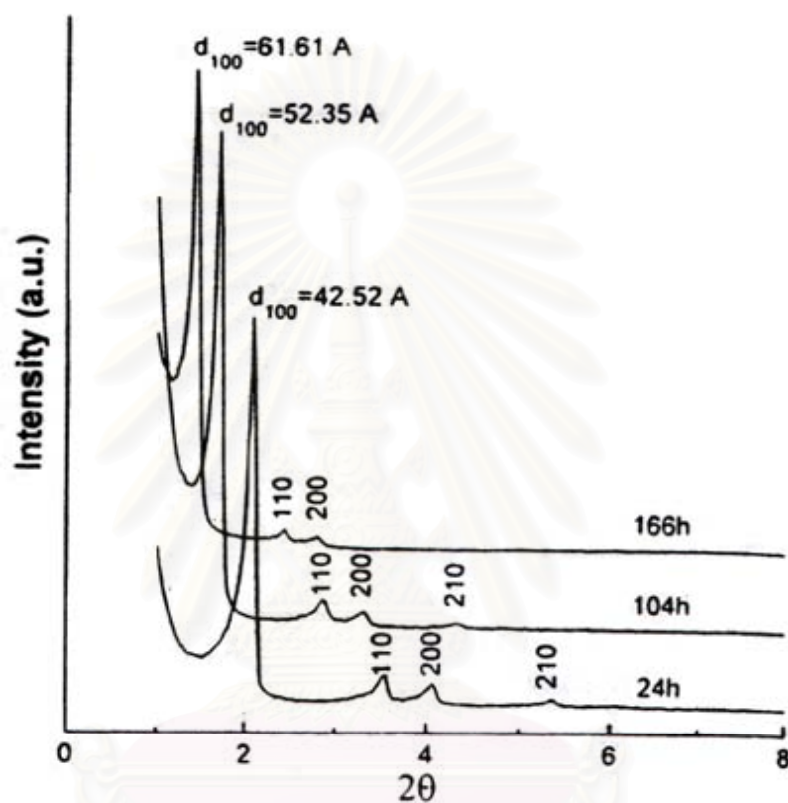
Figure 2.7 XRD of MCM-41 samples with different pore diameter.

In Figure 2.8 a correlation between the unit cell parameter (a_0) of the resulted MCM-41 sample and the crystallization time is given. Variables such as temperature, $CTMA/SiO_2$ ratio, and nature of the cation (TMA^+, TEA^+, Na^+) were found to be important for controlling the process. The swelling mechanism observed might be related to the replacement of some $CTMA^+$ by tetraalkylammonium cations in the interphase formed between the liquid crystal and the silica surfaces.
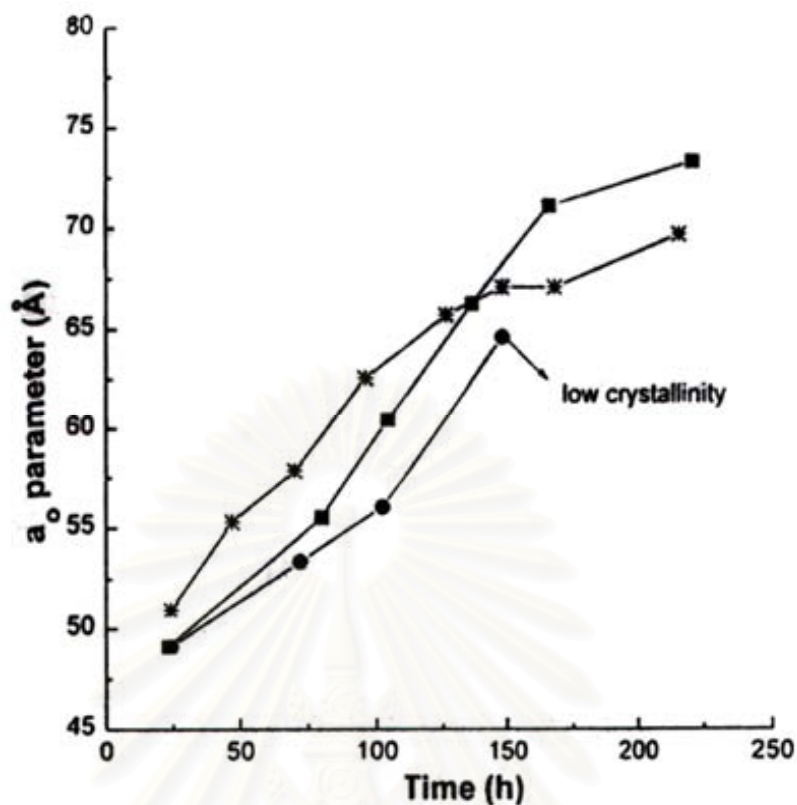
Figure 2.8 Correlation between the unit cell parameter (a_0) of MCM-41 and the crystallization time.

2.7.3 Synthesis Temperature

Klinowski *et al.*[81] showed that with increasing synthesis temperature or crystallization time, the d_{100} spacing, the hexagonal lattice parameter *(a)* in calcined Si-MCM-41 was increased from the unit cell expansion as shown in Table 2.3. The pore-wall thickness was increased as the reaction time increased, The silicate needed for continued wall building must clearly be transported into the channel from the mother liquor. It was likely that the silicate anions and the associated water molecules occupied the free space at the silicate/surfactant interface. The channel diameter (D_{BJH}) of calcined MCM-41 made at 165ºC increased from 26.1 to 36.5 Å as the reaction time increased from 1 to 48 hours, and the final diameter was close to that of the CTMABr micelle (39.7 Å).

Table 2.3 Unit cell parameter ($a = 2d_{100}/\sqrt{3}$), d_{100} spacing, pore diameter D_{BJH}, wall

thickness W, and surface area A_{BJH} of calcined Si-MCM-41[81]

Condition of synthesis	d_{100} (Å)*	a_O (Å)*	D_{BJH} (Å)+	W (Å)+	A_{BJH} (cm^3/g)+
70°C for 48 h	35.1	40.5	27.1	13.4	1380
158°C for 48 h	47.8	55.2	32.4	22.8	1107
165°C for 48 h	54.8	63.3	36.5	26.8	763
165°C for 16 h	45.4	52.4	32.5	19.9	1222
165°C for 1 h	36.7	42.4	26.1	15.3	1462
* calculated from XRD + calculated from sorption study Wall thickness was calculated from W = a_0 - D_{BJH}					

The channel diameter was controlled by the diameter of the surfactant micelles. It was unlikely that the channel enlargement is due to the effect of temperature on the micelle diameter. Since the contraction of the lattice upon calcination was not accompanied by the thinning of the channel walls, it was the channel diameter to be decreased. At very long reaction times, more surfactant decomposed forming neutral molecules which could not be accommodated within the micelle and must escape into the mother liquor.

2.7.4 Surfactant/Si Ratio

Vartuli *et al.*[82] proposed that surfactant/Si molar ratio was a critical variable in the formation of liquid-crystal templated M41S material. Tatsumi *et al.*[18,83-84,] showed when surfactant concentration was increased, the structure changed from hexagonal into cubic, and finally into lamellar. The effects of counter anions of DTMA$^+$ for the synthesis of Ti-MCM-41 are shown in Table 2.4. It was found that the chloride-containing system favored the hexagonal structure in a wider surfactant/Si ratio than the bromide-containing system for DTMA as surfactant while the hexagonal phase was favored over a wider concentration range of CTMABr than CTMACl.

Table 2.4 Effect of anions and surfactant/Si ratio on the structure of Ti-MCM-41.

Surfactant/Si ratio	Anion	
	Cl$^-$	Br$^-$
0.45	hexagonal	Ill-defined mesoporous
0.60	hexagonal	Hexagonal
0.75	hexagonal	Ill-defined mesoporous
0.90	Ill-defined mesoporous	Non-crystalline
Gel composition=TEOS : 0.01TBOT : DTMAX : 0.5TMAOH : 100H$_2$O; X=Cl or Br		

2.7.5 Influence of pH

Stucky *et al.*[85] reported that the structure of the Si-M41S products was affected by the pH and the polymerization degree of the silica source; the lamellar phase was favored at high pH (11.5-13) and for a low degree of polymerization of a silica source i.e.; a monomeric sodium silicate with large amount of Na. The hexagonal phase was obtained at low pH (>9.7 but <11.5) and for highly polymerized silica source.

Tatsumi *et al.*[18] investigated the effect of amount of TMAOH on the structure of Ti-MCM-41 produced from the gel with the composition of TEOS : TBOT : DTMABr : TMAOH : H_2O = 1 : 0.01 : 0.6 : 0.3 : 60. The pH measured just before the hydrothermal treatment and the results are summarized in Table 2.5.

Table 2.5 Effect of amount of TMAOH on products, structure and yield[18]

TMAOH/TEOS	pH	Yield (%)	Structure
0	-	>90	Amorphous
0.15	10.4	>90	Ill-defined mesostructure
0.30	11.3	>90	Hexagonal
0.45	11.5	38	Hexagonal
0.60	12.1	0	Clear solution

Although TEOS was monomeric silicate as sodium silicate, no lamellar phase was produced at all the pH range. The optimal pH for the hexagonal phase was found to be in the range of 11-12. If the pH is too low, it resulted in the formation of amorphous materials. At the higher pH (11.5-12), highly crystalline hexagonal phase was obtained, although the yield was relatively low. No solid product was obtained at pH higher than 12.

2.7.6 Influence of Surfactant Concentration

Influence of surfactant concentration was reported,[83-84] Ti-MCM-41 samples were obtained from the gel with H_2O/surfactant molar ratios of 100 (14.6%wt), 150 (10.2%wt), 200 (7.9%wt). The aqueous DTMACl does not form micelle in such low concentrations. And the same was true for CTMACl and CTMABr at typical synthesis temperature, in the absence of silicates, the hexagonal phase was formed at surfactant concentrations from 25 to 70%wt. Although the

hexagonal structure was obtained in a wide range of surfactant concentrations, the product synthesized from the more concentrated surfactant solution had a higher regularity. The structure was transformed from hexagonal to cubic with increasing concentration of the surfactant as shown in Table 2.6.

Table 2.6 Effect of concentration of surfactant and silica source on the structure of product.

Silica source	Si/Ti	H_2O/CTMA	Structure
TEOS	0	69.8	Hexagonal
TEOS	0	46.5	Cubic
TEOS	100	46.5	Cubic
TEOS	50	46.5	Ill-defined mesostructure
Water glass	0	46.5	Hexagonal

The structure of M41S was affected not only by surfactant/Si and surfactant concentration but also by the silica source and the Si/Ti ratio. The increase in the Ti content to Si/Ti = 50 resulted in the formation of an ill-defined mesoporous materials, which showed only one strong intensity peak at *ca*. $2\theta = 2°$.

2.7.7 Influence of Silica Source

Ti-MCM-41 was also synthesized from various silica source. The Ti-MCM-41 prepared from water glass or colloidal silica stabilized were lower in regularity and surface area than from TEOS. The UV-visible spectra of the Ti-MCM-41 from water glass and colloidal silica showed also the broad shoulder around 270 nm indicated to the extraframework titanium while Ti-MCM-41 from TEOS proved to be free of extraframework titanium.[18,83-84]

2.7.8 Influence of Secondary Crystallization

Increasing the synthesis time[19,23] allows more extensive diffusion of additional silicate units and surfactant molecule into the growing surfactant/silica aggregate; additional silicate condensation while additional surfactant molecules increased the density of the surfactant phase which translates to larger lattice parameter and pore size. Two-step synthesis method was introduced by Mokaya.[13] The MCM-41 was utilized as "silica source" and "seeds" for secondary synthesis. Apart from thicker pore walls, another critical factor in increasing the stability of MCM-41 was greater silica condensation in the pore walls. It was proposed that during crystallization additional silicate units access to the assembling surfactant molecules along the stacking axis. For secondary synthesis, silicate units might also enter the pores of the "seed" primary MCM-41 crystallites, thereby increasing both the wall thickness and the proportion of Q^4 silica units via further condensation in a process similar to silylation. Silicate units also interact with the additional surfactant molecules on the outer surface of the "seed" crystals forming new surfactant/silica aggregates which extend growth in the *ab* plane. The new surfactant/silica aggregates might also act as linkages between primary MCM-41 crystallites, thereby forming larger crystallites. Furthermore, while it was unlikely that the surfactant molecules will enter the pores of the "seed" crystals, they might however interact with silicate units at the pore entrance to extend growth (with the crystallites of the primary MCM-41 acting as "seed") and thus better long-range ordering and thicker pore walls but with no significant change in lattice parameter (a_0) since the wall thick thickness increases within the confines of the existing primary MCM-41 pores.

2.8   Characterization of Mesoporous Molecular Sieves

2.8.1   X-ray Diffraction (XRD)

When one suspects how successfully a mesoporous molecular sieve has been synthesized a well-established methodology must be followed to demonstrate that this is indeed the case. The procedure involves, first, the use of XRD which should be carried out at low angles (2θ) between $1°$ and $8°$ (Figure 2.9).
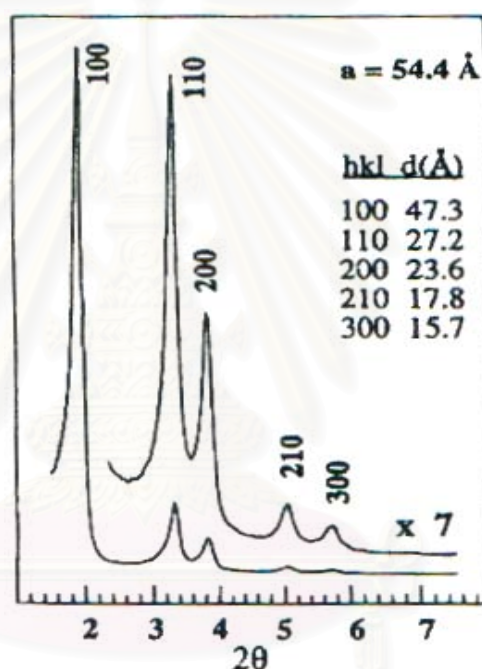
Figure 2.9 X-ray diffraction pattern of high-quality calcined MCM-41.

The reflections are due to the ordered hexagonal array of parallel silica tubes and can be indexed assuming a hexagonal unit cell as (100), (110), (200), (210) and (300). Since the materials are not crystalline at the atomic level, no reflections at higher angles are observed. The unit cell parameter for hexagonal MCM-41 was calculated from $a = 2d_{100}/\sqrt{3}$ and related to Bragg's law ($n\lambda = 2d\sin\theta$).[86]

2.8.2 Transmission Electron Microscopy (TEM)

Two models of pore structures of MCM-41 were proposed using XRD data and molecular dynamics simulation approach.[87] Both models are shown in Figure 2.10.
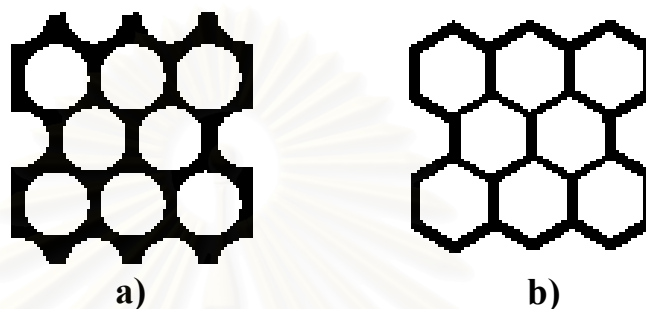
Figure 2.10 Pore structures of MCM-41: a) cylindrical pore and b) hexagonal pore.

Model A[87] represents a cylindrical pore structure with a lattice constant of 44.6 Å and a wall thickness of 8.4 Å based on the LCT mechanism. The simulation shows 10^3-10^4 atoms to model MCM-41 and analyzed models with different values of lattice constants and wall thickness. When comparing their simulation with experimental values, they found that the simulated XRD patterns of amorphous silica with wall thickness larger than 11 Å agreed well with the experiments. The percentage of silicon in the form of silanols obtained from the model (17-28%) also agreed fairly well with the observed diffraction pattern. It has to be pointed out, however, that an inverse relationship between the diameter of the micelle template and the wall thickness of the pores was found. Thus, decreasing the template diameter leads to thicker walls between hexagonal packed cylindrical pores. Model B represents a hexagonal pore structure with an interpore distance of 35 Å based on the lamellar to hexagonal phase transformation mechanism.[64] Both the cylindrical and hexagonal pore structures have been visualized by TEM.

2.8.3 Adsorption Study[60,64,86]

Adsorption of molecules has been widely used to map the pore size distribution of solid catalysts. In this sense the physisorption of gases such as N_2, O_2, and Ar have been used to characterize the porosity of M41S samples and more specifically MCM-41. When adsorption was carried out on a MCM-41 sample with 40 Å pore diameter, the isotherm for N_2 was type IV in the IUPAC classification, and no adsorption-desorption hysteresis was found at the boiling temperature of N_2 (-196°C) as shown in Figure 2.11. In the case of Ar and O_2 the isotherm were also of type IV with hysteresis loops. These results can be attributed to capillary condensation taking place within a narrow range of tubular pores with effective width of 33-43 Å confirming both the high degree of pore uniformity and the dimension of the pore determined by TEM. Further adsorption studies under different experimental conditions and on samples with different pore diameters showed that the presence and size of the hysteresis loop depended on the adsorbate, pore size, and temperature. In this respect, no nitrogen hysteresis loops were found for materials with pore sizes of 25-40 Å, but a nitrogen isotherm on a 45 Å material showed hysteresis. Finally, adsorption of cyclopentane at different temperatures showed that the presence and size of hysteresis depended on the temperature.[64]

a)

b)

c)
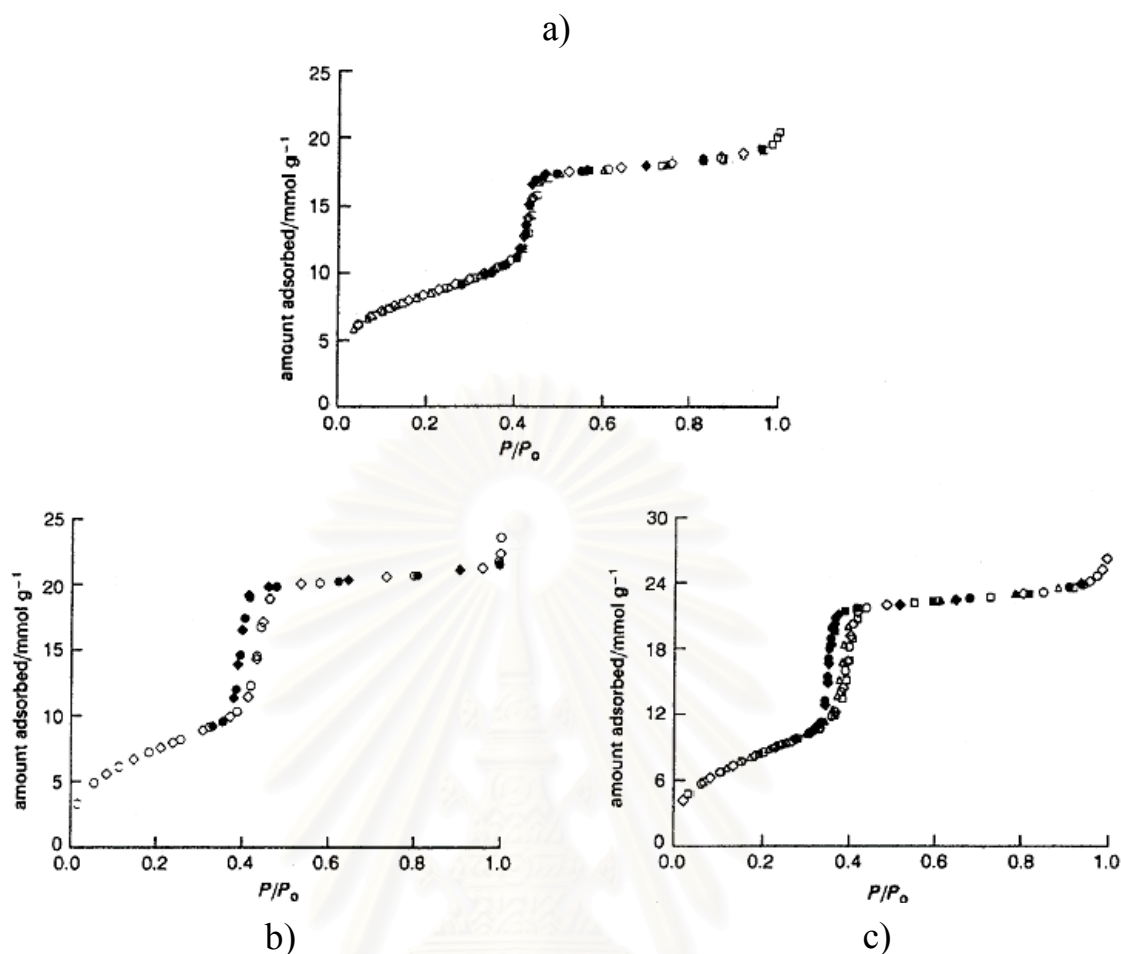
Figure 2.11 Adsorption isotherm of a) nitrogen, b) argon, and c) oxygen on MCM-41 at -196°C. Different symbols denote different runs; filled symbols denote desorption.

Owing to the success of N_2 and Ar adsorption in terms of the determination of the pore diameter, one can combine the XRD results together with the pore size determined from gas adsorption experiments to find the thickness of the wall. The wall thickness can be calculated by determining the difference between the lattice parameter ($a = 2d_{100}/\sqrt{3}$) determined by XRD and the pore size obtained by nitrogen adsorption analysis. The traditional method for analyzing pore-size distributions in the mesopore range is the Barrett-Joyner-Halenda (BJH) method. However, one should bear in mind that the values are only estimates, because so far no reliable

means for pore-size analysis exists. Moreover, the lattice parameters are often calculated from quite broad reflections and therefore do not correspond to an exact value. However, independent studies showed in case of the regular MCM-41 samples the wall thickness was approximately constant at about 10 Å.[64] The value can be changed, having as a consequence important implications on the stability of the sample.[70]

Adsorption studies, besides their convenience for measuring the textural properties of these materials, can also be used to study the interaction of molecules with the walls of the pores, a feature of particular importance from the point of view of the diffusion and catalytic properties of the material. In this sense, adsorption studies of polar and non-polar molecules can be quite useful for measuring the hydrophobic and hydrophilic properties of M41S mesoporous materials. When H_2O was adsorbed at 24°C on a MCM-41 sample, the adsorption isotherm obtained showed a fairly narrow hysteresis loop of type IV as shown in Figure 2.12, indicating relatively weak adsorbent-adsorbate interactions. From these results, one would conclude that the MCM-41 surface is quite hydrophobic, with an uptake of water similar to that given by hydroxylated silica and many carbons.[88] This conclusion is nevertheless surprising if one considers the high number of silanol groups present in these materials. However, the hydrophobic character of MCM-41 has been clearly demonstrated by carrying out the adsorption of cyclohexane in the presence of water, and benzene in the presence of H_2O. The results obtained show that while in a hydrophilic zeolite, such as faujasite, large amounts of benzene and H_2O are adsorbed, when the same adsorbates were used on a sample of siliceous MCM-41, much larger amounts of benzene than H_2O were adsorbed. This adsorption characteristic is of vital importance when reactants with different polarities, for instance H_2O or H_2O_2 and olefins, have to react and certainly it will control the rate of the diffusion-adsorption reaction in those cases.
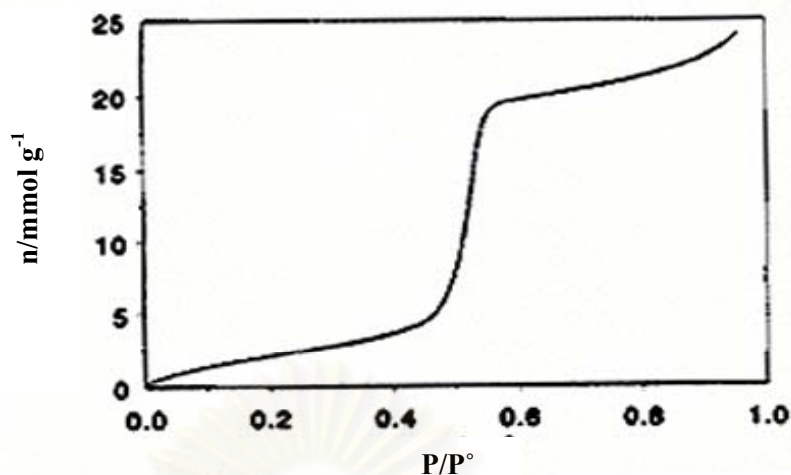
Figure 2.12 Water adsorption isotherm on MCM-41.

2.8.4 Fourier Transformed Infrared (FT-IR) Spectroscopy

In the case of the transition metal-substituted M41S samples, their principal interest resides in their potential use as oxidation catalysts, with this particularly true for the titanium-substituted MCM-41 material. In this case, the isomorphous substitution and, therefore, the incorporation of these elements in the framework is not easy to as certain, and hence, a combination of several techniques is required to provide the necessary information. In the case of Ti-substituted MCM-41, spectroscopic and catalytic techniques should be used to show the incorporation of Ti in the silica framework.[10,89]

Previous work on the characterization of Ti-zeolite can be used as a guide for characterizing the Ti-MCM-41 samples. Thus, an IR absorption band of calcined Ti-MCM-41 as (Figure 2.13) at 960 cm^{-1} attributed to Si-O-Ti stretching with Ti in tetrahedral coordination was used to identify the incorporation of Ti in zeolites and, similarly, has also been used to show the presence of Ti in the framework of Ti-MCM-41.[10,89]
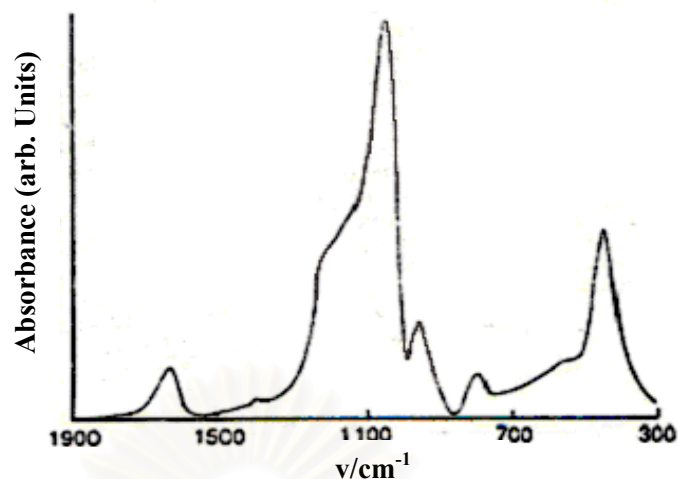
Figure 2.14 Infrared spectra of calcined Ti-MCM-41.

However, this has been questioned on the basis of more recent IR studies on as-synthesized and calcined Ti-zeolite, it was concluded that the band at 960 cm^{-1} can instead be due to the Si-O stretching vibration in the Si-OR group, R being H$^+$ in the calcined state and TEA$^+$ in the as made material. Thus, while all the properly prepared Ti-zeolites and Ti-MCM-41 show the presence of this band, the reverse is not neccesarily true.

2.8.5 Raman Spectroscopy and Diffuse Reflectance UV-Visible (DR-UV) Spectroscopy

Raman spectroscopy,[90] while having the limitation of its relatively high detection limit (0.5%wt), has the advantage that it can visualize if some or all of the Ti has or has not been incorporated and whether indeed some is segregated as TiO$_2$ anatase (140 cm^{-1}). On the other hand, UV-visible spectroscopy gives very valuable information on the coordination of the Ti. A sample containing only framework titanium should give an optical transition at 210 nm, which is assigned to a charge transfer (CT) in [TiO$_4$] and [O3Ti-OH] moieties. Isolated extraframework hexacoordinated Ti would give a CT at about 225 nm. Partially polymerized hexacoordinated Ti species, which contain Ti-O-Ti bonds and belong to a silicon rich

amorphous phase, would give a broad band at 270 nm. Finally, for TiO_2 in the form of anatase the transition occurs in the 330 nm region. UV-visible spectroscopy, which is a widely available technique, is a very useful tool for characterizing Ti-MCM-41 samples since, besides its low detection limit (0.03 %wt), it can give information on framework and extraframework Ti. The diffuse reflectance spectra in the UV-visible region of the calcined Ti-MCM-41 (Figure 2.14), does not show the 330 nm band associated to anatase, but a band at 210-230 nm associated to isolated Ti in tetrahedral (210 nm) and hexacoordination (230 nm).[10,91-92]

Figure 2.14 Diffuse reflectance-UV spectrum of calcined Ti-MCM-41.

Then it can be certainly concluded that in well-prepared Ti-MCM-41 samples, isolated Ti (IV) and Ti (VI) species are present, and therefore the incorporation of Ti to the framework of the walls occurs. This fact opened the
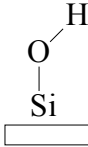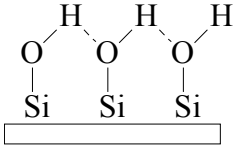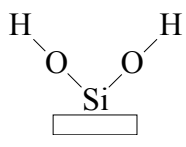
possibility of using these materials as catalysts for the selective oxidation of large molecules.

2.9   Comprehensive Study of MCM-41 Surface

Beck *et al.*[4] reported the Si-NMR of siliceous MCM-41, calcined and uncalcined MCM-41 suggested about $20 \pm 10\%$ and $40 \pm 20\%$ of the silicon atoms, respectively, were silanols (Q^3), similar to the results for amorphous silica.

Lu *et al.*[34-35,37] studied the nature of MCM-41 surface and found that the surface chemistry of MCM-41 was similar to that of typical silica surface. It was found that MCM-41 surface contained many types of SiOH groups, i.e., single, hydrogen-bonded, and geminal SiOH groups. These three observed types of SiOH groups with their characteristic IR sbsorption band and Si-NMR resonances illustrated in Table 2.7. The number of SiOH groups over MCM-41 surface was $2.5\text{-}3.0/nm^2$, whereas the amorphous silica was occupied with the member of $5\text{-}8/nm^2$. This highly condensed surface with less SiOH groups indicated that MCM-41 was better-ordered than amorphous silica. The value of the SiOH number has contributions in all of these three groups on both the external and internal surface.

Table 2.7 Representation of the three types of SiOH groups in MCM-41 and their characteristics

Silanol type	 **Single**	 **Hydrogen-Bonded**	 **Geminal**
IR adsorption band (cm^{-1})	3738	3200-3600	3738
NMR resonance (ppm)	-101	-101	-92

The formation of internal SiOH groups was thought to be related to the formation process of MCM-41 as illustrated in Figure 2.15. When one template molecule is removed, one isolated SiOH group was formed. With increasing temperature, dehydroxylation of hydrogen-boned and geminal SiOH groups took place to from siloxane bonds and simultaneously more free SiOH groups were generated. That was why the intensity of the adsorption band at 3738 cm^{-1} increased gradually at higher outgassing temperatures, and the adsorption band at 3222 cm^{-1} disappeared. Dehydroxylation of single SiOH groups was considered to be impossible since they was too far apart (0.5 nm) and such a process would necessarily involve the unfavorable formation of highly strained linked structures. Dehydroxylation from geminal groups was probably very difficult since siloxane (=Si=O) does not form readily. All SiOH groups the internal surface of MCM-41 should be isolated silanols, including single and hydrogen-bonded SiOH groups; and the geminal SiOH groups should be on the external surface and/or inside lattice defects.[34] Since the IR

absorption band at 3725 cm^{-1}, which was assigned to vibration of lattice SiOH groups, was not detected, the geminal groups were believed to be on the external surface. The number of geminal SiOH groups was directectly proportional to the external surface area of the MCM-41 samples.
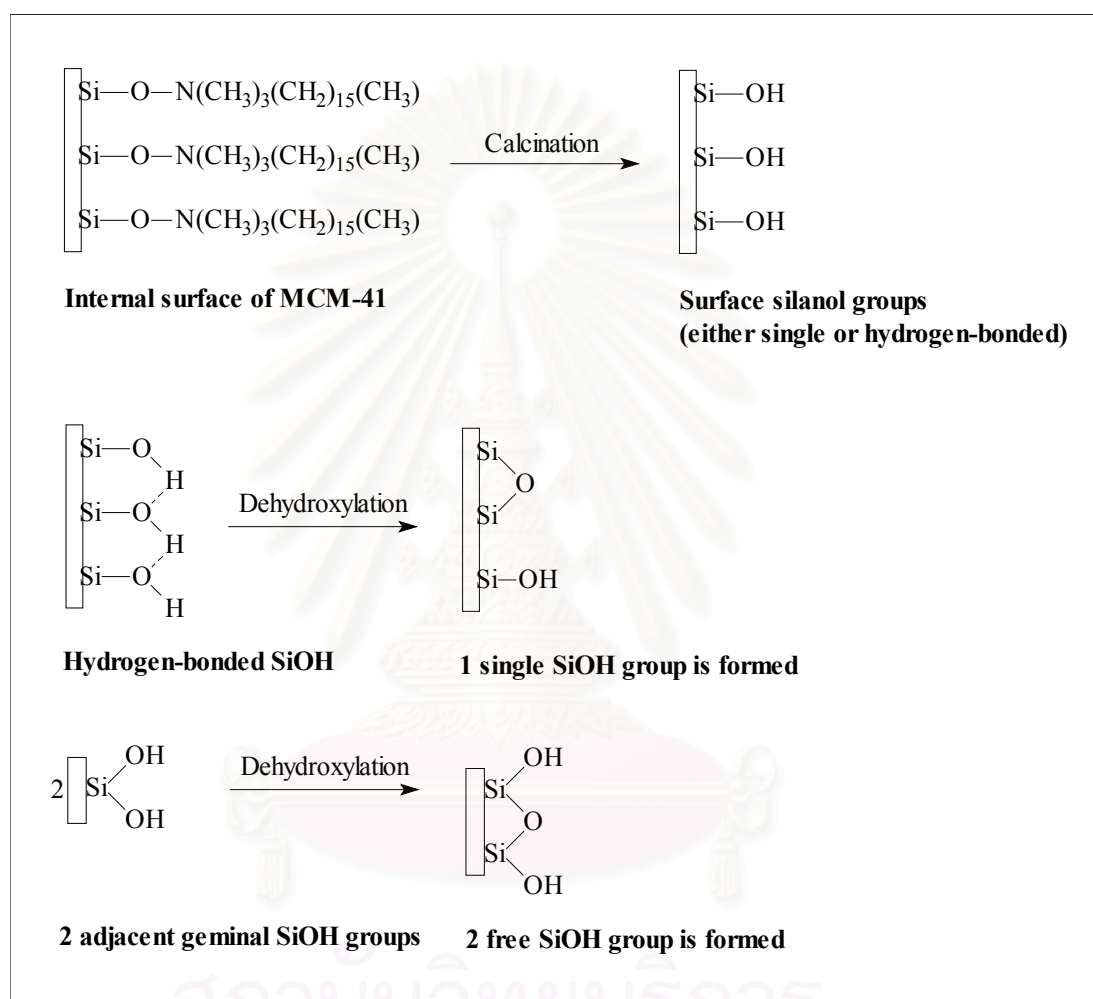
Figure 2.15 Schematic representation of formation and dehydroxylation processes of SiOH groups in MCM-41.

^{29}Si CP/MAS NMR spectra of MCM-41 with and without surface attachments of trimethylsilyl groups as shown in Figure 2.16, also with the chemical shift assignments for the observable resonances. Three resonances at -110, -101, and -92 ppm which were assigned to the silicon sites of Q^4 (a), Q^3 (b), and Q^2 (c), respectively can be observed on the calcined MCM-41. The Q^3 sites were associated

with the isolated SiOH groups (i.e., free and hydrogen-bonded), and the Q^2 sites corresponded to the geminal silanols.
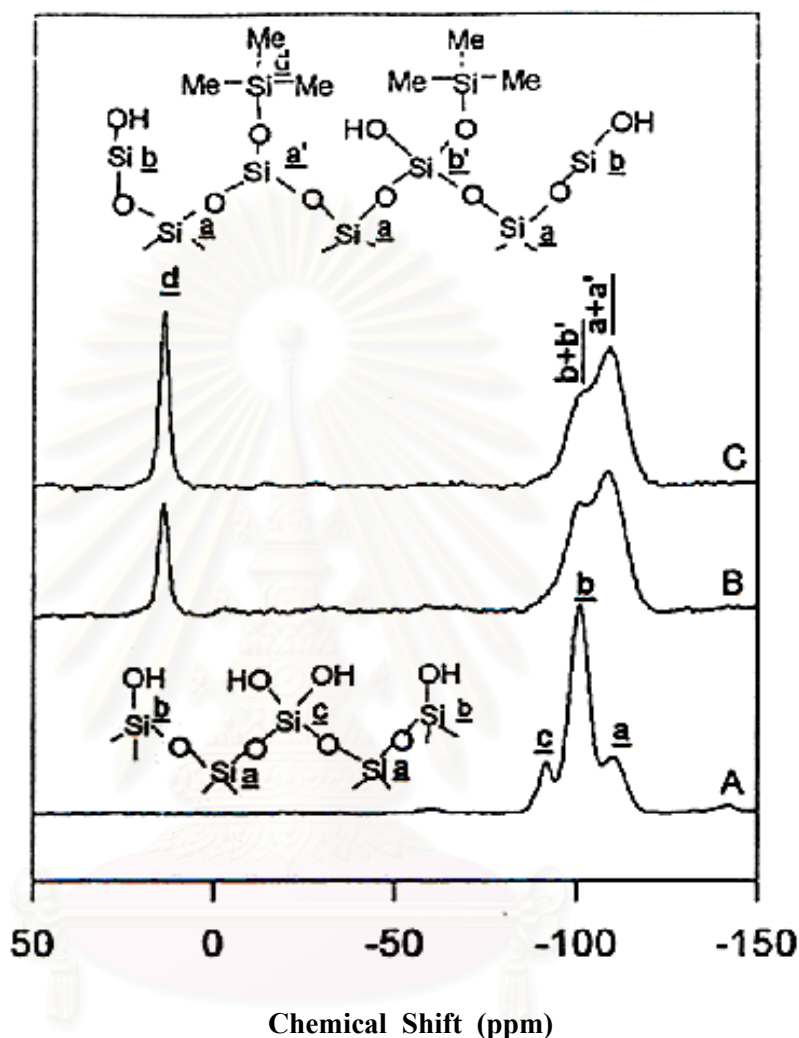
Figure 2.16 ^{29}Si CP/NMR spectra[37] for a) calcined MCM-41, b) partially silylated MCM-41 with coverage of 43%, and c) fully silylated MCM-41.

For the two silylated samples at different degree of silylation, a sharp peak at 14 ppm was ascribed to the attached on the sample before silylation. The intensity for the Q^4 silicons (a + a′) is drastically increased at the expense of Q^3 silicons because these silicon sites were redistributed during silylation. The Q^2 sites for both the partially and fully modified MCM-41 samples are actually featureless in the ^{29}Si

CP/MAS NMR spectra, demonstrating that geminal silanols were not hydrogen-bonded and were also the active sites for silylation as well. These NMR results revealed that both free and geminal SiOH groups were highly accessible to the silylating reagent.[35]

Surface Coverage of trimethylsilyl groups,[35,37] the degree of silylation, can be affected by parameters such as pre-outgassing temperature, silylation temperature, and concentration of a silylating reagent. A systematic study of the surface coverage as a function of pre-outgassing temperature was carried out. The surface coverage of trimethylsilyl groups was calculated based on the followed equation;

$$S = \frac{\triangle W\% \times N_A}{EMW \times S_{BET}} \times 10^{-20} \ (number/nm^2)$$

where S is the number of attached trimethylsilyl groups per nm^2, $\Delta W\%$ represents the weight gain after silylation (%), N_A is Avogadro's number, EMW is the effective molar weight of the attached trimethylsilyl groups (72 g/mol), and S_{BET} is the BET surface area (m^2/g), assuming that each trimethylsilyl group occupies a cylindrical volume of 0.43 nm and the external surface areas are negligible.

XRD patterns of silylated sample with trimethylsilyl reagent were highly resolved and the width of the main (100) peak was narrowed, reflecting a better order pore structure. This was probably related to more homogenous of pore structure brought about by the chemical attachments of a monolayer of trimethylsilyl groups over MCM-41 surfaces. In addition, unavailability of any residual water due to the complete removal of SiOH groups during silylation had a significant impact on the intensity of the main (100) peak.

From N_2 adsorption-desorption isotherms and pore size distributions before and after silylation, respectively, the relative pressure of after partially and fully silylated sample were lower than that before silylated sample, whereas a relatively broad pore size distribution was presented after silylation. The decrease of the pore diameter after

the partial silylation was 5 Å. For the fully silylated sample, the decrease in pore diameters was 6.5 Å, which was fairly consistent with the theoretical prediction. As well documented, the maximum lateral extension of a trimethylsilyl group was roughly 3.7 Å. Assuming a monolayer of trimethylsilyl groups was formed over MCM-41 surfaces after silylation, the reduction of pore diameter should, therefore be about 7.4 Å. The difference of 0.9 Å between the theoretical and BJH calculations was suggested to be associated with the heterogeneity of attached trimethylsilyl groups with a surface coverage of about 85%.

The silanol groups cannot be completely replaced by trimethylsilyl groups as the absorption band of hydrogen-boned at 3200-3600 cm^{-1} was still observable for the silylated MCM-41 sample. In addition, since the intensity of absorption for the silylated MCM-41 was similar to that of the sample before silylation, the hydrogen-boned SiOH groups was believed to be not accessible to the silylating reagent. Accordingly, the concentration of attached trimethylsilyl groups which was about 0.7/nm^2 roughly represented the concentration of single SiOH groups since geminal SiOH groups contributed a negligible portion to the concentration of free SiOH groups, and it was unlikely that reaction of two silylation reagent could react at a given geminal silanol site because of steric hindrance. The concentration of hydrogen-bonded SiOH groups was then be readily calculated to be 1.8–2.3/nm^2. The degree of silylation on MCM-41 surface was determined by the concentration of free (i.e., single and geminal) SiOH groups rather than steric considerations. The trimethylsilyl group estimably occupies a cylindrical volume of space was 0.43 nm^2. The theoretical maximum concentration of attached trimethylsilyl group was only 0.754 /nm^2 This was due neither to steric prohibition nor to the lack of SiOH groups (a significant portion of hydrogen-bonded SiOH groups were still on surface). When the surface hydrogen-boned SiOH groups were totally removed and/or transformed to free SiOH groups, the degree of silylation approached 100%.[34]

2.10   Catalytic Properties of Ti-MCM-41

After the several works on the selective oxidation of paraffins, olefins, and alcohols on Ti-silicalite and its extension to a large pore Ti-zeolite, the door was opened to introduce active Ti in the walls of MCM-41. The first report on the successful preparation of Ti-MCM-41 was published by Corma *et al.* in early 1994,[10-11] and the resulted material was able to selectively epoxidize olefins to epoxides using H_2O_2 as the oxidizing agent as shown in Table 2.8.

Table 2.8 Catalytic oxidation of 1-hexene with H_2O_2 on Ti-MCM-41[11]

Time (h)	Conversion of H_2O_2	Selectivity of H_2O_2	Product selectivity (% molar)		
			Epoxide	Glycol	Ether
0.50	3.9	60	100		
2.00	23.4	70	95.7	1.7	2.6
3.50	28.9	70	94.4	1.6	4.0
5.00	39.9	75	91.2	3.1	5.7

The activity of Ti-MCM-41 to epoxidize small linear olefins with H_2O_2 was lower than when using Ti-silicalite and Ti-zeolite catalysts, indicating that the intrinsic activity of Ti in the MCM-41 was lower than in ZSM-5 and zeolites, at least under the reaction conditions used. However the advantages of Ti-MCM-41 as epoxidation catalyst was in its ability to oxidize large molecules which cannot diffuse in the pores of microporous materials, as well as to use organic hydroperoxides as oxidants. For instance Ti-MCM-41 was found to be much more active than Ti-zeolite to oxidize α-terpineol and norbornene at 70ºC using *tert*-butyl hydroperoxide as oxidant as summarized in Table 2.9.[11]

Table 2.9 Oxidation of α-terpineol and norbornene on Ti-Containing Materials[11]

Catalyst sample	Reaction time (h)	α-Terpineol		Reaction time (h)	Norbornene		
					Epoxides		Alcohol
		Product	Others		Exo	Endo	
Ti-MCM-41	3	23.8	4.02	5	21.7	4.7	3.1
	8	31.5	8.6	11	30.0	12.3	6.4
Ti-Beta	3	4.1	2.5	5	4.7	5.6	6.6
	8	7.6	5.8	11	11.2	7.1	12.8

Ti-MCM-41 showed a very lower activity and lower selectivity toward the use of H_2O_2 for alkene oxidation than either TS-1, TS-2 or Ti-β, owing to their high hydrophilicity.[11] After these catalysts were treated with trimethylsilylation, the catalytic activities in oxidation of alkenes (Table 2.10) with H_2O_2 were enhanced remarkably.[40]

Table 2.10 Effect of trimethylsilylation on catalytic activities of Ti-MCM-41 for alkenes and alkanes

Catalyst	Conversion	TON	Selectivity (%)			
			Alcohol	Ketone	Epoxide	Diol
Cyclohexene						
Ti-MCM-41 (non-sil)	0.72	5.4	30.0	15.2	0	54.7
Ti-MCM-41 (sil)	13.3	112.1	14.4	21.0	13.9	50.7
			trans- Epoxide	*cis-* Epoxide	*trans-* Diol	*cis-* Diol
Cyclododecene						
Ti-MCM-41 (non-sil)	1.9	10.9	46.0	47.0	7.1	0
Ti-MCM-41 (sil)	6.5	40.0	29.6	63.0	7.4	0

Ti-MCM-41 (non-sil) exhibited low activity in the oxidation of cyclohexene. However, trimethylsilylation of Ti-MCM-41 resulted in a *ca*. 20-fold increase in the activity in the oxidation of cycloxene. The tureover number (TON) per hours was ever higher than that observed with Ti-β. The selectivity for epoxide/diol was increased at the expense of allylic oxidation

In the oxidation of cyclododecene, trimethylsilylation led to a 3 to 4-fold increase although the attained activity was relatively low. Unlike cyclohexene, allylic oxidation of cyclododecene hard occurred and epoxides were selectively obtained without their extensive hydrolysis. Besides, it had been observed that trimethylsilylated catalysts exists in the organic phase because of their hydrophobicity, resulting in migration of the inhibition of oxidation caused by water. No leaching of Ti was observed during the oxidation.

Table 2.11 Effect of trimethylsilylation on catalytic activity of Ti-MCM-41 for alkenes

Catalyst	Conversion	TON	Selectivity (%)		
			2-Pentenal		Epoxide
2-Penten-1-ol					
Ti-MCM-41 (non-sil)	32.4	242	81.0		19.0
Ti-MCM-41 (sil)	14.7	124	81.6		18.4
			Epoxide	Pyran	Others
α-Terpineol					
Ti-MCM-41 (non-sil)	2.2	19.4	44.3	45.4	10.3
Ti-MCM-41 (sil)	8.1	74.3	14.2	32.0	53.8

The activity of Ti-MCM-41 for hexane oxidation was negligible before trimethylsilylation. 2-penten-1-ol containing a polar hydroxyl group more easily migrates into the pores of non-trimethylsilylated catalysts than simple alkenes in competition with water, showing a much higher reactivity than cyclohexene.

Trimethylsilylated sample Ti-MCM-41 (sil) exhibited lower activity in the oxidation of 2-penten-1-ol than the corresponding non-trimethylsilylated samples. Partial removal of silanol groups would reduce the capability to absorb the allylic alcohols through hydrogen bonding. The decrease activity might be also due to the difficulty in access to the active site caused by the introduction of rather bulky trimethylsilyl groups. The oxidation of α-terpineol, trimethylsilylation resulted in enhancement of activity for oxidation. This is interpreted in terms of high hydrophobicity of α-terpineol compared to 2-penten-1-ol.

CHAPTER III

EXPERIMENTS

3.1   Equipment and Instruments

Ovens and Furnaces

In this study, reactant mixture and solid products heated at the temperature of 100ºC was carried out using a Memmert UM-500 oven. Calcination of the solid catalysts at 540ºC was achieved in a Carbolite RHF 1600 muffle furnace with programmable heating rate of 2ºC/min.

XRD

Synthesized samples were identified for the structure using a Rigaku D/MAX-2200 X-ray diffractometer (XRD) at the Petroleum and Petrochemical College, Chulalongkorn University with nickel filtered Cu Kα radiation (30 kV, 30mA) at an angle of 2Θ range from 1.5 to 10°. The scan speed was 2°/min and the scan step was 0.02°. The three slits (scattering, divergent and receiving slits) are fixed at 0.5°, 0.5° and 0.15 mm, respectively.

ICP Spectrometer

Titanium contents in the catalysts were analyzed using the Perkin Elmer Plasma 1000 inductively coupled plasma-atomic emission (ICP-AE) spectrometer at the Scientific and Technological Research Equipment Center of Chulalongkorn University.

FTIR Spectrometer

Vibration of metal-oxygen bonds in the catalysts were measured in the wave number range from 600 to 1500 cm^{-1} using a Nicolet Impact 410 Fourier transformed infrared (FTIR) spectrometer with the KBr pellet technique at Department of Chemistry, Faculty of Science, Chulalongkorn University.

<u>DR-UV-VIS Spectrometer</u>

The diffused reflectance-ultraviolet-visible (DR-UV-VIS) spectra of the catalysts were measured in the range of 200-600 nm using a Perkin Elmer LAMBDA 14 DR-UV-VIS spectrometer at Institute of Analytical Chemistry Training, Ministry of Science and Technology.

3.2   Chemicals and Gases

To remove a trace amount of moisture nitrogen, highly pure grade purchased from Thai Industrial Gases (TIG) was passed through a 40 cm x 2.5 cm tube of the molecular sieve 4A. Tetraethyl orthosilicate (98% TEOS), tetramethylammonium hydroxide (TMAOH), *n*-hexadecyltrimethylammonium chloride (CTMACl), *n*-dodecyltrimethylammonium chloride (DTMACl) were commercially available from TCI, Japan.   Trimethylchlorosilane,   hexamethyldisiloxane,   hexamethyldisilazane, trimethylethoxysilane, trimethylsilyltrifluoroacetate reagents of Analar grade were purchased from Fluka and used without any treatment. Toluene, acetone and 2-propanol solvents were dehydrated by mixing with the activated molecular sieves 4A (zeolite NaA) prior to use. An ICP standard titanium solution of 1000 ppm was purchased from BDH. Liquid nitrogen was supplied by PRAXAIR Thailand. Other chemicals were from Merck or Fluka, otherwise specifically identified.

3.3   Synthesis of C_{12}-Ti-MCM-41 with Various Si/Ti Ratios in Gel

Using DTMACl as template C_{12}-Ti-MCM-41 samples with various Si/Ti ratios in gel were prepared. According to the procedure reported by Tatsumi *et al.*[18] a gel with a molar composition of SiO_2 : x TiO_2 : 0.6 DTMACl : 0.3 TMAOH : 60 H_2O was prepared under nitrogen atmosphere as follows. Into a 500-cm^3 round bottom flask with 4 necks an amount of 17.59 g of the template DTMACl was dissolved in 53.86 g of water. The mixture was stirred vigorously until a clear solution was obtained. The flask was cooled down in an ice/water bath at the temperature of 5ºC.   From

each addition funnel 23.15 g of TEOS liquid and 3.04 g of 20% TMAOH solution were simultaneously added dropwise to the cold template solution. In this step TEOS was partially hydrolyzed in basic solution. After stirring for 30 min a solution of required amount of TBOT in 2-propanol was slowly added to the mixture in the flask with stirring. The stirring was continued for 16 h before 48.0 g of water were added. After 30 min, alcohols existing as both solvent and by-product were evaporated from the mixture at the temperature of 85°C for about 3 h. The composition of gel was corrected by adding water to the total weight of 164.5 g. The resulted gel was crystallized in a tightly capped Teflon bottle which was heated in an oven at 100°C for 10 days. After cooling the Teflon bottle with running tap water, the solid was filtered off, wash several times with deionized water and dried in an oven at the temperature of 100°C. Apparatus for the gel preparation and alcohol removal was shown in Figure 3.1, and 3.2, respectively. A schematic diagram of preparation of Ti-MCM-41 is shown in Scheme 3.1. A so-called as-synthesized C_{12}-Ti-MCM-41 sample was obtained as a white solid product at a yield of 12.85 g. The organic template was removed from the channels of the material by calcination of the as-synthesized sample at 540°C for 6 h resulted in the so-called calcined C_{12}-Ti-MCM-41 sample. The heating program for template removal is shown in Scheme 3.2. The samples with various Si/Ti ratios were characterized using XRD, ICP-AES and DR-UV-VIS techniques.

3.4   Synthesis of C_{16}-Ti-MCM-41 with Various Si/Ti Ratios in Gel

Using CTMACl as template C_{16}-Ti-MCM-41 samples with various Si/Ti ratios in gel was prepared. A gel with a molar composition of SiO_2 : x TiO_2 : 0.6 CTMACl : 0.36 TMAOH : 75 H_2O was prepared as follows. Into a 500-cm^3 four necked round bottom flask an amount of 21.33 g of the template CTMACl was dissolved in 53.86 g of water. The mixture was stirred vigorously until a clear solution was obtained. The flask was cooled down in an ice/water bath at the temperature of 5ºC. From each addition funnel 23.15 g of TEOS liquid and 3.65 g of 20% TMAOH solution were simultaneously added dropwise to the cold template solution. After stirring for 30 min a solution of required amount of TBOT in 2-propanol was slowly added to the mixture in the flask with stirring. The stirring was continued for 16 h before 63.0 g of water were added. After 30 min, alcohols existing as both solvent and by-product were evaporated from the mixture at the temperature of 85ºC for about 3 h. The composition of gel was corrected by adding water to the total weight of 198.7 g. The resulting gel was crystallized in a tightly capped Teflon bottle which was heated in an oven at 100ºC for 10 days. After cooling the Teflon bottle with running tap water, the solid was filtered off, washed several times with deionized water and dried in an oven at the temperature of 100ºC. A so-called as-synthesized C_{16}-Ti-MCM-41 sample was obtained as a white solid product at a yield of 11.9 g. The organic template was removed from the channels of the material by calcination of the as-synthesized sample at 540ºC for 6 h resulted in the so-called calcined C_{16}-Ti-MCM-41 sample. The samples with various Si/Ti ratios were characterized using XRD, ICP-AES and DR-UV-VIS techniques.
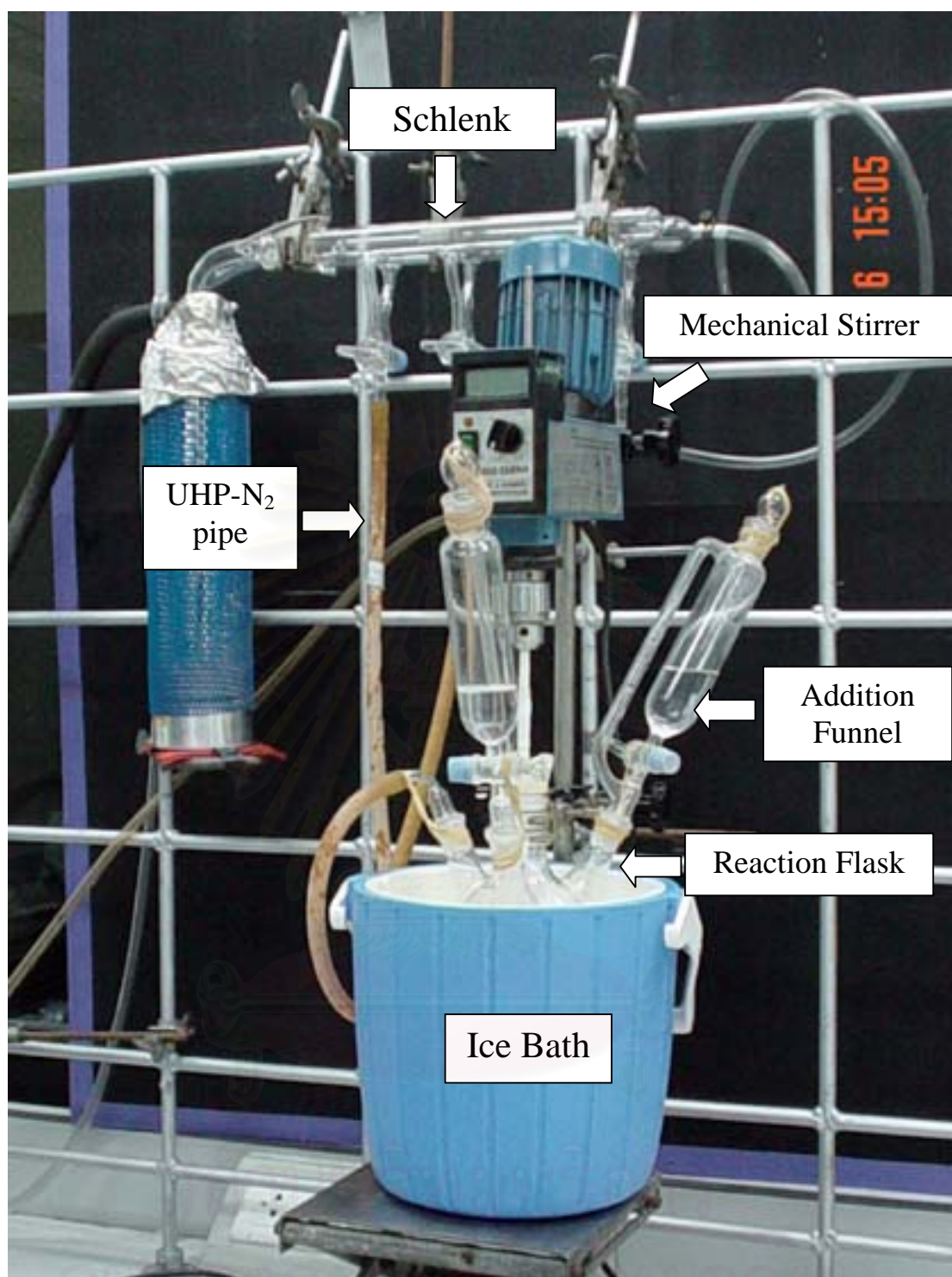
Figure 3.1 Apparatus for the gel preparation.
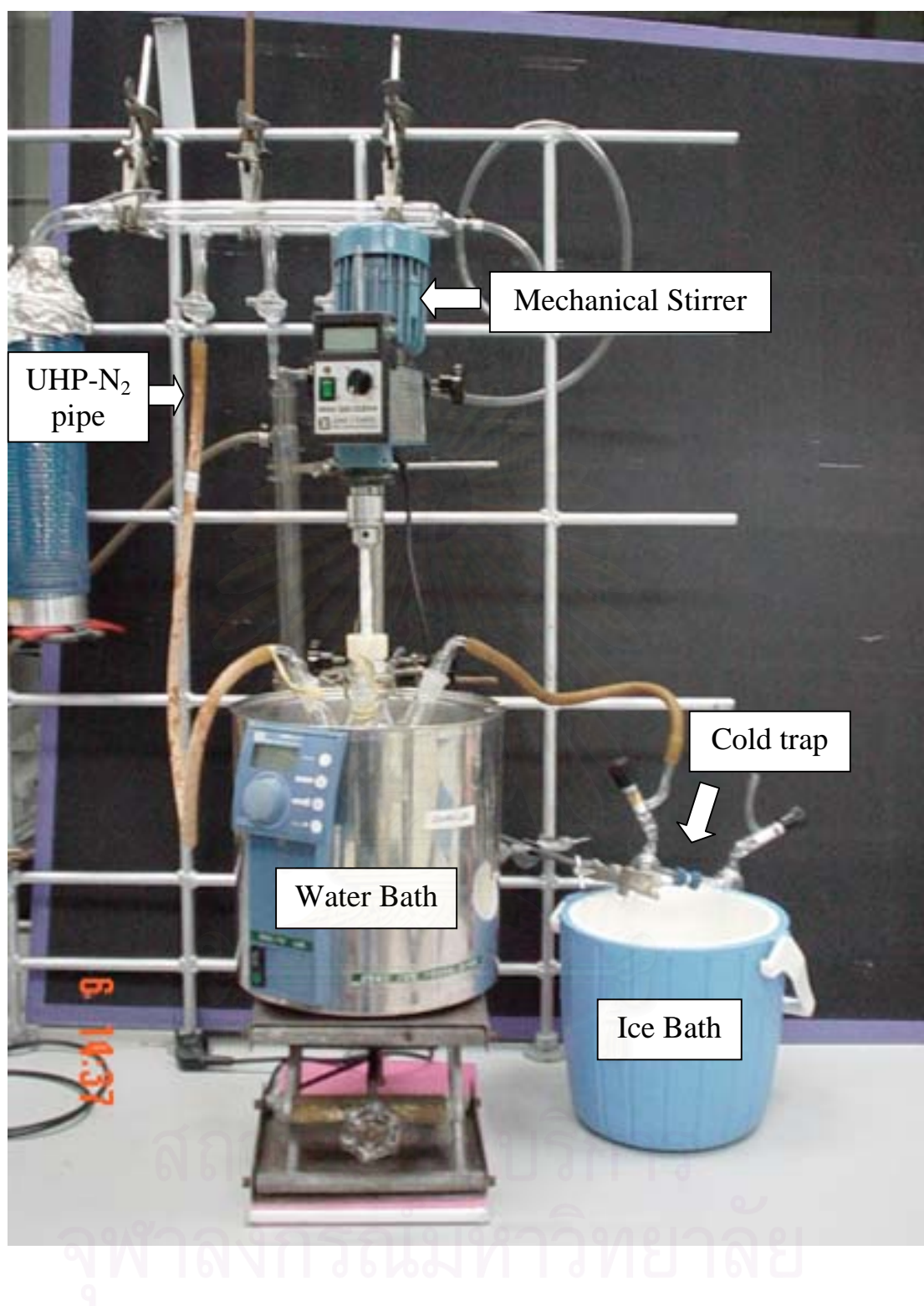
Figure 3.2 Apparatus for evaporation of alcohol from the reactant mixture.
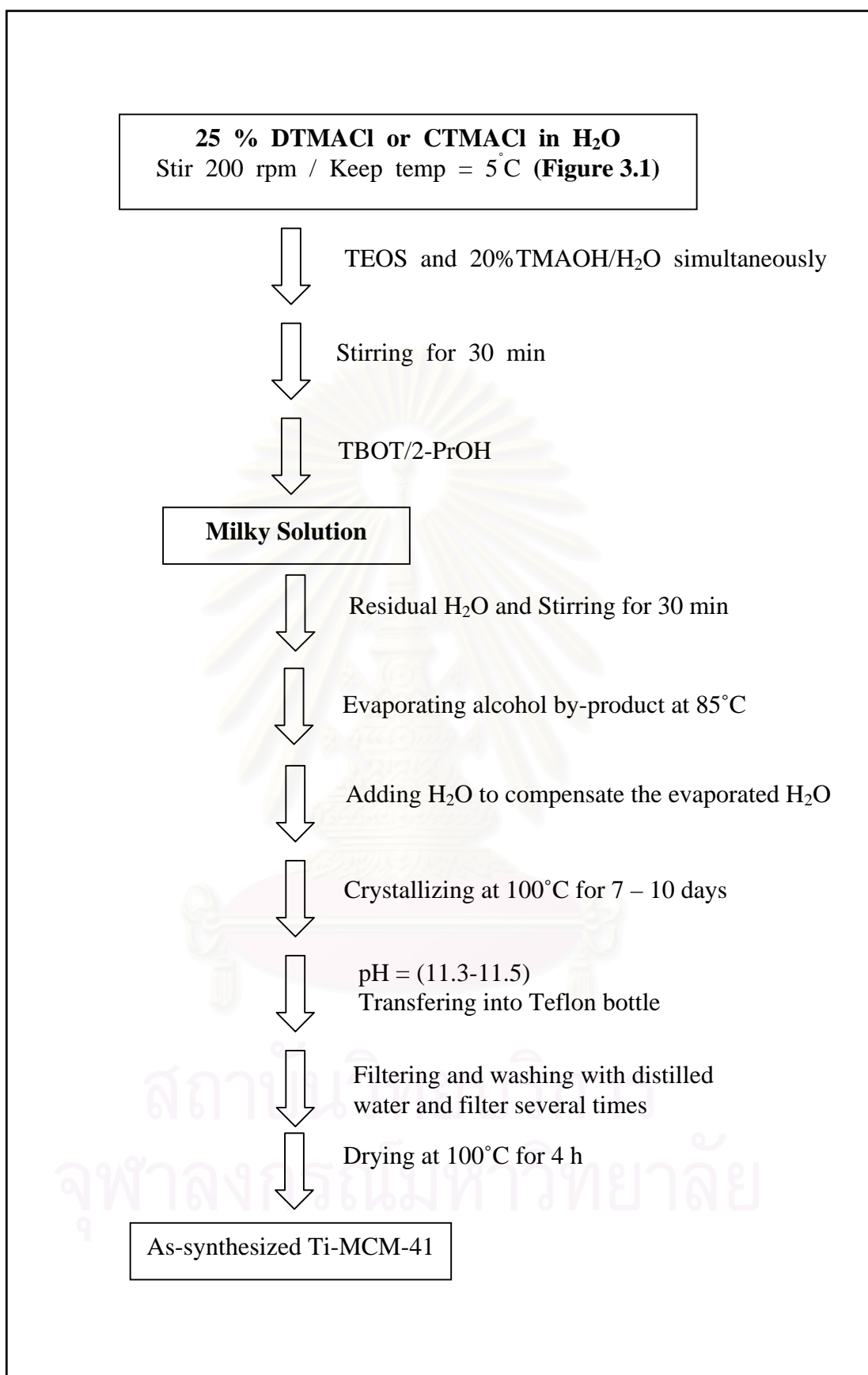
Scheme 3.1   Schematic diagram of preparation of Ti-MCM-41.
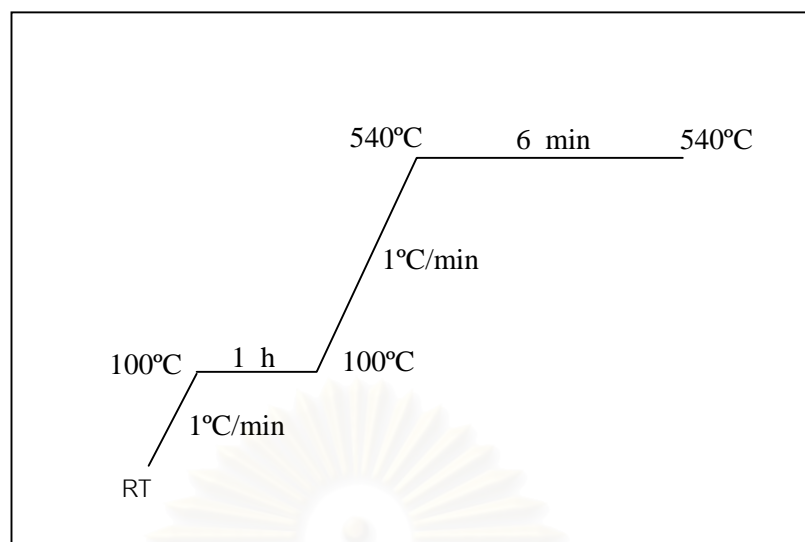
Scheme 3.2 Heating program for removal of template from Ti-MCM-41 channels.

3.5 Preparation of ICP-AES Samples

In a 100-cm^3 Teflon beaker, 0.0400 g of a calcined catalyst was soaked with 10 cm^3 of 6 M HCl and subsequently with 10 cm^3 of 48% hydrofluoric acid to get rid of silica in the form of volatile SiF$_4$ species. The solid was heated but not boiled to dryness on a hot plate. The fluoride treatment was repeated twice more. An amount of 10 cm^3 of a mixture of 6 M HCl and 6M HNO$_3$ at a ratio 1 : 3 was added and further heated to nearly dryness. An amount of 5 cm^3 of 6 M HCl was added to the beaker and warmed for 5 min to complete dissolution. An amount of 10-cm^3 deionized water was added to the beaker and warmed for 5 min to complete dissolution. The solution was transferred to a 100-cm^3 polypropylene volumetric flask and made to the volume by adding deionized water. The flask was capped and shaken thoroughly. If the sample was not analyzed for titanium content immediately, the solution was then transferred into a plastic bottle with a treaded cap lined under with a polyethylene seal. The standard solutions of titanium ions of 0, 2, 5, and 10 ppm were used to construct a calibration curve.

3.6   Restructuring of C$_{12}$-Ti-MCM-41 and C$_{16}$-Ti-MCM-41

A hydrothermal method for restructuring of C$_{12}$-Ti-MCM-41 and C$_{16}$-Ti-MCM-41 samples was investigated in this study. It was carried out right after the resulted gel was already crystallized for either 7 days or 10 days. After quenching step, the solid was filtered off without washing and mixed with a certain amount of deionized water, 10 g of water per gram of as-synthesized sample. After stirring for 30 min, the mixture was transfer to the Teflon bottle and heated to 120ºC for various periods of 1-3 days. The solids were filtered and washed several times until no base. The samples were dried in an oven at the temperature of 125ºC for 2 h. They were calcined in a muffle furnace at the temperature of 540ºC for 6 h and resulted in the so-called cal-RS-C$_{12}$-Ti-MCM-41 and cal-RS-C$_{16}$-Ti-MCM-41 samples and characterized using XRD.

3.7   Silylation of Restructured Ti-MCM-41

The calcined restructured Ti-MCM-41 samples, cal-RS-C$_{12}$-Ti-MCM-41 and cal-RS-C$_{16}$-Ti-MCM-41, were treated with various silyl reagents such as trimethyl-chlorosilane (TMCS), hexamethyldisiloxane (HMDSO), hexamethyldisilazane (HMDS), trimethylethoxysilane (TMES), and trimethylsilyltrifluoroacetate (TMSTFA). The structures of the silyl compounds are shown in Figure 3.3. As mentioned in Section 2.9 that about 40% of surface of Ti-MCM-41 was Q^3 type silanol groups. The ten-fold excess amount of those silyl compounds were used and are shown in Table 3.1. These compounds are moisture sensitive, thus the glassware and solvents used in this study were neatly free from moisture. Apparatus for silylation of Ti-MCM-41 samples was shown in Figure 3.4.

To remove air and moisture, a 250-cm^3 a pear shape flask with a side arm sealed with a septum was evacuated and filled with nitrogen for 3 times alternately. An amount of 1.0 g of powder sample and 50 cm^3 of toluene were put into the 250-

cm³ flask under a nitrogen flow. A silyl reagent was injected at a required amount by a syringe into the flask through the septum. The reflux distillation of the slurry was operated using an oil bath at 120°C for 16 h. Volatile matters were stripped off by evacuation to a cold trap. The powder remained in the flask was washed three times with 50 cm³ acetone. The silylated sample was separated from the solvent by centrifugation, followed by drying at 125°C for 2 h. The sample was characterized using XRD and FTIR.
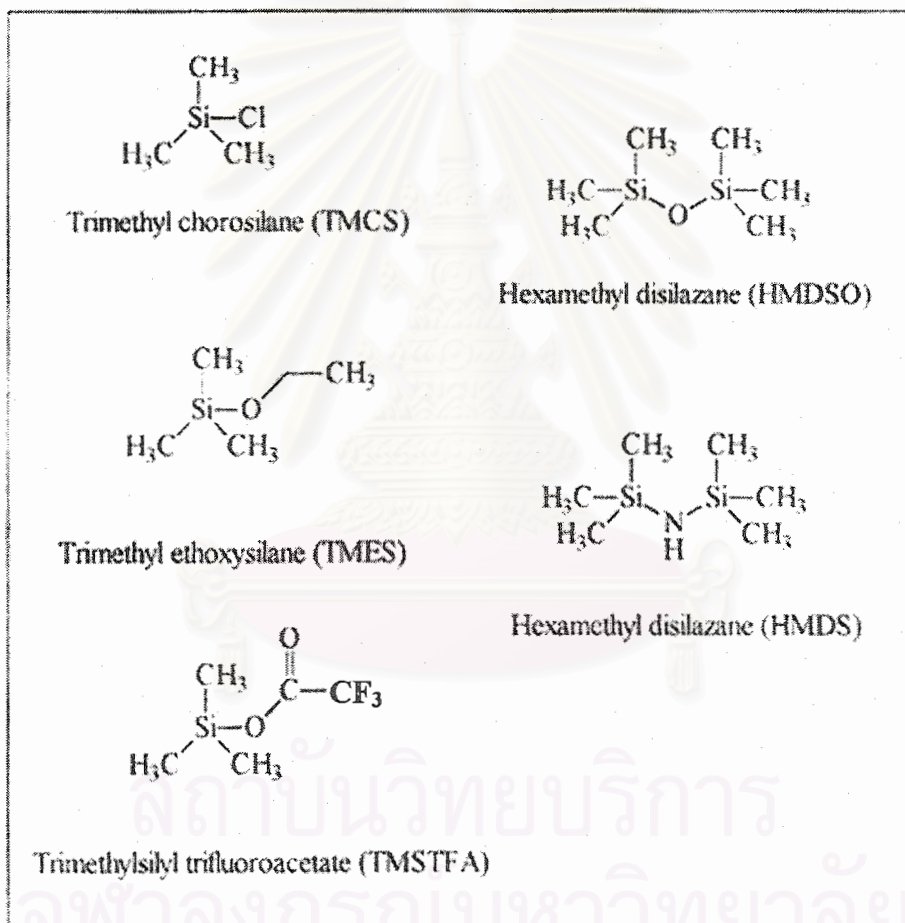
Figure 3.3 Structures of various silyl reagents.

Table 3.1 Required amounts and properties of silyl compounds for silylation of 1 g
of calcined Ti-MCM-41 samples

Silyl Compound	MW (g/mol)	Density (g/cm³)	No. of silyl group per molecule	Weight of compound (g)	Volume of compound (cm³)
TMCS	108.64	0.859	1	7.2330	8.42
TMES	118.25	0.758	1	7.8728	10.39
TMSTFA	186.21	1.076	1	12.1312	11.27
HMDSO	162.38	0.764	2	5.4055	7.08
HMDS	161.40	0.774	2	5.3728	6.94
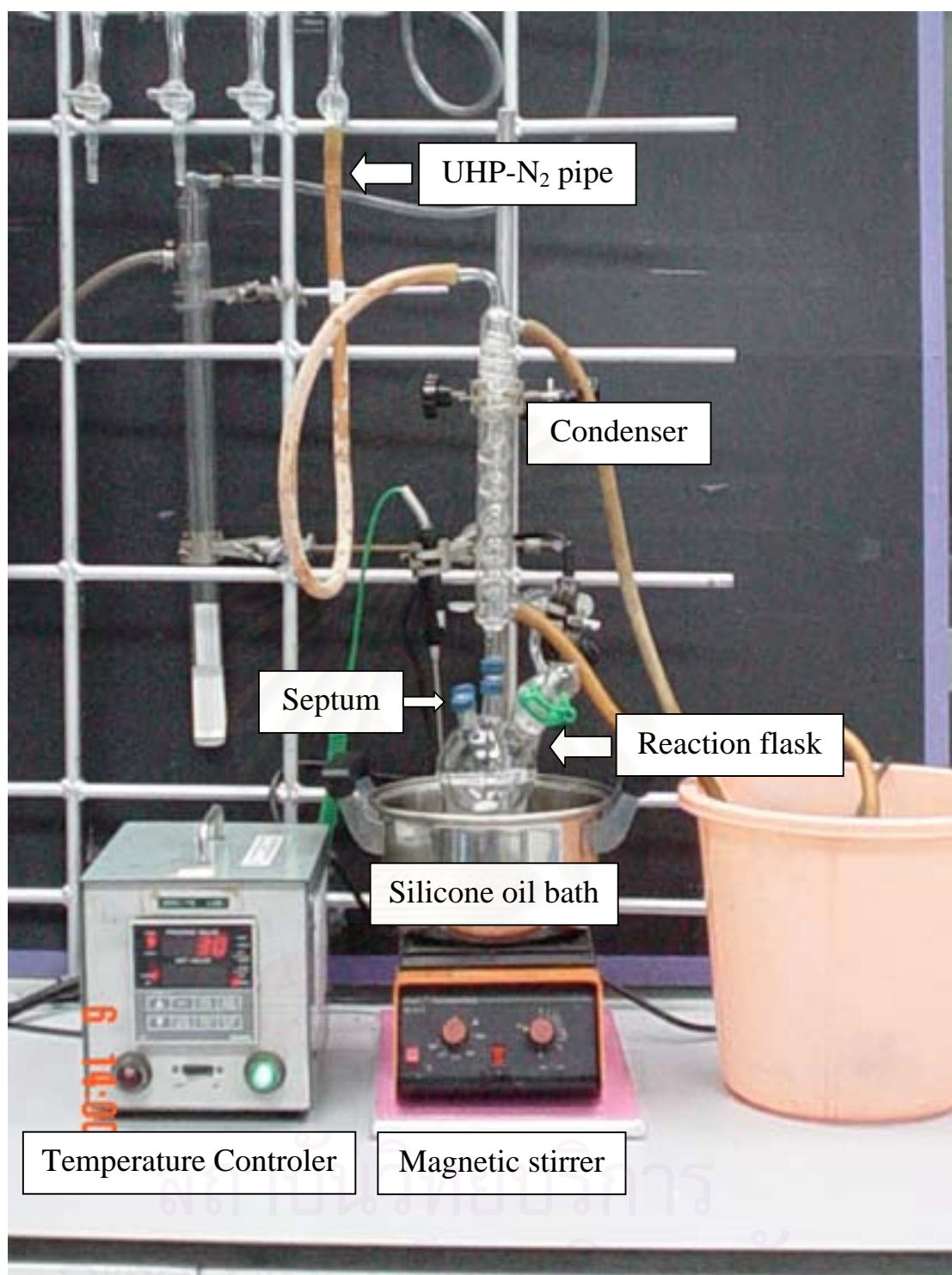
Figure 3.4 Apparatus for silylation of Ti-MCM-41 samples.

3.8   Stability Test of Ti-MCM-41 Samples

3.8.1   Hydrothermal Stability

A reflux distillation of the slurry of 0.1 g of Ti-MCM-41sample in 50 cm^3 of deionized water was operated at 100ºC for 12 h under nitrogen atmosphere. The sample was then filtered off and dried in an oven heated at 100ºC for 2 h. It was then characterized for structure change using XRD.

3.8.2   Stability to Moisture

A sample was exposed to moisture over saturated aqueous solution of ammonium chloride at room temperature for various periods of 1-3 days. The sample was dried in an oven heated at 100ºC for 2 h. Apparatus for testing the sample for its stability to moisture is shown in Figure 3.4. The sample was then characterized for structure change using XRD.
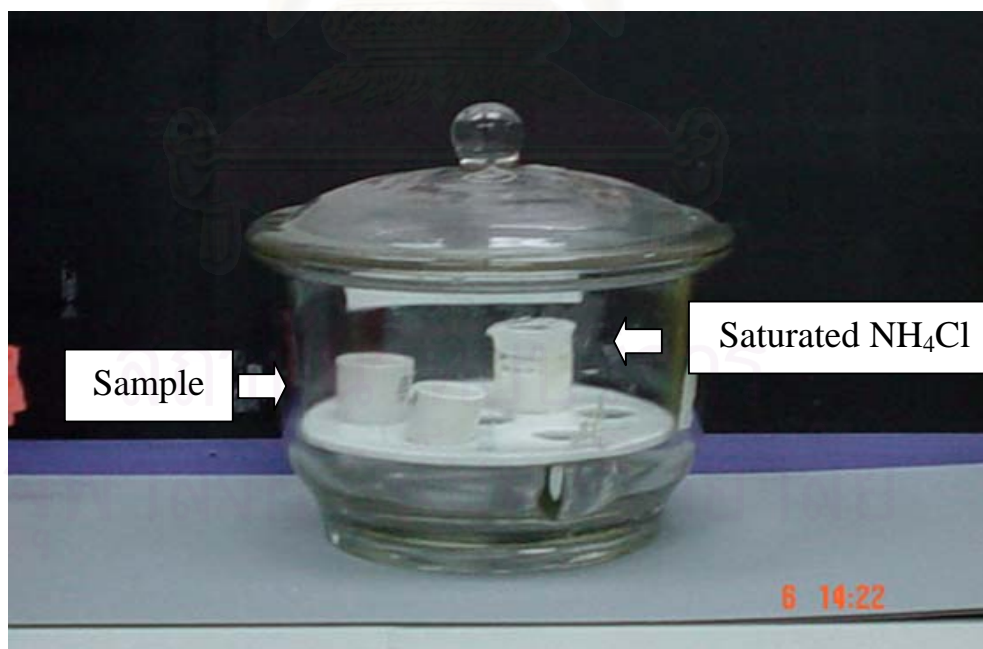
Figure 3.4 Apparatus for testing the sample for its stability to moisture.

3.8.3 Mechanical Stability

An amount of 0.50 g sample was pressed in a stainless steel die of 13-mm diameter by a dynamic press of various pressure values of 500, 1000, 1500, and 2000 kg/m^2. The pressure was held for 10 min. It was then characterized for structure change using XRD.

CHAPTER IV

RESULTS AND DISCUSSION

4.1 Ti-MCM-41 Samples without Treatment

4.1.1 XRD Results

XRD patterns of as-synthesized and calcined samples of C_{12}-Ti-MCM-41 and C_{12}-Ti-MCM-41 are shown in Figure 4.1 and the corresponded data are shown in Table 4.1. The XRD patterns of both as-synthesized samples with Si/Ti in gel of 100 (Figures 4.1. a and c) exhibit the characteristic reflection peaks of hexagonal structure of MCM-41 structure. After removal of template by calcination at elevated temperature, reflection peaks in the XRD pattern of calcined C_{12}-Ti-MCM-41 have twice intensity of that before calcination, while the XRD pattern of calcined C_{16}-Ti-MCM-41 becomes only one very broad peak with less intensity. The results indicate that under the synthesis condition, C_{12}-Ti-MCM-41 structure has ordered structure better than that of C_{16}-Ti-MCM-41 and this is responsible for higher structural stability of C_{12}-Ti-MCM-41 than C_{16}-Ti-MCM-41. The partial collapse of structure in C_{16}-Ti-MCM-41 was also indicated by the shrinkage of d-spacing from 37.72 to 29.43 Å or 20% d-spacing reduction. On the contrary, the d-spacing shrinkage is only 2% for C_{12}-Ti-MCM-41 but the uniformity was markedly improved after calcination. The restructuring in C_{12}-Ti-MCM-41 occurred by increasing degree of silanol group condensation. Upon removal of the pillared template between the walls, the structure of C_{16}-Ti-MCM-41 tends to collapse more easily than that of C_{12}-Ti-MCM-41. This observation is in agreement with several reports[12,66] on the less stability of larger pore Ti-MCM-41 upon template removal. This is the reason why a stabilization of C_{16}-Ti-MCM-41 structure is needed.

Table 4.1 XRD data of as-synthesized and calcined samples of C_{12}-Ti-MCM-41 and C_{16}-Ti-MCM-41 with Si/Ti ratio in gel of 100

Sample	Bragg's angle, 2θ (degree)	d-spacing (Å)	Intensity (counts)
As-synthesized C_{12}-Ti-MCM-41 (100)	2.72	32.45	16,733
Calcined C_{12}-Ti-MCM-41 (100)	2.88	30.65	41,396
As-synthesized C_{16}-Ti-MCM-41 (100)	2.34	37.72	15,130
Calcined C_{16}-Ti-MCM-41 (100)	3.00	29.43	10,754
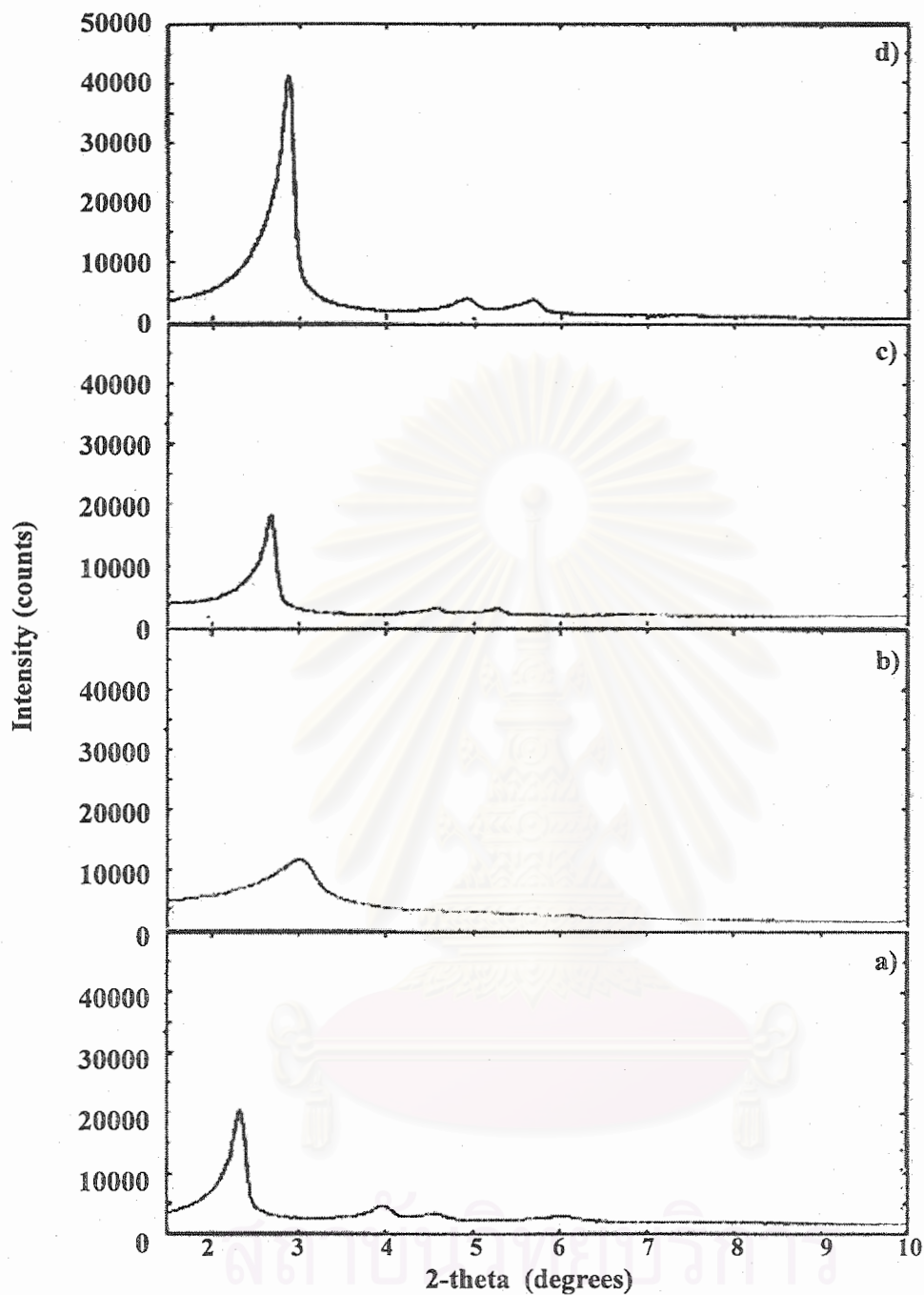
Figure 4.1 XRD patterns of Ti-MCM-41 samples, a) as-synthesized C_{16}-Ti-MCM-41 with Si/Ti of 100, b) calcined C_{16}-Ti-MCM-41 with Si/Ti of 100, c) as-synthesized C_{12}-Ti-MCM-41 with Si/Ti of 100 and d) calcined C_{16}-Ti-MCM-41 with Si/Ti of 100.

4.1.2 Si/Ti Ratios in Ti-MCM-41 Samples

Titanium contents and corresponding Si/Ti ratios in the C_{12}-Ti-MCM-41 and C_{16}-Ti-MCM-41 samples are shown in Table 4.2. With decreasing the Si/Ti ratio in gel, the Si/Ti ratio in product also decreases, i.e. more titanium amount can be loaded into the products of Ti-MCM-41. However, the titanium content determined by ICP-AES includes all sites of titanium existing in the Ti-MCM-41 samples. To identify which site Ti occupies the most, DR-UV-VIS is a more informative method.

Table 4.2 Titanium contents and corresponding Si/Ti ratios in C_{12}-Ti-MCM-41 and C_{16}-Ti-MCM-41 samples

Sample	Si/Ti ratio in gel	Si content (mmol SiO_2)	Ti content (mmol SiO_2)	Si/Ti ratio in product
C_{12}-Ti-MCM-41 (100)	100	0.66901	0.00842	79
C_{12}-Ti-MCM-41 (60)	60	0.66009	0.01179	56
C_{16}-Ti-MCM-41 (100)	100	0.66941	0.00728	92
C_{16}-Ti-MCM-41 (60)	60	0.66035	0.01076	61

4.1.3 DR-UV-VIS Spectra

To identify the titanium sites in the Ti-MCM-41 sample, DR-UV-VIS spectra of as-synthesized samples of C_{12}-Ti-MCM-41 and C_{16}-Ti-MCM-41 were measured and shown in Figure 4.2. All spectra present only one absorption band at the wavelength about 215 nm that is a characteristic band ascribed for tetrahedral coordinated titanium.[10,88] It is proven that all Ti-MCM-41 samples have titanium incorporated in the framework tetrahedral sites. There is no observation of

extraframework or non-framework titanium site at any longer wavelength. There is no band around 330 nm due to the TiO_2 of anatase phase.

C$_{12}$-Ti-MCM-41   **C$_{16}$-Ti-MCM-41**
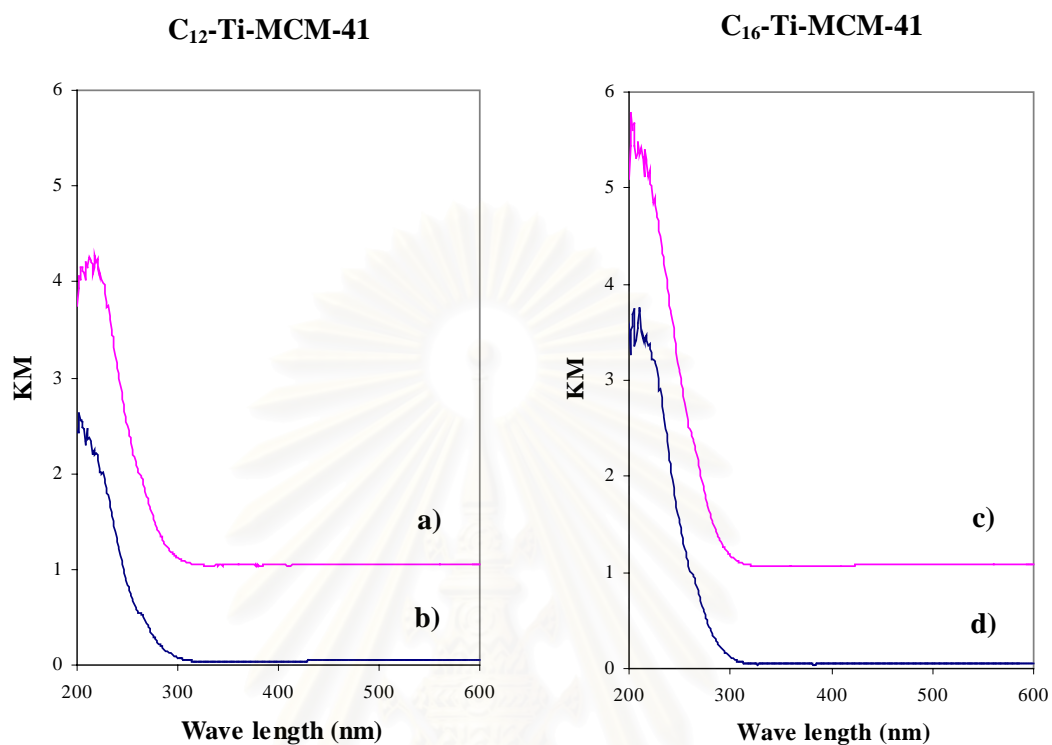
Figure 4.2 DR-UV-VIS spectra of Ti-MCM-41 samples, a) calcined C$_{12}$-Ti-MCM-41 with Si/Ti of 60, b) calcined C$_{12}$-Ti-MCM-41 with Si/Ti of 100, c) calcined C$_{16}$-Ti-MCM-41 with Si/Ti of 60 and d) calcined C$_{16}$-Ti-MCM-41 with Si/Ti of 100.

4.2   Ti-MCM-41 Treated under Restructuring Conditions

4.2.1   Restructuring of Wet As-synthesized Ti-MCM-41 Samples

4.2.1.1   C$_{16}$-Ti-MCM-41(100) Samples

The C$_{16}$-Ti-MCM-41 samples were synthesized with crystallization period of either 7 or 10 days, and XRD patterns of as-synthesized C$_{16}$-Ti-MCM-41(100) samples with and without restructuring treatment are shown in Figures 4.3 and 4.4. The XRD patterns are not much different between that before and those after the treatment in hot water for 3 days or shorter if the sample was obtained with crystallization period of 10 days. In contrast, if the similar treatment was performed on the wet as-synthesized C$_{16}$-Ti-MCM-41(100) sample obtained with crystallization period of 7 days, there is some change observed in XRD patterns in Figure 4.4. The change was significant after the restructuring of the wet as-synthesized C$_{16}$-Ti-MCM-41(100) sample for 2 and 3 days. For 2-day treatment, the XRD pattern shows only one broad band with lower intensity compared to that of the as-synthesized C$_{16}$-Ti-MCM-41(100) sample. For 3-day treatment, the XRD shows a mixed phase of MCM-41 and MCM-50 structures. The observation reveals that crystallization of C$_{16}$-Ti-MCM-41(100) within 7 days results in the incomplete condensation of silica on the mesostructure. The incomplete mesostructure collapses easily under the hydrothermal treatment and results in phase transformation from MCM-41 to MCM-50 structure upon prolongation of the treatment period.
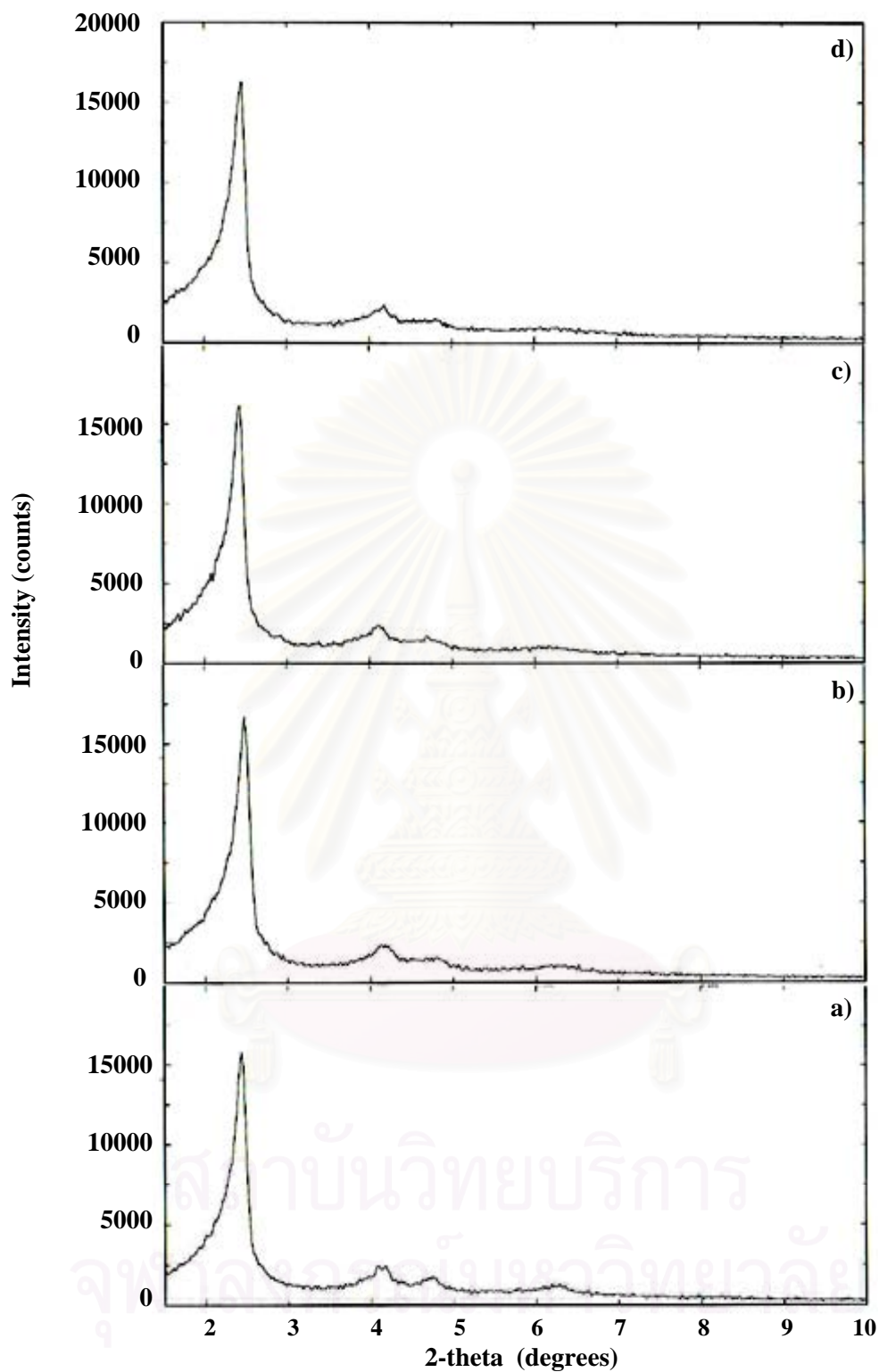
Figure 4.3 XRD patterns of C_{16}-Ti-MCM-41(100) samples crystallized for 10 days, a) as-synthesized sample; b) wet as-synthesized sample treated in hot water for 1 day; c) wet as-synthesized sample treated in hot water for 2 days, and d) wet as-synthesized sample treated in hot water for 3 days.
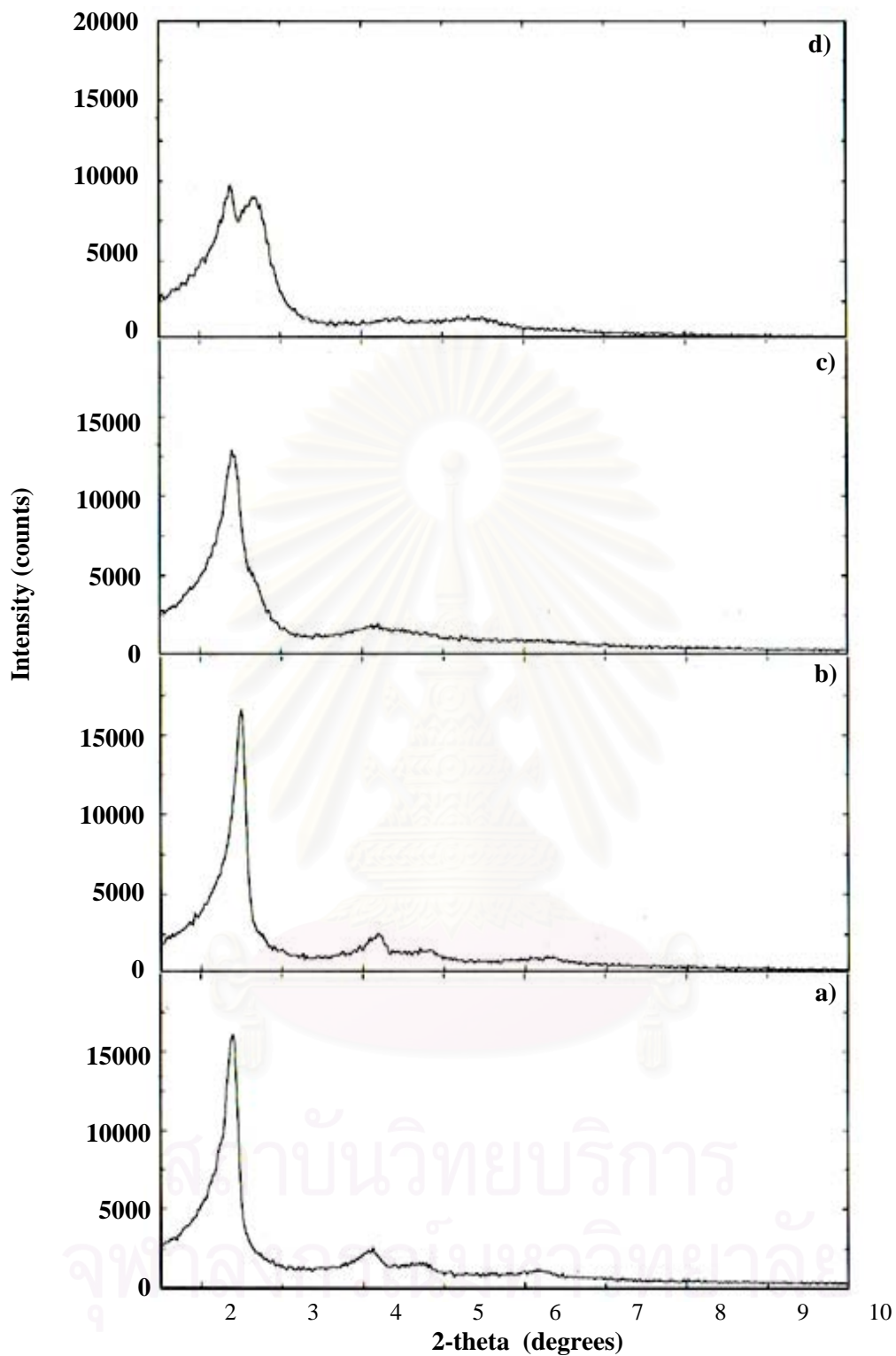
Figure 4.4   XRD patterns of C_{16}-Ti-MCM-41(100) samples crystallized for 7 days, a) as-synthesized sample; b) wet as-synthesized sample treated in hot water for 1 day; c) wet as-synthesized sample treated in hot water for 2 days, and d) wet as-synthesized sample treated in hot water for 3 days.

4.2.2 Restructuring of Calcined Ti-MCM-41 Samples

According to the results from restructuring treatment in the previous section, the effect of restructuring on unstable samples such as C_{16}-Ti-MCM-41 results in structural collapse similar to the effect of thermal treatment. The period of restructuring treatment was maintained for only 1 day to prevent the loss in structure upon the prolonged hydrothermal treatment.

4.2.2.1 C_{12}-Ti-MCM-41 Samples

It is found excitedly that the calcined C_{12}-Ti-MCM-41 samples can be restructured by the treatment in hot water for 1 day. The restructured sample exhibits the higher crystallinity, based on intensity of (100) reflection peak, than that of the untreated sample C_{12}-Ti-MCM-41(100) by 28% and C_{12}-Ti-MCM-41 (60) by 32% as shown in Figure 4.5 and Table 4.3. In addition, the *d*-spacing shrinkage after calcination (1-2% contraction) is less than that of the untreated sample (4% contraction).

Table 4.3 Comparison of intensities of (100) the reflection peak before and after restructuring treatment of the C_{12}-Ti-MCM-41 with Si/Ti ratio in gel of 60 and 100

Sample	Bragg's angle, 2θ (degree)	d-spacing (Å)	Intensity (counts)
No treated C_{12}-Ti-MCM-41 (60)	2.76	31.98	23,076
Treated C_{12}-Ti-MCM-41 (60)	2.72	32.94	30,374
No treated C_{12}-Ti-MCM-41 (100)	2.90	30.44	34,727
Treated C_{12}-Ti-MCM-41 (100)	2.80	31.53	44,587
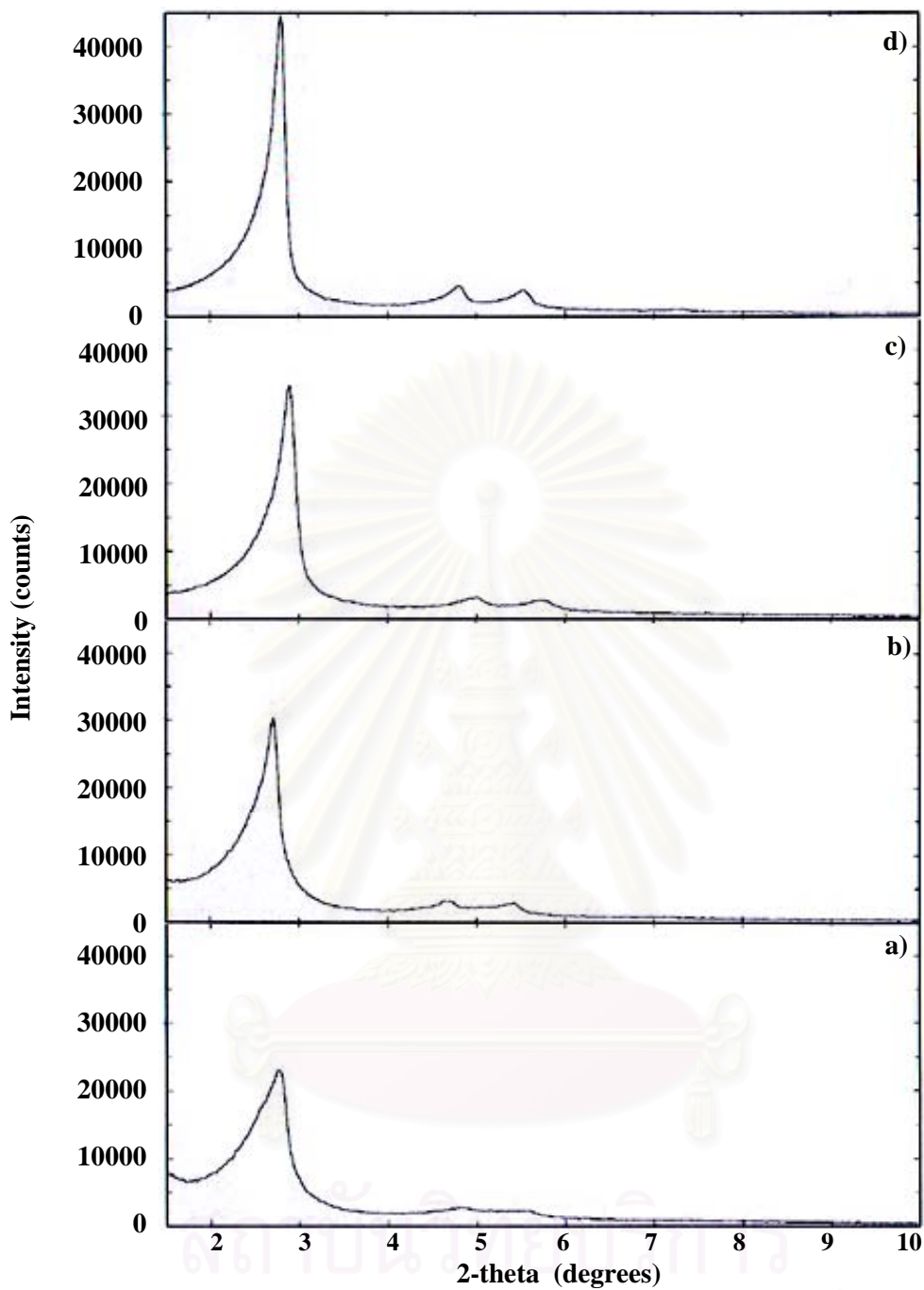
Figure 4.5 XRD patterns of calcined C_{12}-Ti-MCM-41 samples, a) Non treated C_{12}-Ti-MCM-41 sample with Si/Ti of 60; b) C_{12}-Ti-MCM-41 sample with Si/Ti of 60 sample treated in hot water for 1 day; c) Non treated C_{12}-Ti-MCM-41 sample with Si/Ti of 100; d) C_{12}-Ti-MCM-41 sample with Si/Ti of 100 sample treated in hot water for 1 day.

4.2.2.2 C_{16}-Ti-MCM-41 Samples

The calcined C_{16}-Ti-MCM-41 restructured in hot water for 1-day exhibits differently. It has lower crystallinity than that of the untreated sample C_{16}-Ti-MCM-41(100) by 21% and C_{16}-Ti-MCM-41(60) by 30% as shown in Figure 4.6 and Table 4.4. In addition, the d-spacing shrinkage after calcination (15% contraction) is less than that of the untreated sample (20-22% contraction).

The thermal stability improvement is resulted from the thicker wall resulted the restructuring at the pore wall of the C_{16}-Ti-MCM-41 mesostructure. This is implied by the reduction in d-spacing value.

Table 4.4 Comparison of intensities of (100) the reflection peak before and after restructuring treatment of the C_{16}-Ti-MCM-41 with the Si/Ti ratio in gel of 60 and 100

Sample	Bragg's angle, 2θ (degree)	d-spacing (Å)	Intensity (counts)
No treated C_{12}-Ti-MCM-41 (60)	3.04	29.04	10,666
Treated C_{12}-Ti-MCM-41 (60)	2.84	31.08	13,912
No treated C_{12}-Ti-MCM-41 (100)	3.00	29.43	10,754
Treated C_{12}-Ti-MCM-41 (100)	2.76	31.98	13,057
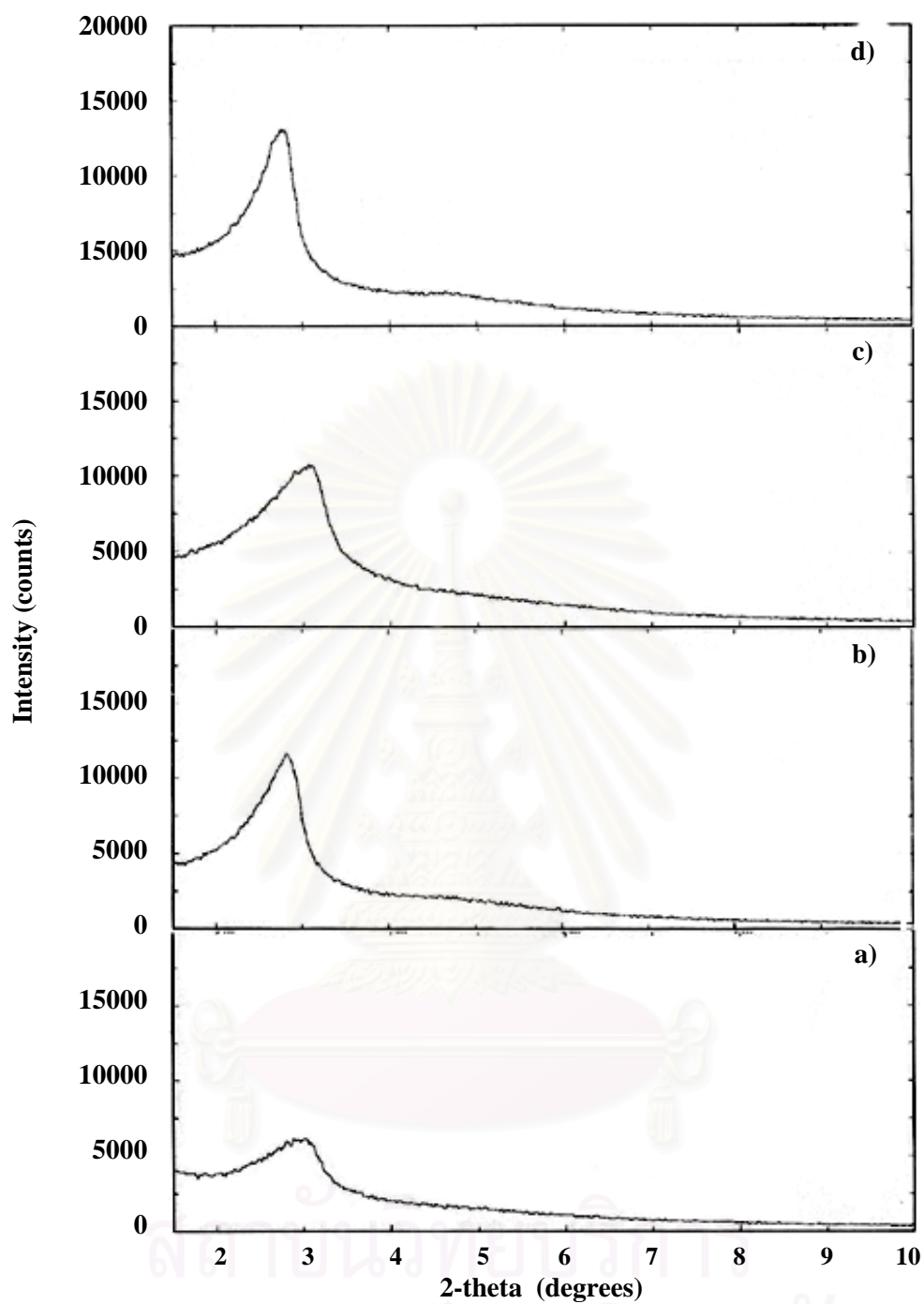
Figure 4.6 XRD patterns of calcined C_{12}-Ti-MCM-41 samples, a) Non treated C_{16}-Ti-MCM-41 sample with Si/Ti of 60; b) C_{16}-Ti-MCM-41 sample with Si/Ti of 60 sample treated in hot water for 1 day; c) Non treated C_{16}-Ti-MCM-41 sample with Si/Ti of 100; d) C_{16}-Ti-MCM-41 sample with Si/Ti of 100 sample treated in hot water for 1 day.

The restructured samples give similar DR-UV-VIS spectra to that of untreated sample as shown in Figure 4.7. That is a good sign that upon treatment no leaching of titanium from the framework sites to other undesired sites.
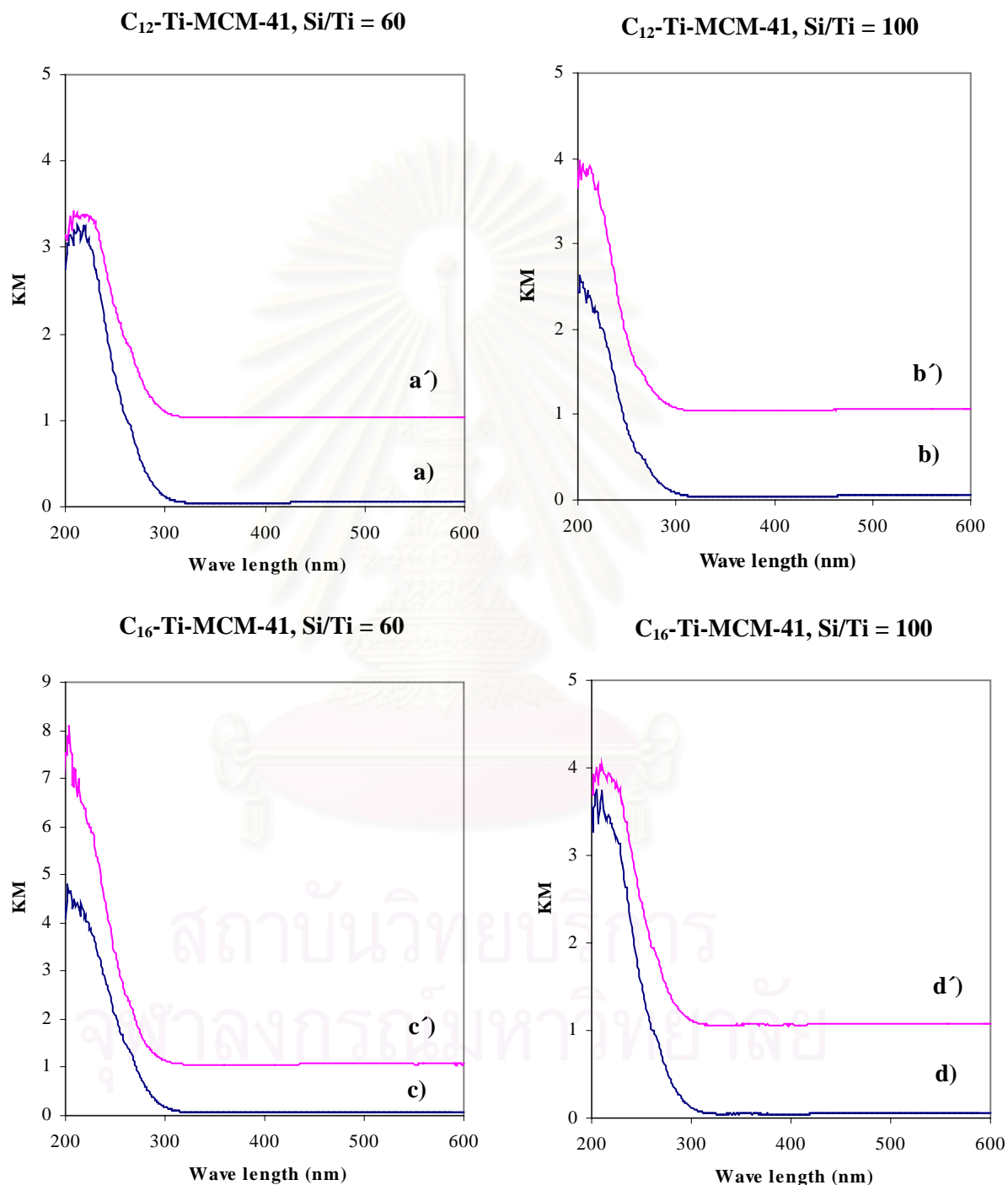
Figure 4.7 DR-UV-VIS spectra of calcined Ti-MCM-41 samples, a), b), c), d) without restructuring treatment and a´), b´), c´), d´) with restructuring treatment in hot water for 1 days.

4.3   Silylation of Ti-MCM-41

4.3.1   Conditions for Silylation of Ti-MCM-41

To investigate conditions for silylation of Ti-MCM-41, the calcined C_{12}-Ti-MCM-41 (100) one was a representative among those samples. According to [28]Si-NMR data reported in literature,[4] the amount of silanol groups on the surface of Ti-MCM-41 was found in the range of 20 to 40% of silicon atoms existing in the material. The maximum value of 40% was then utilized to calculate for the required amount of silyl group in various silyl reagents. Among silyl reagents, trimethylchlorosilane, TMCS was selected as a probing reagent in such investigation.

Intensities of the (100) reflection peak of the calcined C_{12}-Ti-MCM-41 (100) samples silylated with trimethylchlorosilane (TMCS), before and after hydrothermal treatment are compared in Table 4.5. The data indicate that the loss in crystallinity of the Ti-MCM-41 samples is reflected by the decrease in intensity of the (100) reflection peak from XRD data and it is affected by the amount of TMCS and silylation temperature. With increasing the amount of TMCS, the crystallinity is decreased. With increasing temperature, the crystallinity is decreased as well. The decrease of peak intensity by 29% is the least and relates to greatest stability to hydrothermal treatment of the sample obtained at the condition using TMCS at 10-fold excess whereas up to the decrease by 80% is obtained when 2-fold excess of TMCS was used. Therefore, the condition using 10-fold excess of other silyl reagents at the temperature of 120ºC is maintained for the rest of silylation studies.

Table 4.5   Comparison of intensities of (100) the reflection peak before and after hydrothermal treatment of the C_{12}-Ti-MCM-41 sample silylated with trimethylchlorosilane (TMCS)

Excess amount of TMCS based on Q^3 Si	Temperature (ºC)	Peak intensity of (100) plane (counts)		Change in intensity (%)
		Before hydrothermal treatment	After hydrothermal treatment	
2 fold	110	35,396	6977	-80
10 fold	110	35,396	20483	-42
10 fold	120	35,396	25141	-29

The IR spectra of the calcined C_{12}-Ti-MCM-41 sample before and after treatment with TMCS are shown in Figure 4.8. The bands at around 3500 and 1640 cm^{-1} are assigned to the OH stretching and bending vibration, respectively, in water molecules adsorbed on the Ti-MCM-41 surface. It is obviously seen that the amount of adsorbed water is remarkably decreased after silylation. This reveals that the silylated material has less hydrophilicity, or in another word more hydrophobicity than the non-silylated sample.
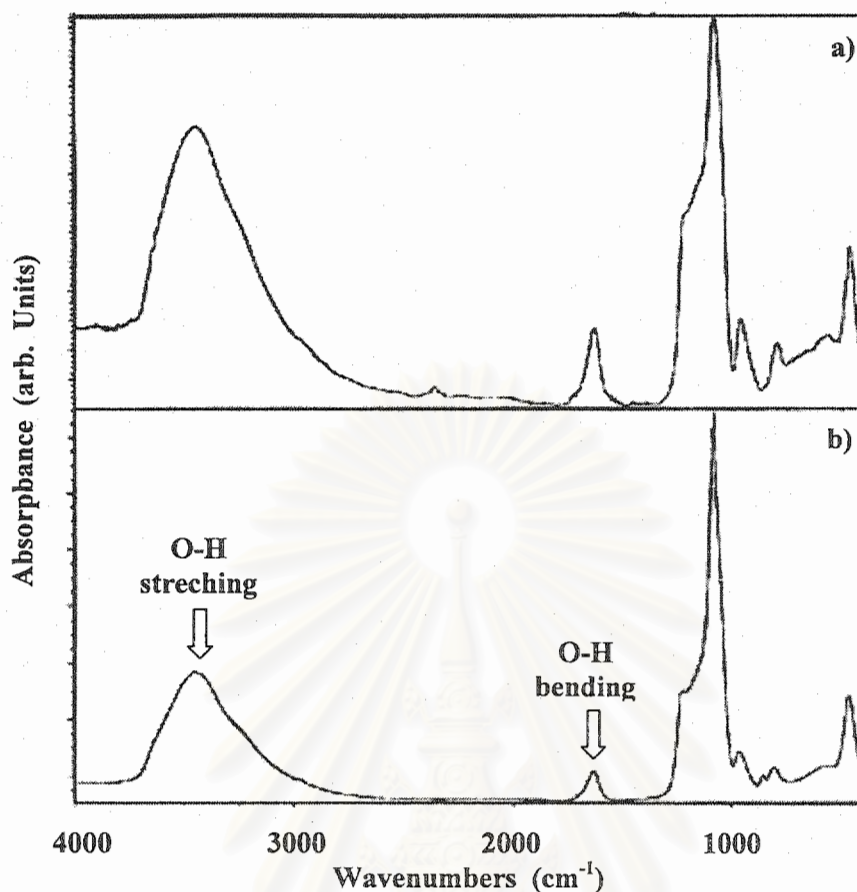
Figure 4.8 FT-IR Spectra of Ti-MCM-41 a) before and b) after silylation.

4.3.2 Stability of Ti-MCM-41 Samples Treated with Various Silyl Reagents

After silylation, the crystallinity of the C_{12}-Ti-MCM-41 treated with TMCS slightly increases by 10% compared to that before silylation while the treatments with other silyl reagents, result in decrease of crystallinity by 3, 7 and 29% when treated with TMES, TMSTFA, and HMDSO. The effects of the nature of the compound can be accounted for the losses in crystallinity of silylated compounds. The fluoro-compound is the most corrosive but HCl, a by-product form TMCS was found to promote the improvement of crystallinity. Water, a by-product from HMDSO is harmful to the mesostructure of Ti-MCM-41. Organic leaving group is naïve.

After treated with various silyl reagents, the Ti-MCM-41 was tested for the stability to hydrothermal treatment. According to the principal of more difficulty in diffusion of trimethylsilyl compounds into the relatively small pore C_{12}-Ti-MCM-41 than that into C_{16}-Ti-MCM-41, the former was chosen as the testing sample. If a trimethylsilyl compound has good performance in silylation of C_{12}-Ti-MCM-41, it should be able to enter the relatively large pore of C_{12}-Ti-MCM-41 and react with the surface of the latter in similar way. The silyl reagents used in this study were divided into two groups, possessing one and two silyl functional groups per molecule. For examples, TMCS, TMES, and TMSTFA possess one silyl functional group per molecule while HMDS and HMDSO contain two silyl functional groups per molecule. Intensities of the (100) reflection peak of the calcined C_{12}-Ti-MCM-41 (100) samples silylated with various silyl reagents, before and after hydrothermal treatment are compared in Table 4.7. From the XRD data in Table 4.6, the decrease of intensity, or the loss in crystallinity increases for HMDS (by 13%) < TMCS (by 29%) < TMES (by 50%) < HMDSO (by 55%) < TMSTFA (by 70%) < no treatment (by 79%). It is concluded that HMDS is the most efficient silyl reagent for reacting with the surface of Ti-MCM-41 to give the silylated material with the greatest stability to hydrothermal treatment. The presence of two silyl functional groups per molecule is accounted for the high activity of HMDS. The small size is responsible for the secondly active TMSC despite only one silyl group per molecule. Among the compounds possessing one silyl group, the bulkiness of TMSTFA > TMES > TMCS and that makes TMSTFA at the lowest activity while TMSC at the highest activity. Similarly, the bulkiness of HMDSO > HMDS, therefore HMDSO has lower activity than HMDS despite the equal presence of two silyl groups per molecule. The good leaving group of chloride seems to be accounted for the high activity of TMSC as well. Furthermore, it may be that water can be generated as a by-product from

HMDSO and it may cover the surface silanol groups of Ti-MCM-41 that have not yet accessible to of low mobility HMDSO.

Table 4.6 Comparison of intensities of (100) the reflection peak before and after hydrothermal treatment of the C_{12}-Ti-MCM-41 sample silylated with various silyl reagents

Silyl reagent	Peak intensity of (100) plane (counts)		Change in intensity (%)
	Before hydrothermal treatment	After hydrothermal treatment	
No treatment	32,142	6,787	-79
TMCS	35,371	25,141	-29
HMDSO	22,773	10,231	-55
TMSTFA	29,948	9,007	-70
TMES	31,018	15,537	-50
HMDS	31,026	26,935	-13

By exposure to moisture in the controlled atmosphere, the loss in crystallinity was reported in Table 4.7. The loss in crystallinity increases for TMES (by 2%) ~ TMSTFA (by 3%) < HMDS (by 9%) < TMCS (by 22%) < no treatment (by 38%) < HMDSO (by 48%).

Table 4.7 Comparison of intensities of (100) the reflection peak before and after exposure of the C_{12}-Ti-MCM-41 sample silylated with various silyl reagents, to moisture

Silyl reagent	Peak intensity of (100) plane (counts)		Change in intensity (%)
	Before exposure to moisture	After exposure to moisture	
No treatment	41,396	25,566	-38
TMCS	45,554	35,635	-22
HMDSO	29,330	15,319	-48
TMSTFA	38,570	37,576	-3
TMES	39,948	38,960	-2
HMDS	39,959	36,369	-9

4.4 Coupled Restructuring and Silylation of Ti-MCM-41

The crystallinities of the C_{12}-Ti-MCM-41 and C_{16}-MCM-41 samples were much improved by the coupled treatment of restructuring in hot water and silylation with HMDS as shown in Table 4.8. The coupled treatment sample exhibits the very higher crystallinity than a single technique of restructuring or silylation as shown in Table 4.9, based on intensity of (100) reflection peak, than untreated sample. The crystallinity of C_{16}-Ti-MCM-41(100) and C_{16}-Ti-MCM-41(60) are increased by 74 and 79% and C_{12}-Ti-MCM-41(100) and C_{12}-Ti-MCM-41(60) are increased by 8 and 24%. The effect of coupled treatment is found stronger on the C_{16}-MCM-41 sample. The reason is the C_{16}-Ti-MCM-41 sample is so less stable than C_{12}-Ti-MCM-41 that can be seen from the previous sections. The restructuring of Q^3 silicon is possible upon restructuring or

silylation. This is the first report using a coupled method of restructuring in hot water and silylation with HMDS.

Table 4.8 The crystallinities of the C_{12}-Ti-MCM-41 and C_{16}-MCM-41 samples improved by the coupled treatment of restructuring in hot water and silylation with HMDS

Sample	Peak intensity of (100) plane (counts)		Change in intensity (%)
	Before coupled treatment	After coupled treatment	
C_{12}-Ti-MCM-41(60)	23076	28584	+8
C_{12}-Ti-MCM-41(100)	34727	37447	+24
C_{16}-Ti-MCM-41(60)	10666	19119	+79
C_{16}-Ti-MCM-41(100)	10754	18447	+74

Table 4.9 The crystallinities of the C_{12}-Ti-MCM-41 and C_{16}-MCM-41 samples improved by the silylation with HMDS

Sample	Peak intensity of (100) plane (counts)		Change in intensity (%)
	Before silylated treatment	After silylated treatment	
C_{12}-Ti-MCM-41(60)	23,778	24,120	+1
C_{12}-Ti-MCM-41(100)	32,143	31,026	-4
C_{16}-Ti-MCM-41(60)	10,666	14,086	+32
C_{16}-Ti-MCM-41(100)	10,754	16,262	+51

The stability to hydrothermal treatment and moisture was tested as well and the results are shown in Tables 4.10 and 4.11. It is obvious that the coupled treatment of restructuring and silylation can remarkably increase the stability to hydrothermal treatment and moisture of both C_{12}-Ti-MCM-41 and C_{16}-MCM-41. Upon hydrothermal treatment and exposure to moisture the crystallinity is almost constant for C_{12}-Ti-MCM-41 and slightly affected for C_{16}-MCM-41. The increase in their stability is resulted from the successfully increased wall thickness after restructuring and attachment of trimethylsilyl group at the wall of the materials.

Table 4.10 Stability to hydrothermal treatment of the C_{12}-Ti-MCM-41 and C_{16}-MCM-41 samples improved by the coupled treatment of restructuring in hot water and silylation with HMDS

Sample	Peak intensity of (100) plane (counts)		Change in intensity (%)
	Before hydrothermal treatment	After hydrothermal treatment	
C_{12}-Ti-MCM-41(60)	28584	31004	+9
C_{12}-Ti-MCM-41(100)	37447	36246	-3
C_{16}-Ti-MCM-41(60)	19119	16989	-11
C_{16}-Ti-MCM-41(100)	18750	18638	-1

Table 4.11 Stability to moisture of the C_{12}-Ti-MCM-41 and C_{16}-MCM-41 samples improved by the coupled treatment of restructuring in hot water and silylation with HMDS

Sample	Peak intensity of (100) plane (counts)		Change in intensity (%)
	Before exposure to moisture	After exposure to moisture	
C_{12}-Ti-MCM-41(60)	28584	30830	+8
C_{12}-Ti-MCM-41(100)	37447	40874	+9
C_{16}-Ti-MCM-41(60)	19119	18102	-5
C_{16}-Ti-MCM-41(100)	18750	18574	-1

4.5 Mechanical Stability of C_{12}-Ti-MCM-41 (100)

The C_{12}-Ti-MCM-41 shows the highest stability from the later section. C_{12}-TiMCM-41 is selected to test mechanical stability and results are shown in Figure 4.9 and Table 4.12. It shows that the improved stability by a coupled restructuring and silylation exhibits mechanical stablity than no treatment sample and restructuring treatment. The restructuring treatment improves the wall polymerization but at the same time the pore diameter and the *d*-spacing are enlarged as a result the mechanical stability becomes low. But its mechanical stability dramatically improves after it is silylated with HMDS.

Table 4.12 The comparative mechanical stability of C$_{12}$-Ti-MCM-41

Sample	Pressure (kg cm^{-2})				
	0	**500**	**1000**	**1500**	**2000**
	Peak intensity of (100) plane (counts)				
No treatment	32,142	13,063	12,793	12,232	10,125
Restructuring	44,587	7,074	6,250	6,187	6,234
Couple restructuring and silylation	37,447	36,594	35,032	31,416	30,669
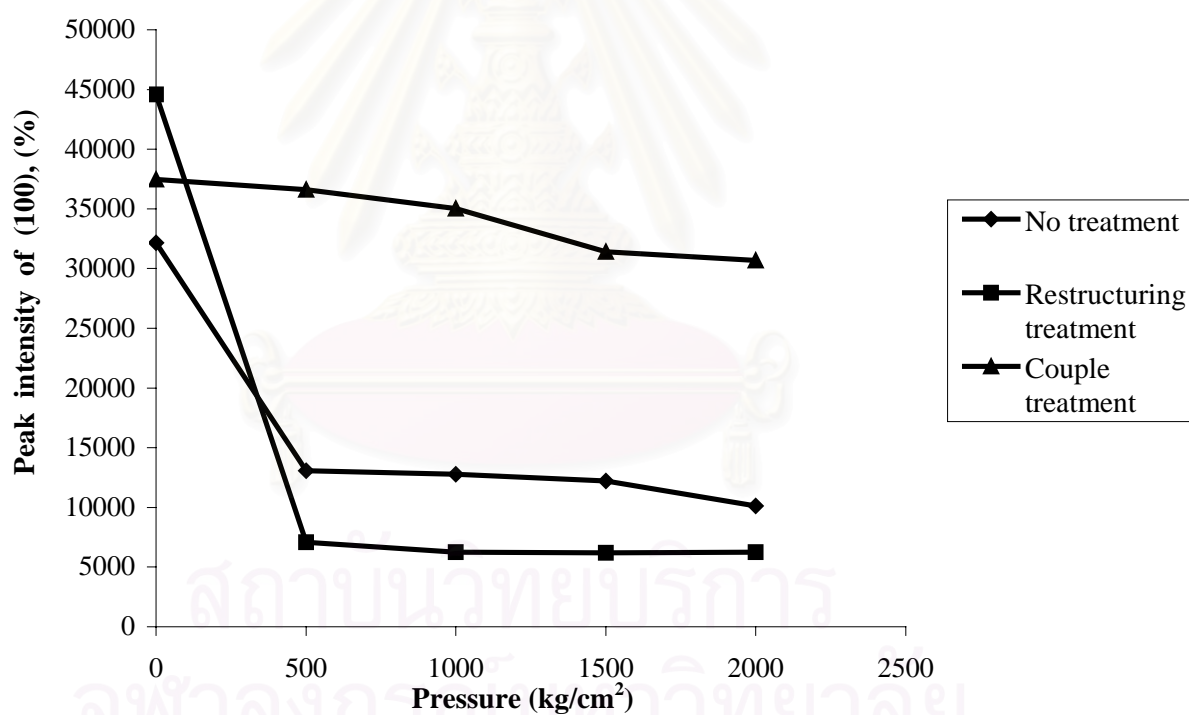
Figure 4.9 Influence of external pressure to crystallinity of C$_{12}$-Ti-MCM-41.

CHAPTER V

CONCLUSION

The mesoporous Ti-MCM-41 was successfully synthesized with improvement of the stability by the post-synthesis coupled restructuring in hot water followed by silylation. A high-stability mesoporous Ti-MCM-41, synthesized using $C_{12}TMA^+$ (smaller pore) or $C_{16}TMA^+$ (larger pore) as template, was prepared by the alkaline-free hydrothermal synthesis reported by Tatsumi *et al.*[18] The Si/Ti ratios of 100 and 60 were utilized in order to monitor the effect of titanium content to their properties. The secondary wall-polymerization by a post-synthesis hydrothermal treatment increases crystallinity and stability of C_{12}-Ti-MCM-41 and C_{16}-Ti-MCM-41. Finally, the Ti-MCM-41 samples were increased their hydrophobicity by trimethylsilylation with trimethylsilyl reagents. After the hydrothermal restructuring treatment, the DR-UV-Vis results indicate upon treatment no leaching of titanium from the tetrahedral sites on framework to octahedral site. In silylation step, silyl reagent was varied for investigation of the most active silyl reagent, the hexamethyldisilazane (HMDS) was the best among tested silyl reagents.

The tests for hydrothermal stability to hydrothermal treatment and stability to moisture indicate that the mesoporous Ti-MCM-41 which improved stability by a combination of hydrothermal restructuring and silylation exhibits the unique higher hydrothermally stable and stability to moisture than using a single technique, not only the improvement of stability, but also the improvement of crystallinity. After the application of the combination technique, in case of C_{16}-Ti-MCM-41, the crystallninity was totally increased by 74% - 79% and in case of C_{12}-Ti-MCM-41, the crystallinity was totally increased by 7% - 24% compared to the calcined sample of untreated

sample. The effect of improvement of the crystallinity depends on the titanium contents and the their initial crystallinity. These modified Ti-MCM-41 materials exhibit the larger pore than the typical silylated Ti-MCM-41 which can overcome the problem of the lower accessibility from the void occupy of trimethylsily (TMS) group. The mechanical stability test also shows that the improvement using the combination techniques results in the highest stability compared to the calcined sample obtained from typical hydrothermal synthesis or with only hydrothermal restructuring improvement.

The suggestion for future work :

1. Studying the catalytic activity for oxidation of these improved Ti-MCM-41 with various substrates in order to compare the effect of the crystallinity increment and the higher hydrophobicity.

2. Fully characterization of these stable Ti-MCM-41 for their other physical properties.

3. Application of this method of improvement of stability and hydrophopicity to other silica materials.

REFERENCES

1. IUPAC <u>Manual of Symbols and Terminology, Appendix 2, Part 1.</u> *Colloid and Surface Chemistry, Pure Appl. Chem.* **1972**, *31*, 578.

2. Szostak, R. <u>Molecular Sieves Principles of Synthesis and Identification,</u> New Van Nostrand Reinhold, New York, **1988**, p.1-45.

3. Whitehurst, D. D. "Method to Recover Organic Templates from Freshly Synthesized Molecular Sieves" U.S. Patent 5,143,879, **1992**.

4. Beck, J. S.; Vartuli, J. C.; Roth, W. J.; Leonowicz, M. E.; Kresge, C. T.; Schmitt, K. D.; Chu, C. T-W.; Olson, D. H.; Sheppard, E. W.; McCullen, S. B.; Higgins, J. B.; Schlenker, J. L. "A New Family of Mesoporous Molecular Sieves Prepared with Liquid Crystal Templates" *J. Am. Chem. Soc.* **1992**, *114*, 10834.

5. Tatsumi, T. "Metallozeolites and Applications in Catalysis" Solid *State & Material Science* **1997**, *2*, 76.

6. Gontier, S.; Tuel, A. "Liquid Phase Oxidation of Aniline over Various Transition-Metal-Substituted Molecular Sieves" *J. Catal*. **1995**, *157*, 124.

7. Blasco, M. T.; Camblor, M. A.; Corma, A.; Pérez-Pariente, J. "Synthesis of a Titanoaluminosilicates Isomorphous to Zeolites Beta and its Application as a Catalyst for the Selective Oxidation of Large Organic Molecules" *J. Chem. Soc., Chem. Commun.* **1992**, *8*, 589.

8. Blasco, T.; Camblor, M. A.; Corma, A.; Pérez-Pariente, J. "The State of Ti in Titanoaluminosilicates Isomorphous with Zeolites β" *J. Am. Chem. Soc.* **1993**, *115*, 11806.

9. Blasco, T.; Camblor, M. A.; Corma, A.; Esteve, P.; Guil, J. M.; Martínez,

A.; Perdigón, J. A.; Valencia, S. "Direct Synthesis and Characterization of Hydrophobic Aluminum-free Ti-Beta Zeolites" *J. Phys. Chem. B* **1998**, *102*, 75.

10. Corma, A.; Navarro, M. T.; Pérez-Pariente, J. "Synthesis of an Ultralarge Pore Titanium Silicate Isomorphous to MCM-41 and its Application as a Catalyst for Selective Oxidation of Hydrocarbons" *J. Chem. Soc., Chem. Commun.* **1994**, 147.

11. Blasco, T.; Corma, A.; Navarro, M. T.; Pérez-Pariente, J. "Synthesis, Characterization, and Catalytic Activity of Ti-MCM-41 Structures" *J. Catal.* **1995**, *156*, 65.

12. Ryoo, R.; Kim, J. M. "Structural Order in MCM-41 Controlled by Shifting Silicate Polymerization Equilibrium" *J. Chem. Soc., Chem. Commun.* **1995**, 711.

13. Mokaya, R. "Improving the Stability of Mesoporous MCM-41 Silica via Thicker More Highly Condensed Pore Walls" *J. Phys. Chem. B* **1999**, *103*, 10204.

14. Ryoo, R.; Kim, J. M.; Ko, C. H.; Shin, C. H. "Disordered Molecular Sieve with Branched Mesoporous Channel Network" *J. Phys. Chem.* **1996**, *100*, 17718.

15. Koyano, K. A.; Tatsumi, T.; Tanaka, Y.; Nakata, S. "Stabilization of Mesoporous Molecular Sieves by Trimethylsilylation" *J. Phys. Chem. B* **1997**, *101*, 9436.

16. Cheng, C. F.; Zhou, W. Z.; Park, D. H.; Klinowski, J.; Hargreaves, M.; Gladden, F. "Modification of MCM-41 by Surface Silylation with Trimethylchlorosilane and Adsorption Study" *J. Chem Soc., Faraday Trans.* **1997**, *93*, 359, 193.

17. Rhee, C. H.; Lee, J. S. "Thermal and Chemical Stability of Titanium-

Substituted MCM-41" *Catal. Lett*. **1996**, *40*, 261.

18. Koyano, K. A.; Tatsumi, T. "Synthesis of Titanium-Containing MCM-41" *Microporous Materials* **1997**, *10*, 259.

19. Gusev, V. Y.; Feng, X.; Bu, Z.; Haller, G. L.; O'Brien, J. A. "Mechanical Stability of Pure Silica Mesoporous MCM-41 by Nitrogen Adsorption and Small-Angle X-ray Diffraction Measurements" *J. Phys. Chem*. **1996**, *100*, 1985.

20. Ishikawa, T.; Matsuda, M.; Yasukawa, A.; Kandori K.; Inagaki, S.; Fukushima, T.; Kondo, S. "Surface Silanol Groups of Mesopourous Silica FSM-16" *J. Chem. Soc. Faraday Trans*. **1996**, *98*, 1985.

21. Tatsumi, T.; Koyano, K. A.; Tanaka, Y.; Nakata, S. "Mechanochemical Collapse of M41S Mesoporous Molecular Sieves through Hydrolysis of Siloxane Bonds" *Chem. Lett*. **1997**, 469.

22. Tatsumi, T.; Koyano, K. A.; Tanaka, Y.; Nakata, S. "Mechanical Stability of Mesoporous Materials, MCM-48 and MCM-41" *J. Porous. Mater*. **1999**, *6*, 13.

23. Coustel, N.; Renzo, F. D.; Fajula, F. "Improved Stability of MCM-41 through Textural Control" *J. Soc., Chem. Commun*. **1994**, 967.

24. Kim, J. M.; Kwak, J. H.; Jun, S.; Ryoo, R. "Ion Exchange and Thermal Stability of MCM-41" *J. Phys. Chem.* **1995**, *99*, 16742.

25. Ryoo, R.; Ko, C. H.; Howe, R. F. "Imaging the Distribution of Framework Aluminum in Mesoporous Molecular Sieve MCM-41" *Chem. Mater*. **1997**, *9*, 1607.

26. Edler, K. J.; White, J. W. "Further Improvements in the Long-Range Order of MCM-41 Materials" *Chem. Mater*. **1997**, *9*, 1226.

27. Das, D.; Tsai, C. –M.; Cheng, S. "Improvement of Hydrothermal Stability of MCM-41 Mesoporous Molecular Sieve" *Chem. Commun*. **1999**, 473.

28. Kim, W. J.; Yoo, J. C.; Hayhurst, D. T. "Synthesis of Hydrothermally Stable MCM-41 with Initial Adjustment of pH and Direct Addition of NaF" *Micropor. and Mesopor. Mater.* **2000**, *39*, 177.

29. Xia, Q. -H.; Hidajat, K.; Kawi, S. "Improvement of the Hydrothermal Stability of Fluorinated MCM-41 Material" *Mater. Lett.* **2000**, *42*, 102.

30. Sayari, A.; Liu, P.; Kruk, M.; Jaroniec, M. "Characterization of Large-Pore MCM-41 Molecular Sieves Obtained via Hydrothermal Restructuring" *Chem. Mater.* **1997**, *9*, 2499.

31. Chen, L.; Horiuchi, T.; Mori, T.; Maeda, K. "Postsynthesis Hydrothermal Restructuring of M41S Mesoporous Molecular Sieves in Water" *J. Phys. Chem. B* **1999**, *103*, 1216.

32. Kruk, M.; Jaroniec, M.; Sayari, A. "Influence of Hydrothermal Restructuring Condition on Structural Properties of Mesoporous Molecular Sieves" *Micropor. and Mesopor. Mater.* **1999**, *27*, 217.

33. Biz, S.; White, M. G. "Effect of Post-Synthesis Hydrothermal Treatment on the Adsorptive Volume of Surfactant-Templated Mesostructures" *Micropor. and Mesopor. Mater.* **2000**, *40*, 159.

34. Zhao, X. S.; Lu, G. Q.; Whittaker, A. K.; Millar, G. J.; Zhu, H. Y. "Comprehensive Study of Surface Chemistry of MCM-41 Using ^{29}Si CP/MAS NMR, FTIR, Pyridine-TPD, and TGA" *J. Phys. Chem. B* **1997**, *101*, 6525.

35. Zhao, X. S.; Lu. G. Q. "Modification of MCM-41 by Surface Silylation with Trimethylchlorosilane and Adsorption Study" *J. Phys. Chem. B* **1998**, *102*, 1556.

36. Park, M.; Komarneni, S.; "Stepwise Functionalization of Mesoporous Crystalline Silica Materials" *Micropor and Mesopor Mater.* **1998**, *25*, 75.

37. Zhao, X. S.; Audsley, F.; Lu, G. Q. "Irreversible Change of Pore Structure of MCM-41 upon Hydration at Room Temperature" *J. Phys. Chem. B* **1998**, *102*, 4143.

38. Corma, A.; Domine, M.; Gaona, J. A.; Jordá, J. L.; Navarro, M. T.; Rey, F.; Pérez-Pariente, J.; Tsuji, J.; McCulloch, B.; Nemeth, L. T. "Strategies to Improve the Epoxidation Activity and Selectivity of Ti-MCM-41" *Chem. Commun*. **1998**, 2211.

39. D'Amore, M. B.; Schwarz, S. "Trimethylsilylation of Ordered and Disordered Titanosilicates: Improvements in Epoxidation with Aqueous H_2O_2 from Micro- to Mesopores and Beyond" *Chem. Commun*. **1999**, 121.

40. Tatsumi, T.; Koyano, K. A.; Igarashi, N. "Activity Enhancement by Trimethylsilylation of Ti-containing Mesoporous Molecular Sieve Catalysts for Oxidation of Alkenes and Alkanes with H_2O_2" *Study. Surf. Sci Catal.* **1998**, 221.

41. Tatsumi, T.; Koyano, K. A.; Igarashi, N. "Remarkable Activity Enhancement by Trimethylsilylation in Oxidation of Alkenes and Alkanes with H_2O_2 Catalyzed by Titanium-Containing Mesoporous Molecular Sieves" *Chem. Commun*. **1998**, 325.

42. Corma, A.; García, H.; Navarro, M. T.; Palomares, E. J.; Rey, F. "Observation of a 390-nm Emission Band Associated with Framework Ti in Mesoporous Titanosilicates" *Chem. Mater.* **2000**, *12*, 3068.

43. Anwander, R.; Nagl, I.; Widenmeyer, M.; Engelhardt, G.; Groeger, O.; Palm, C.; Röser, T. "Surface Characterization and Functionalization of MCM-41 Silicas via Silazane Silylation" *J. Phys. Chem. B* **2000**, *104*, 3532.

44. Antochshuk, V.; Jaroniec, M. "Simultaneous Modification of Mesoporoes

and Extraction of Template Molecules from MCM-41 with Trialkylchlorosilanes" *Chem. Commun*. **1999**, 2373.

45. Antochshuk, V.; Araujo, A. S.; Jaroniec, M. "Functionalized MCM-41 and Ce-MCM-41 Materials Synthesized via Interfacial Reactions" *J. Phys. Chem. B* **2000**, *104*, 9713.

46. Lin, H. –P.; Yang, L. –Y.; Mou, C. –Y.; Liu, S. –B.; Lee, H. –K. "A Direct Surface Silyl Modification of Acid-Synthesized Mesoporous Silica" *New J. Chem*. **2000**, *24*, 253.

47. Wu, P.; Tatsumi, T.; Komatsu, T.; Yashima, T. "Postsynthesis, Characterization, and Catalytic Properties in Alkene Epoxidation of Hydrothermally Stable Mesoporous Ti-SBA-15" *Chem. Mater*. **2002**, *14*, 1657.

48. Bhaumik, A.; Tatsumi, T. "Organically Modified Titinium-Rich Ti-MCM-41, Efficient Catalysts for Epoxidation Reactions" *J. Catal*. **2000**, *189*, 31.

49. Igarashi, N.; Tanaka, Y.; Nakata, S.; Tatsumi, T. "Increased Stability of Organically Modified MCM-41 Synthesized by a One-step Procedure" *Chem. Lett*. **1999**, 1.

50. Peña, M. L.; Dellarocca, V.; Rey, F.; Corma, A.; Coluccia, S.; Marchese, L. "Elucidating the Local Environment of Ti (IV) Active Sites in Ti-MCM-48: a Comparison between Silylated and Calcined Catalysts" *Micropor and Mesopor Mater*. **2001**, *44-45*, 345.

51. Ryoo, R.; Jun, S.; "Improvement of Hydrothermal Stability of MCM-41 Using Salt Effects During the Crystallization Process" *J. Phys. Chem. B* **1997**, *101*, 317.

52. Kim, J. M.; Jun, S.; Ryoo, R. "Improvement of Hydrothermal Stability of Mesoporous Silica Using Salts: Reinvestigation for Time-Dependent Effects" *J. Phys. Chem. B* **1999**, *103*, 6200.

53. Corma, A.; Kan, Q.; Rey, F. "Synthesis of Si and Ti-Si-MCM-48 Mesoporous Materials with Controlled Pore Sizes in the Absence of Polar Organic Additives and Alkali Metal Ions" *Chem. Commun.* **1998**, 579.

54. Jun, S.; Kim, J. M.; Ryoo, R.; Ahn, Y. –S.; Han, M. –H. "Hydrothermal Stability of MCM-48 Improved by Post-Synthesis Restructuring in Salt Solution" *Micropor. and Mesopor..Mater.* **2000**, *41*, 119.

55. He, N.; Lu, Z.; Yuan, C.; Hong, J.; Yang, C.; Bao, S.; Xu, Q. "Effect of Trivalent Elements on the Thermal and Hydrothermal Stability of MCM-41 Mesoporous Molecular Materials" *Supramolecular Science* **1998**, *5*, 553.

56. Chen, L. Y.; Jaenicke, S.; Chuah, G. K. "Thermal and Hydrothermal Stability of Framework-Substituted MCM-41 Mesoporous Materials" *Micropor. Mater.* **1997**, *12*, 323.

57. Corma, A.; Grande, M. S.; Gonzalez-Alfaro, V.; Orchillest, A. V. "Cracking Activity and Hydrothermal Stability of MCM-41 and Its Comparison with Amorphous Silica-Alumina and a USY Zeolite" *J. Catal.* **1996**, *159*, 375.

58. Landau, M. V.; Varkey, S. P.; Herskowitz, M.; Regev, O.; Pevzner, S.; Sen, T.; Luz, Z. "Wetting Stability of Si-MCM-41 Mesoporous Material in Neutral, Acidic and Basic Aqueous Solutions" *Micropor and Mesopor Mater.* **1999**, *33*, 149.

59. Hartmann, M.; Bischof, C. "Mechanical Stability of Mesoporous Molecular Sieve MCM-48 Studied by Adsorption of Benzene, *n*-Heptane, and Cyclohexane. *J. Phys. Chem. B* **1999**, *103*, 6230.

60. Khushalani, D.; Kuperman, A.; Ozin, G. A.; Tanaka, K.; Garces, J.; Olken,

M. M.; Coombs, N. "Metamorphic Materials-Restructuring Siliceous Mesoporous Materials" *Adv Mater*. **1995**, *7*, 847.

61. Huo, Q.; Margolese, D. I.; Stucky, G. D. "Surfactant Control of Phases in the Synthesis of Mesoporous Silica-Based Materials" *Chem. Mater*. **1996**, *8*, 1147.

62. Meier, W. M.; Oison, D. H. Atlas of Zeolite Framework Types, 5 nd. ed. Revised; Elsevier: Amsterdam, **2001**.

63. Treacy, M. M. J.; Higgins, J. B. "Collection of Simulated XRD Powder Patterns for Zeolites" 4 nd. Ed., Elsevier: Amsterdam, **2001**.

64. Corma, A. "From Microporous to Mesoporous Molecular Sieves Materials and Their Use in Catalysis" *Chem Rev*. **1997**, *97*, 2373.

65. Behrens, P.; Glaue, A.; Haggenmüller, C.; Schechner, G. "Structure-Directed Materials Syntheses: Synthesis Field Diagrams for the Preparation of Mesostructured Silicas" *Solid State Ionics* **1997**, *101-103*, 255.

66. Chen, C. –Y.; Burkett, S. L.; Li, H. –X.; Davis, M. E. "Studies on Mesoporous Materials II. Synthesis Mechanism of MCM-41" *Micropor. Mater*. **1993**, *2*, 27.

67. Sayari, A. "Catalysis by Crystalline Mesoporous Molecular Sieves" *Chem. Mater*. **1996**, *8*, 1840.

68. Huo, Q. S.; Margolese, D.; Ciesla, U,; Feng P. Y.; Gier, T. E.; Sieger, P.; Leon, R.; Petroff, P. M.; Schuth, F. Stucky, G. D. "Generalized Synthesis of Periodic Surfactant Inorganic Composite-Materials" *Nature* **1994**, *368*, 317.

69. Huo, Q.; Margolese, D. I.; Stucky, G. D. "Surfactant Control of Phase in the Synthesis of mesoporous Silica-Based Materials" *Chem. Mater*. **1996**, *8*, 1147.
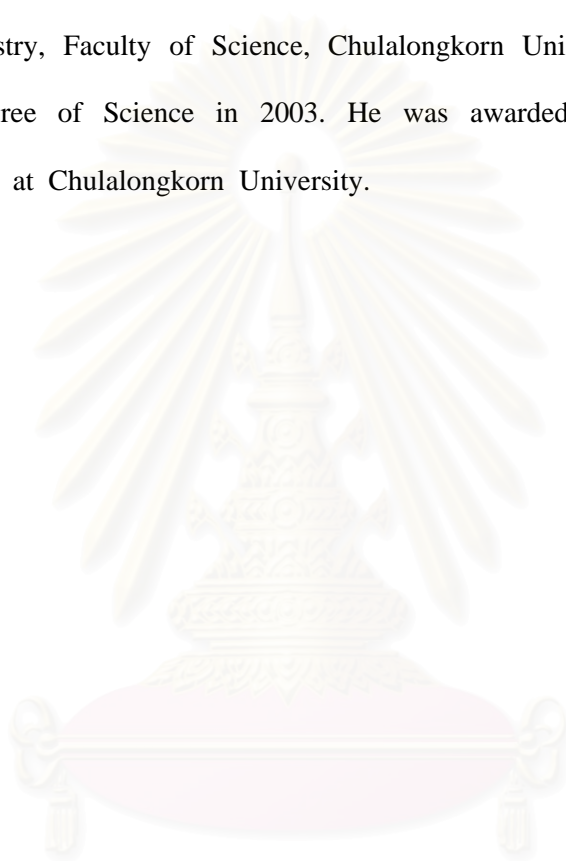
70. Zheo, X. S.; Lu, G. Q.; Millar, G. J. "Advances in Mesoporous Molecular Sieves MCM-41 *Ind. Eng. Chem. Res.* **1996**, *35*, 2075.

71. Reddy, J. S.; Sayari, A. "Oxidation of Propylamine over Titanium Silicate Molecular Sieves" *Appl. Catal A* **1995**, *128*, 231.

72. Attard, G. S.; Glyde, J. C.; Goltner, C. G. "Liquid-Crystalline Phases as Templates for the Synthesis of Mesoporous Silica" *Nature* **1995**, *378*, 366.

73. Alba, M. D.; Becerro, A. I.; Klinowski, J. "Pore Structure Analysis of the Mesoporous Titanosilicate Molecular Sieve MCM-41 by ^{1}H NMR and N_2 sorption" *J. Chem. Soc., Faraday Trans.* **1996**, *92*, 849.

74. Alba, M. D.; Luan, Z.; Klinowski, J. "Titanosilicate Mesoporous Molecular Sieve MCM-41: Synthesis and Characterization" *J. Phys. Chem.* **1996**, *100*, 2178.

75. Zhang, W.; Fröba, M.; Wang, J.; Tanev, P. T.; Wong, J.; Pinnavaia, T. J. "Mesoporous Titanosilicate Molecular Sieves Prepared at Ambient Temperature by Electrostatic (S^+I^-, $S^+X^-I^+$) and Neutral ($S°I°$) Assembly Pathways: A Comparison of Physical Properties and Catalytic Activity for Peroxide Oxidations" *J. Am. Chem. Soc.* **1996**, *118*, 9164.

76. Wu, P.; Iwamoto, M. "Metal-ion-Planted MCM-41. Part 3. Incorporation of Titanium Species by Atom-Planting Method" *J. Chem. Soc., Faraday Trans.* **1998**, *94*, 2871.

77. Ahn, W. S.; Lee, D. H.; Kim, T. J.; Kim, J. H.; Seo, G.; Ryoo, R. "Post-Synthetic Preparations of Titanium-Containing Mesopore Molecular Sieves" *Appl. Catal. A* **1999**, *181*, 39.

78. Beck, J. S.; Vartuli, J. C., Kennedy, G. J.; Kresge, C. T., Roth, W. J.,

Schramm, S. E. "Molecular or Supramolecular Templating: Defining the Role of Surfactant Chemistry in the Formation of Microporous and Mesoporous Molecular Sieves" *J. Am. Chem. Soc*. **1994**, *6*, 1816.

79. Grün, M.; Unger, K. K.; Matsumoto, A.; Tsutsumi, K. "Novel Pathways for the Preparation of Mesoporous MCM-41 Materials: Control of Porosity and Morphology" *Micropor. and Mesopor. Mater*. **1999**, *27*, 207.

80. Corma, A.; Kan, Q.; Navarro, M. T.; Pérez-Pariente, J.; Rey, F. "Synthesis of MCM-41 with Different Pore Diameters without Addition of Auxiliary Organics" *Chem Mater* **1997**, *9*, 2123.

81. Luan, Z.; He, H.; Zhou, W.; Klinoski, J. "Transformation of Lamella Silicate into the Mesoporous Molecular Sieve MCM-41" *J. Chem. Soc., Fraday Trans*. **1998**, *94*, 979.

82. Vartulli, J.; Schmitt, K. D.; Kresge, C. T.; Roth, W. J.; Leonowicz, M. E.; McCullen, S. B.; Hellring, S. D.; Beck, J. S.; Schlenker "Effect of Surfactant/Silica Molar Ratios on the Formation of Mesoporous Molecular Sieves: Inorganic Mimicry of Surfactant Liquid-Crystal Phases and Mechanistic Implications" *Chem matter* **1994**, *6*, 2317.

83. Koyano, K. A.; Tatsumi, T. "Synthesis of Titanium-Containing Mesoporous Molecular Sieves with a Cubic Structure" *Chem. Commun*. **1996**, 145.

84. Koyano, K. A.; Tatsumi, T. "Synthesis of Titanium-Containing Mesoporous Molecular Sieves with a Cubic Structure" *Stud. Surf. Sci. Catal*. **1997**, *105*, 93.

85. Monnier, A.; Schüth, F.; Huo, Q.; Kumar, D.; Margolese, D.; Maxwell, R. S.; Stucky, G. D.; Krishamurty, M.; Petroff, P.; Fiouzi, A.; Janicke, M.; Chmelka, B. F. "Cooperative Formation of Inorganic-Organic Interfaces in the Synthesis of Silicate Mesostructures" *Science* **1993**, *261*, 1299.

86. Ciesla, U.; Schuth, F. "Ordered Mesoporous Materials" *Micropor. and Mesopor. Mater*. **1999**, *27*, 131.

87. Feuston, B. P.; Higgins, J. B. "Model Structures for MCM-41 Materials: A Molecular Dynamics Simulation" *J. Phys. Chem*. **1994**, *98*, 4459.

88. Llewellyn, P. L.; Schüth, F.; Grillet, Y.; Rouquerol, F.; Rouquerol, J.; Unger, K. K.."Water Sorption on Mesoporous Aluminosilicate MCM-41" *Langmuir* **1995**, *11*, 574.

89. Camblor, M. A.; Corma, A.; Pérez-Pariente, J. "Infrared Spectroscopic Investigation of Titanium in Zeolites. A New Assignment of the 960 cm^{-1} Band" *J. Chem. Soc., Chem. Commun*. **1993**, 557.

90. Morey, M.; Davidson, A.; Stucky, G. "A New Step Toward Transition Metal Incorporation in Cubic Mesoporous Materials: Preparation and Characterization of Ti-MCM-48" *Micropor. and Mesopor. Mater*. **1996**, *6*, 99.

91. Marchese, L.; Maschmeyer, T.; Gianotti, E.; Coluccia, S.; Thomas, J. M. "Probing the Titanium Sites in Ti-MCM-41 by Diffuse Reflectance and Photoluminescence UV-Vis Spectroscopies" *J. Phys. Chem. B* **1997**, *101*, 8836.

92. Prakash, A. M.; Sung-Suh, H. M.; Kevan, L. "Electron Spin Resonance Evidence for Isomorphous Substitution of Titanium into Titanosilicate TiMCM-41 Mesoporous Molecular Sieve" *J. Phys. Chem. B* **1998**, *102*, 857.

VITAE

Mr. Dachochai Wilairat was born on October 11, 1977 in Nakornpathom, Thailand. He received a Bachelor's Degree of Science in Chemistry from Chulalongkorn University in 1998 and continued his Master study in program of inorganic chemistry, Faculty of Science, Chulalongkorn University and graduated with his Master Degree of Science in 2003. He was awarded by research grants from Graduate School at Chulalongkorn University.